



TECHNISCHE
UNIVERSITÄT
WIEN
Vienna University of Technology

Master Thesis

Investigation of Zn-alloy coatings for corrosion protection of installation systems

Carried out for the purpose of obtaining the degree
Master of Science (MSc or Dipl. Ing. or DI)
submitted at the
Institute of Chemical Technologies and Analytics.

Supervisor:

Ao. Univ. Prof. Dipl.-Ing. Dr. techn. Linhardt Paul

Author:

Eva Walkner, BSc

April 2022

Die approbierte gedruckte Originalversion dieser Diplomarbeit ist an der TU Wien Bibliothek verfügbar
The approved original version of this thesis is available in print at TU Wien Bibliothek.



I confirm, that going to press of this thesis needs the confirmation of the examination committee.

Affidavit

I declare in lieu of oath, that I wrote this thesis and performed the associated research myself, using only literature cited in this volume. If text passages from sources are used literally, they are marked as such.

I confirm that this work is original and has not been submitted elsewhere for any examination, nor is it currently under consideration for a thesis elsewhere.

Feldkirch, April 2022



Signature

Die approbierte gedruckte Originalversion dieser Diplomarbeit ist an der TU Wien Bibliothek verfügbar
The approved original version of this thesis is available in print at TU Wien Bibliothek.



Abstract

It is known that Zn and Zn-alloy coatings protect steel from corrosion. A standard method to apply such coatings is hot dip galvanizing (HDG). The process works either by dipping finished parts (batch HDG) or continuously immersing a steel strip into a liquid zinc bath.

The continuous hot dip galvanization is suitable for long products like strut channels. In this case the steel strip for the strut channels gets coated before the roll forming step. Smaller parts like connectors are produced mainly by batch hot dip galvanizing.

To increase the lifetime of different Hilti MT-system parts there are some possibilities: for the strut channels made from continuously coated steel an increase of the coating thickness and adding alloying elements like Al and Mg to the coating bath is the simplest way. However, for the connectors the thickness obtained by batch HDG is limited by the process itself.

Therefore, in this work two coating processes were evaluated to increase the corrosion protection of the connector parts: the double dip HDG process on sample plates and Hilti parts, and the zinc diffusion process on Hilti parts.

The double dip approach opposed to the standard batch HDG process adds a second dip step into a suitable Zn-alloy bath after the first standard zinc dip step. In the zinc diffusion process fine powder containing zinc and other additives are put together with the parts in an airtight container. Heat is introduced and through thermal diffusion the zinc finds its way into the metal substrate while an intermetallic layer is formed.

The coated samples were investigated by metallographic analytics including SEM and EDX, standard electrochemical methods and accelerated lab corrosion tests. Based on the results the plating parameters like dipping time, bath temperature and alloy composition for the double dip approach were optimized. Parallel to that, existing zinc diffusion samples were investigated equally and compared to the double dip zinc approach.

The double dip zinc process was found to be promising when using a dipping time of 5 minutes for both dips. An aluminium and iron-rich ternary zinc layer formed next to the steel substrate in the microstructure. An increasing zinc content towards the outer top area of the coating was found which was providing a suitable corrosion protection in the test. For the connectors tested for corrosion properties in the project, the zinc diffusion coated samples and the mechanically plated reference samples performed best.

Die approbierte gedruckte Originalversion dieser Diplomarbeit ist an der TU Wien Bibliothek verfügbar
The approved original version of this thesis is available in print at TU Wien Bibliothek.



Kurzfassung

Es ist bekannt, dass Beschichtungen aus Zn und Zn-Legierungen Stahl vor Korrosion schützen. Ein Standardverfahren zum Aufbringen solcher Überzüge ist die Feuerverzinkung im Schmelztauchverfahren (HDG). Das Verfahren funktioniert entweder durch Eintauchen fertiger Teile (= Stückverzinkung) oder durch kontinuierliches Eintauchen eines Stahlbandes in ein flüssiges Zinkbad (= Bandverzinkung).

Die Bandverzinkung eignet sich für lange Produkte wie profilierte Querträger. In diesem Fall wird das Stahlband für die Querträger vor dem Profilieren beschichtet. Kleinere Teile, wie z.B. Verbindungsstücke, werden hauptsächlich im Stückverzinkungsverfahren gefertigt.

Um die Lebensdauer der verschiedenen Teile des Hilti MT-Systems zu erhöhen, gibt es folgende Möglichkeiten: Für die Querstreben ist eine Erhöhung der Schichtdicke und die Zugabe von Legierungselementen wie Al und Mg zum Beschichtungsbad die einfachste Möglichkeit. Bei den Verbindungselementen ist die mit dem Stückverzinkungsprozess erzielbare Schichtdicke jedoch, durch das Verfahren selbst, begrenzt.

Daher wurden in dieser Arbeit zwei Beschichtungsverfahren zur Erhöhung des Korrosionsschutzes der Verbindungsstücke des MT-Systems bewertet: das Doppeltauch-Stückverzinkungsverfahren auf Probeplatten und Hilti-Teilen und das Diffusions-Verzinken auf Hilti-Teilen.

Beim Doppeltauch-Stückverzinkungsverfahren wird im Gegensatz zum Standard-Stückverzinkungsverfahren nach dem ersten Zinkbad-Tauchschrift ein zweiter Tauchschrift in einem geeigneten Zn-Legierungsbad hinzugefügt. Beim Diffusionsverfahren wird feines Pulver, das Zink und andere Additive enthält, zusammen mit den Hilti-Teilen in einen luftdichten Behälter gegeben. Durch Wärmezufuhr und thermischer Diffusion diffundiert das Zink in das Metallsubstrat wodurch sich eine intermetallische Schicht bildet.

Die beschichteten Proben wurden metallographisch aufbereitet und mithilfe von REM und EDX analysiert. Weiters wurden die Proben mit elektrochemischen Standardmethoden und beschleunigten Laborkorrosionstests untersucht. Anhand der Ergebnisse wurden die Beschichtungsparameter wie Tauchzeit, Badtemperatur und Legierungszusammensetzung für das Doppeltauchverfahren optimiert. Parallel dazu wurden auch bestehende Zinkdiffusionsproben untersucht und mit dem Doppeltauchverfahren (DDZ) verglichen.

Das DDZ für Zink erwies sich als vielversprechend, wenn eine Tauchzeit von 5 Minuten für beide Tauchvorgänge verwendet wurde. Im Gefüge bildete sich anschliessend zum Stahlsubstrat eine aluminium- und eisenreiche ternäre Zinkphase aus. Es wurde ein zunehmender Zinkgehalt im äußeren oberen Bereich der Beschichtung festgestellt, der im Test einen geeigneten Korrosionsschutz bot. Bei den Verbindungsstücken, die im Rahmen des Projekts auf ihre Korrosionseigenschaften geprüft wurden, schnitten die zinkdiffusionsbeschichteten Proben und die mechanisch beschichteten Referenzproben am besten ab.

Die approbierte gedruckte Originalversion dieser Diplomarbeit ist an der TU Wien Bibliothek verfügbar
The approved original version of this thesis is available in print at TU Wien Bibliothek.



Foreword

Acknowledgement

After a long journey I am prepared to finish my studies in Technical Chemistry with this thesis.

I am thankful for all the support I got at TU Vienna, especially for the freedom of choices I was given during my master's degree. I was always guided when help was needed, and knowledge transfer was easy and open.

For the conduction of the thesis, I would like to thank Ao. Univ. Prof. Dipl.-Ing. Dr. techn. Paul Linhardt, Head of the research group Corrosion at TU Vienna. He was always understanding and supportive, adapted to my needs and his social and communication skills are on point. He was always reachable, if I had any questions and his patience and trust in me added to my motivation to strive for excellent work.

The thesis wouldn't have been possible without Dr. Alexander Tomandl, Expert of Corrosion at Hilti AG. I want to thank him for being flexible and open to new ideas and that he made this arrangement possible. He supported me on a professional level, and I appreciated the guidance and inputs he gave me along the way. A special thanks goes to the CR&T team members who were always very helpful and inspiring.

I would like to thank Hilti AG in Schaan, Liechtenstein for financing my research work and the well-equipped work environment I was able to use for my investigations.

Along the way, I learned a lot about myself and grew tremendously as a person. It marks an end of an era for me personally and a huge milestone in my life.

I love to thank my partner David and my family, who not only carried the mental weight with me in the hard times of my journey but where there to celebrate my victories as well.

I am happy you were loving, forgiving and patient during all those years.

This work is dedicated to my partner David and my family.

I love you with all my heart.

Die approbierte gedruckte Originalversion dieser Diplomarbeit ist an der TU Wien Bibliothek verfügbar
The approved original version of this thesis is available in print at TU Wien Bibliothek.



1 Table of Contents

Abstract.....	4
Kurzfassung	6
Foreword.....	8
1 Table of Contents.....	10
2 Introduction	13
3 Theory.....	14
3.1 Atmospheric corrosion of zinc coated steel	14
3.1.1 Steel.....	14
3.1.2 Zinc.....	14
3.1.3 Atmospheric corrosion of zinc	14
3.2 Effect of Al and Mg as alloying components in coating technologies	16
3.2.1 Al	16
3.2.2 Mg.....	16
3.2.3 Al and Mg alloys.....	16
3.3 Coating Technologies.....	17
3.3.1 Continuous steel sheet hot dip galvanizing “pre-galv”	17
3.3.2 Batch hot dip galvanizing “HDG”	18
3.3.3 Single Dip Zinc Project Findings.....	18
3.3.4 Double Dip HDG Process.....	18
3.3.5 Zinc Diffusion Coating (Sherardizing)	19
3.3.6 Mechanical Plating (Multilayer Coating, Duplex Coating System).....	19
3.4 Phase diagrams and microstructure properties	20
3.4.1 Properties of the Fe-Zn System.....	20
3.4.2 Properties of the Fe-Zn-Al System	23
4 Experimental methods.....	25
4.1 Metallography.....	25
4.2 SEM	25
4.3 Corrosion tests	26
4.3.1 ISO 9227 Neutral Salt Spray Test	26
4.3.2 ISO 16701 Cyclic Corrosion Test	26
4.3.3 Condensation Water Test Climate DIN 50017	27
4.3.4 Electrochemical Measurements	28
4.4 Sample overview.....	29
5 Overview of investigations.....	30
5.1 Double Dip Zinc WP1.....	30
5.2 Double Dip Zinc WP2.....	33
5.3 Zinc Diffusion Coatings	34

5.4	Multilayer Coating	35
6	Results	36
6.5	Double Dip Zinc Coatings WP1	36
6.5.1	Photographs of DDZ WP1	36
6.5.2	Cross sections LOM images of DDZ WP1	39
6.5.3	Coating thickness measurements of DDZ WP1	45
6.5.4	SEM images and EDX mapping of DDZ WP1	46
6.6	Double Dip Zinc WP2	55
6.6.1	Photographs of DDZ WP2	55
6.6.2	Cross sections LOM images of DDZ WP2	56
6.6.3	Coating thickness measurements of DDZ WP2	58
6.6.4	SEM images and EDX mapping of DDZ WP2	59
6.6.5	Accelerated corrosion: Photographs of DDZ WP2	62
6.6.6	Accelerated corrosion: LOM of DDZ WP2	64
6.6.7	Electrochemistry measurements of DDZ WP2	65
6.7	Zinc Diffusion Coatings	66
6.7.1	Photographs of Zinc Diffusion samples	66
6.7.2	Cross sections LOM images of Zinc Diffusion coatings	67
6.7.3	SEM images of Zinc Diffusion Coatings	69
6.7.4	Accelerated corrosion: Photographs of Zinc Diffusion Coatings	70
6.7.5	Accelerated corrosion: LOM of Zinc Diffusion Coatings	72
6.7.6	Electrochemistry of Zinc Diffusion Coatings	73
6.8	Multilayer Zinc Coating	75
6.8.1	Photographs of Multilayer Zinc Coatings	75
6.8.2	Cross sections LOM images of Multilayer Zinc Coatings	76
6.8.3	Accelerated corrosion: Photographs of Multilayer Zinc Coatings	77
7	Discussion	79
7.1	Double Dip Zinc WP1	79
7.1.1	Sandelin samples	79
7.1.2	MM standard construction steel samples	80
7.2	Double Dip Zinc WP2	82
7.3	Zinc Diffusion Coatings	83
7.3.1	ZAD Coating	83
7.3.2	ZND Coating	84
7.4	Multilayer Coatings	84
7.5	Comparison	85
8	Conclusion	86
8.1	Single- and Double Dip Zinc coatings: plain specimen	86
8.1.1	Sandelin samples	86
8.1.2	Standard construction steel samples	86

8.2	Double Dip Zinc on connectors	86
8.3	Zinc Diffusion Coatings on screws and connectors	86
8.4	Multilayer Zinc Coatings on screws and connectors	86
9	Outlook for the future.....	87
10	Acronyms.....	88
11	Table of Pictures.....	89
12	Tables.....	90
13	Equations.....	91
14	References	92

2 Introduction

To enlarge the lifespan of a product it is crucial, that customers have trust in the long-term corrosion protection of steel products in general. But there is much more to it, as we live on an extraordinary planet where resources should be used wisely, we have a desire to follow a sustainable approach. To balance the interest of building homes for people while maintaining a world to live in for future generations, new methods for increasing the corrosion protection of the Hilti MT-installation system should be investigated.

The MT-System is a multi-duty strut channel and girder system used to install all kinds of pipe supports, ventilation ducts or cable trays in moderately corrosive environments. The MT-System not only consists of strut channels and girders, but there are also connectors, base plates and screws needed to mount it. For the corrosion protection of all different parts included in the system, Zn and Zn-alloy coatings are used. (1)

A standard method to apply such coatings is hot dip galvanizing (HDG). The process works either by dipping finished parts (batch HDG) or continuously immersing steel strip into a liquid zinc bath.

The continuously hot dip galvanization is suitable for long products like strut channels. In this case the steel strip for the strut channels gets coated before the roll forming step. Smaller parts like connectors are produced mainly by batch hot dip galvanizing. The screws and bolts in the system are currently coated with a multilayer coating.

To increase the lifetime of different parts of the system we have some possibilities: for the strut channels made from continuously coated steel an increase of the coating thickness and adding alloying elements like Al (or Mg) to the coating bath is the simplest way. However, for the connectors the thickness obtained by batch HDG is limited by the process itself.

Therefore, in this work two coating processes are to be evaluated in detail to increase the corrosion protection of the connector parts: the double dip HDG process and the zinc diffusion process.

The double dip approach opposed to the standard batch HDG process adds a second dip step into a suitable Zn-alloy bath after the first standard zinc dip step. In the zinc diffusion process fine powder containing zinc and other additives are put together with the parts in an airtight container. Heat is introduced and through thermal diffusion the zinc finds its way into the metal substrate and an intermetallic layer is formed.

The main objective of this work is a comparison of the double dip zinc coatings to the zinc diffusion coatings, the single dip zinc coatings and the multilayer zinc coatings in the microstructure and its corrosion properties to ensure a homogeneous corrosion protection for all parts of the MT-System.

The coated samples are investigated with metallographic analytics including SEM and EDX, standard electrochemical methods and accelerated lab corrosion tests. Based on the results plating parameters like dipping time, bath temperature and alloy composition for the double dip approach should be optimized. Parallel to that, existing zinc diffusion samples, are to be investigated equally and compared to the double dip zinc approach. For an overall system comparison, the multilayer coating and the single dipped samples are also included. The investigation of the properties is done on test plates and Hilti-parts with different geometries.

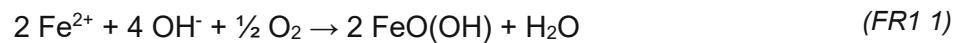
3 Theory

3.1 Atmospheric corrosion of zinc coated steel

3.1.1 Steel

The main component of steel is iron (Fe). It is a very commonly occurring transition metal of the VIII. group in the periodic table of elements and it is the technically most important heavy metal. Steel is iron with up to 1.7 % carbon and commonly other alloying elements for example Si, Mn, Cr, Al, N, Nb, S, Ti, V or W. (2) (3)

Iron appears as silver-white metal and has a density of 7.873 g/cm³. The melting point of iron is 1535 °C. In air, iron is forming a thin protective oxide layer and it is not affected by concentrated sulfuric acid or nitric acid. Whereas in humid, carbon dioxide rich air, or in carbon dioxide or air rich water, iron forms mainly FeO(OH) (FR1 1) and other oxide-rich and hydroxide-rich components known as red rust. Depending on the atmospheric corrosion constituents the corrosion products can contain carbonates, sulphates, and chlorides as well. (3)



This process is widely known and a common problem for the construction industry.

3.1.2 Zinc

Zinc is an element of the second transition metal group of the periodic table of elements. In nature it is found most likely as ZnS (in cubic form as "Sphalerit" or in hexagonal form as "Wurzit"). Furthermore, it is found often as Oxosalt and as ZnCO₃. (2) (3)

The physical appearance of zinc is described as blueish-silvery shiny metal with a density of 7.140 g/cm³. At room temperature zinc is brittle and it softens from a temperature of 100 – 150 °C, so it can be rolled out to a thin metal sheet or drawn to a wire. Above 200 °C it gets brittle again and the melting point lies at 419,6 °C. (3)

For the chemical properties of zinc, it is important that zinc is stable in air, because a colourless protective layer forms based on an oxide- and alkaline carbonate or sulphate layer. Due to that, it is widely used as a protective coating layer for steel substrates. The electrochemical series marks a standard reduction potential of zinc with $\epsilon_0 = -0.7626 \text{ V vs SHE}$ (Standard hydrogen electrode), so it offers sacrificial protection regarding the steel substrate. The various corrosion products forming from zinc on a steel substrate are called white rust. (3)

3.1.3 Atmospheric corrosion of zinc

Steel on itself is a metal with a high corrosion rate. Traditionally, a zinc coating on a steel substrate is used to protect the substrate by building a stable barrier layer and by galvanic action. (4)

Under standard conditions, both reactions, the anodic and the cathodic reactions (AR1 2), (KR1 3), (KR2 4) and (KR3 5) are happening at the same time in different neighbouring positions on the surface. (2)

In the anodic oxidation as in (AR1 2), metallic zinc is forming zinc ions.



For the cathodic reduction the reactions are happening as indicated in (KR1 3), (KR2 4) and (KR3 5).



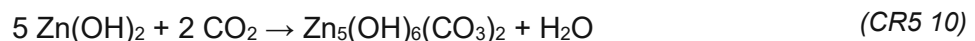
Under acidic conditions the cathodic reaction (KR1 3) is dominating and the main reaction is a formation of H₂. In standard, neutral conditions in water the (KR2 4) reaction is dominant. In oxygen deprived water the (KR3 5) reaction is dominant. (2)

In far less than a second, after fresh preparation of a zinc sample, an oxide layer consisting of ZnO is formed on specimen surfaces when exposed to air. If the atmosphere appears to be humidified or wet, a zinc hydroxide layer (Zn(OH)₂) forms rapidly according to the (CR1 6) reaction. After the zinc hydroxide is formed, water is released, and the zinc oxide forms according to (CR2 7). (2)

This layer varies upon alkaline or acidic conditions. (5)

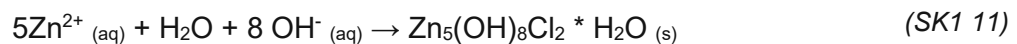


A special property of zinc oxide as well as of zinc hydroxide is their amphoteric character, so they dissolve in acidic (CR3 8) and in alkaline (CR4 9) conditions. (2)



In the atmosphere and in pH-neutral water, the zinc hydroxide is forming a basic zinc carbonate (CR5 10), resembling the naturally occurring mineral hydrozincite leading to a protective layer. (2)

In chloride rich atmosphere, the formation of simonkolleite is the most prominent reaction. It is proposed that zinc ions, hydroxide ions and chloride ions lead to the formation according to (SK1 11). (6)



The scheme is not fully resembling the real formation mechanism, which is proposed to be via hydrated zinc oxide on the surface of the zinc coating forming simonkolleite after an interaction with the chloride ion. Small amounts of iron are found to stabilize simonkolleite. (6)

The reaction is predicted to slow down after some time. When HCO₃²⁻ is present in the electrolyte, hydrozincite Zn₅(OH)₆(CO₃)₂ is also formed. (6)

3.2 Effect of Al and Mg as alloying components in coating technologies

To increase the protection of the steel substrate even further, alloying components like Al and Mg can be introduced to the zinc coating.

3.2.1 Al

Cathodic protection of the steel substrate is found in all atmospheres in zinc and zinc-rich aluminium alloys.

Small amounts (0.001%) of aluminium protect the zinc melt from oxidation through air by forming a small Al_2O_3 -layer on the zinc bath. Furthermore, with increasing Al content, on the barrier between steel and zinc a well adhering aluminium rich Al_5Fe_2 layer is forming. Aluminium addition enhances the visual appearance of the samples as they appear shinier. Due to its ductility properties, Al helps to insert bending strength properties. (2)

On the negative side, too much aluminium can lead to uncoated “black” spots on the coated substrates. (2)

Zn-Al-coatings are estimated to triple the corrosion protection compared to coatings with Zn alone. (7)

3.2.2 Mg

When Mg is added to the zinc bath, without any Al, the Mg reacts quickly with oxygen and the formation of dross at the zinc bath leads to very low product quality. However, this is prevented by addition of small quantities of aluminium. It is found, that by adding Mg to the zinc coating, a higher microhardness is measured opposed to the standard Zn coating. (8)

As for the microstructure, when adding Mg to the bath, the Zn grain size was found to be refined and the eutectic areas near Zn grain boundaries increased when the Mg content was increased. (8)

An $\text{Al}_5\text{Fe}_2\text{Zn}_{0.4}$ inner layer is formed, while on the outer layer zinc grains surrounded by a Zn-Mg eutectic is formed. Usually, this eutectic is Zn_2Mg and is more active than pure Zn, causing preferential corrosion. (8)

3.2.3 Al and Mg alloys

When aluminum is present as well, also ternary eutectics are formed, including zinc lamellas alternating with Zn_2Mg layers and Al “rings” in the Zn_2Mg phases (*Figure 1*). The inner layer containing Al is found to have an increased microhardness, and the outer layer is used to increase the corrosion resistance properties. It is believed, that the improvement of the corrosion resistance with Mg^{2+} is due to the formation of the protective corrosion products simonkellite ($=\text{Zn}_5(\text{OH})_8\text{Cl}_2 \cdot \text{H}_2\text{O}$) and zinc hydroxysulfate ($\text{Zn}_4(\text{OH})_6\text{SO}_4 \cdot \text{H}_2\text{O}$). The stabilizing effect could be due to pH buffering or to consumption of excess anions instead of their transformation into soluble and therefore less stable hydroxides, carbonates, or sulfides. (9) (10)

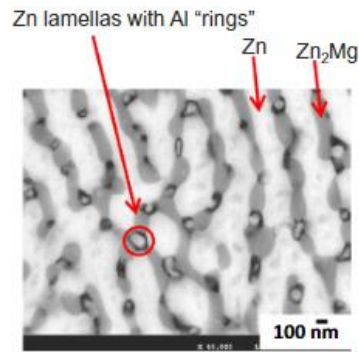


Figure 1 Microstructure of ZnAlMg cross section (9)

3.3 Coating Technologies

The current technologies used to apply coatings for Hilti products are continuous steel sheet hot dip galvanizing referred to as “pre-galv” and batch hot dip galvanizing referred to as “HDG”.

In addition to that, the sherardizing process, and multilayer coatings are used mainly for screw bolts and connectors. (9)

3.3.1 Continuous steel sheet hot dip galvanizing “pre-galv”

For the pre-galv method steel sheet coil is passed continuously at a speed up to 200 m/min through different baths and rolled back up in a coated coil after processing (Figure 2). First, the steel sheet is passing various cleaning (degreasing) baths with rinsing baths to get a clean surface for the following zinc plating step. (11) (12) (13)

Afterwards, the steel sheet is passed through an oven with a burning-, oxidation- and reduction-zone to be subject to fulfil the annealing because all oxides were removed. This is conducted by heating up a steel sheet to 450 - 500°C. Afterwards, the sheet is dipped in a molten zinc bath. Air knives or rollers allow a variation of the coating thickness and a smooth surface finish. The freshly coated endless sheet is cooled down before being recoiled. (13) (11)

A special form of the process is called “galvannealing”, referring to the words “galvanizing and annealing”. For galvannealing a heat step is included after the dipping step, where the zinc is annealed to the steel substrate due to diffusion forming an Zn/Fe coating. (13)

The endless coated sheet can be cold formed and stamped afterwards according to the product specifications. (13) (11)

This process is mainly used to manufacture Hilti strut channels and girders.

A coating containing Al and Mg (up to 8% in total) “ZM 310” (310 g/m² with 25µm) is currently used. Coating weights up to ZM1000 can be produced.

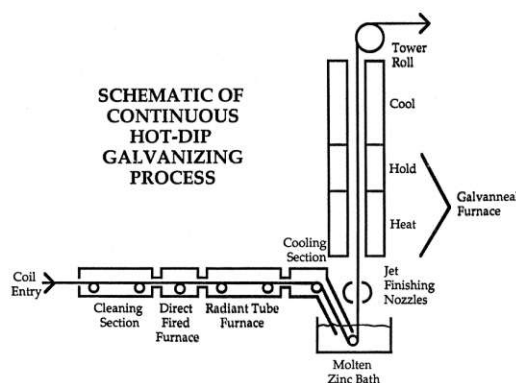


Figure 2 Process schematic of continuous hot dip galvanizing (12)

3.3.2 Batch hot dip galvanizing “HDG”

The major difference of this process in comparison to the continuous process is, that the steel is not continuously rolled from a coil and formed after coating, also the oven procedure is not included. For the HDG process already finished parts are used, where no forming steps after coating are needed.

The process again consists of several steps (*Figure 3*). Cleaning, degreasing, and rinsing with water, pickling (HCl or H₂SO₄) and rinsing again in flowing water are widely accepted process steps.

After that, the parts are dipped in the flux bath, which are typically salt solutions.

They are dried in an oven at about 60 – 120 °C for up to five minutes. The dry fluxed products are immersed into a hot zinc bath (440 – 460 °C) for a duration of 1 - 10 minutes. The immersion time is varied to gain different thicknesses.

For this process DIN EN ISO 1461 requires a minimum coating thickness of 45 µm for parts with a minimum of 2 mm steel thickness. Sometimes the parts are centrifuged to get rid of excess zinc in the thread of screws after dipping. After the process the parts are cooled in a controlled way to prevent further alloying. (13) (11) (12)

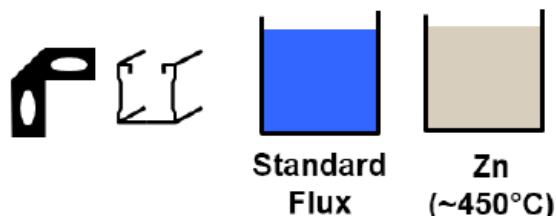


Figure 3 Process schematic of single dip batch hot dip galvanizing (Source: Hilti internal)

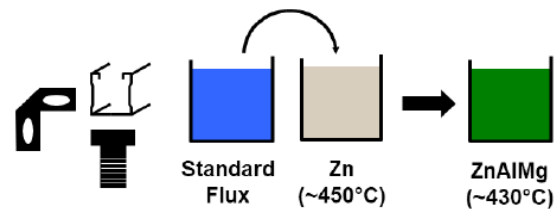


Figure 4 Process schematic of double dip batch hot dip galvanizing (Source: Hilti internal)

One zinc dipping bath is used for this process (*Figure 3*), it is also called the single dip method in the thesis.

3.3.3 Single Dip Zinc Project Findings

This thesis should investigate the double dip method, where the first dip step is carried out with pure zinc or technical zinc and the second step with a zinc alloy bath (using Al or Mg alloys). (14)

Findings from a previous Hilti internal single dip (*Figure 3*) project (15) were, that outdoor exposure tests indicated an improvement factor > 5 for the quenched ZnAlMg alloy compared to a simple Zn coating. Therefore, a reduction to 1/5 of the coating layer thickness when using ZnAlMg is found to lead to a comparable substrate protection. Furthermore, ZnAl and ZnAlMg single dip coatings were found to be even more corrosion resistant using wet paint and flake coatings on top. While on the alloyed zinc coated samples, these wet paint or flake coatings showed better adhesion, than on pure zinc coatings.

But all in all, the coating quality was not feasible in a single dip approach and a quick white rust appearance after exposure to accelerated corrosion tests was found. It is proposed that the new double dip method should fix the issue while providing a long-lasting corrosion resistance. (15)

3.3.4 Double Dip HDG Process

In the process described under 3.3.2 the samples are immersed once in a metallic bath. With the double-dip approach (referred to as DDZ in this thesis), samples are immersed in two different baths (*Figure 4*) with an additional cooling-step in between the dipping steps. The first dip step for the double dipped samples in this thesis is a pure zinc or technical zinc bath and the second dip step is a zinc alloy bath containing Zn/Al. (15)

3.3.5 Zinc Diffusion Coating (Sherardizing)

Sherardizing is a zinc diffusion coating process named after Sherard Osborn Cowper-Coles (1866-1936). It is also referred to as vapor galvanizing or dry galvanizing. (16)

Before sherardizing, there is a pre-treatment step so that the coating will attach accordingly. This includes, if needed: pickling, degreasing or shot blasting. The pre-treatment differs: for example, if the parts were rusty, they are shot-blasted beforehand while machined parts only need degreasing in alkaline baths. (16)

The sherardizing process is conducted by heating up steel parts to 300 – 500 °C which are inserted afterwards in a sealed rotating drum, containing zinc dust and inert fillers (e.g., sand). The process is normally carried out below the melting point of zinc (419°C). In the oven, there is nitrogen atmosphere present to prevent oxidation of specimen by exposure to air. The low partial pressure of zinc allows sufficient coating only if the zinc vapor is in close contact with the iron substrate material. The sherardizing furnace is rotated, so an even coating for all parts is obtainable. The inert fillers (e.g., aluminium oxides) prevent the formation of zinc droplets and work as a cushion, so the parts are not damaged during rotation. After the zinc transfer and deposition step, the chemical diffusion transfers the coating into a solid-state form. The zinc powder diffuses into the steel substrate building a gradient rich of iron on the substrate side of the coating and rich of zinc near the surface. (16)

After the process is completed, the furnace is cooled down and remaining zinc and fillers are recycled. A matte finish is typical for sherardized diffusion coatings. A passivation step where mostly a diluted phosphate acid bath is used to get rid of loose zinc powder on the surface follows. It is recommended to prevent the formation of zinc-oxides or other harmful zinc salts prematurely on the surface while the parts are stored on stock. Commonly, a paint layer can be applied as well. (16)

The sherardizing process is known for its high coating hardness characteristics. It is assumed, that the process induces a high number of defects which leads to the hardness of the coating. However, it is assumed that also the densities of the growing phases and the substrate don't match so coatings with thicknesses > 80 µm are brittle. (16)

3.3.6 Mechanical Plating (Multilayer Coating, Duplex Coating System)

Small parts are tumbled in a drum, where zinc and chemicals are present. For this method, only smaller parts (max. dimensions: 20 - 30 cm and 0.5 kg) are suitable. These parts are cleaned and typically copper coated before they are loaded into the plating barrel. In the plating barrel, the chemicals, small glass beads and zinc powder are present and during tumbling, zinc powder is compacted and adhered to the parts by the glass beads. The process is conducted without the use of electric current or applied heat. The finished parts can be post-treated with a passivation film, dried, and packaged. (17) (18)

After mechanical plating, the coating is often combined with a painting layer, this is referred to as multilayer or duplex coating in this thesis.

For the duplex coating, an additional organic coating layer is applied to the zinc metal coating. It helps enhancing properties like wear resistance, optical appearance (e.g., when adding colour) or corrosion protection. It is estimated that the additional step increases the service life by a factor up to 2.5. Mostly a chemically resistant epoxide resin is used when density is to be increased, as it evens out the surface layer. Also, polyester, or polyurethane based coatings are used in the industry. (19)

The microstructure of a mechanical plated sample is found in the literature, a scheme is shown in *Figure 5*. (20)

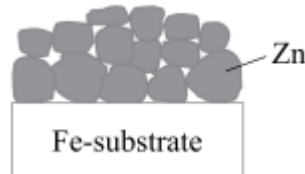


Figure 5 Microstructure example of mechanically plated sample cross section (20)

3.4 Phase diagrams and microstructure properties

3.4.1 Properties of the Fe-Zn System

The basics of the galvanizing processes is the reaction between zinc and iron (in steel). Intermetallic phases are formed through diffusion of both reaction partners. The thermodynamics of the reaction is shown in the phase diagram, the kinetic aspect is obtained by variation of temperature and zinc exposure times. (2)

In Figure 6 a widely accepted Fe-Zn-system from the year 2000 is shown, it has been modified several times as the first presentation of the diagram was in 1938. Detailed information regarding the zinc-rich part of the diagram is shown in Figure 7. (12)

Recently this was evaluated further and process differences regarding the diffusion couple method and the alloying method were found to be alternating the phase diagram. The according phase diagrams from 2021 are shown in Figure 8 and Figure 9. The δ -phase was considered a single phase for a long time, but recent studies have shown, that there are two. In this thesis, only one δ -phase will be discussed regardless, as the theory is not generally accepted yet. (12) (20) (21)

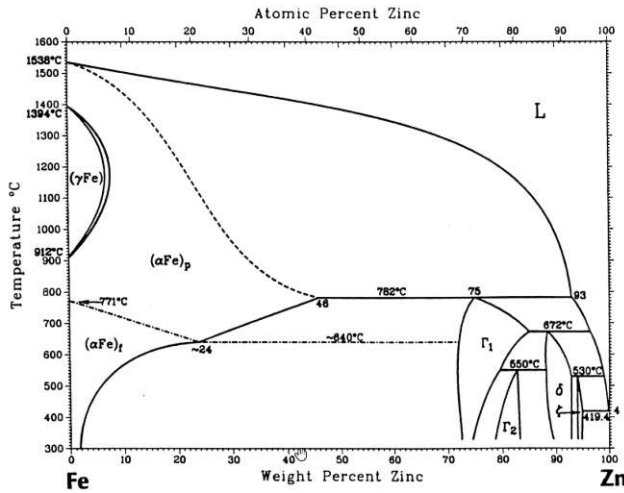


Figure 6 Phase diagram of Fe-Zn-system (12)

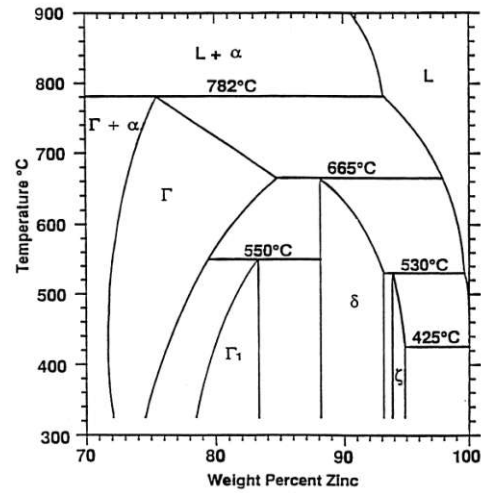


Figure 7 Phase diagram of Fe-Zn system (Zn-rich region) (12)

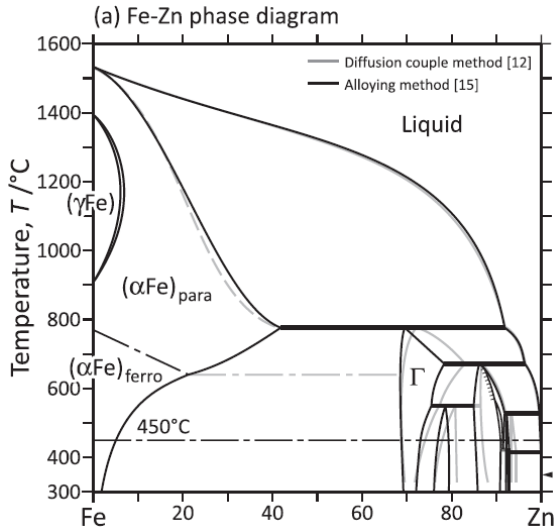


Figure 8 Phase diagram 2021 of Fe/Zn phase diagram including differences regarding method (21)

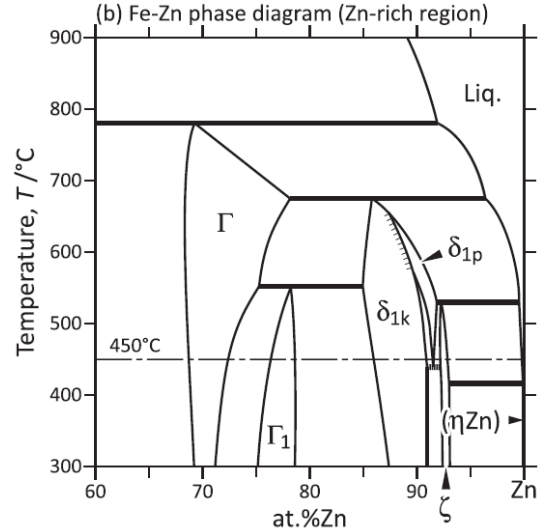


Figure 9 Phase diagram 2021 of Fe-Zn system (Zn-rich region) differences regarding method (21)

The phases shown in Figure 7 are described in Table 1.

Table 1 Phases of Fe/Zn phase diagram (2)

Phases	Formula	Iron (%)	Chrystal structure	Microhardness HV
α-iron	Fe	100	BCC	115 (construction steel)
Γ-phase	Fe ₃ Zn ₁₀	25-28	BCC	
Γ ₁ -phase	Fe ₅ Zn ₂₁	17-21	FCC	> 350
δ-phase	FeZn ₇ -FeZn ₁₀	7 - 12	Hexagonal	> 250
ζ-phase	FeZn ₁₃	6 - 6.2	Monoclitic	100 - 120
η-zinc	Zn (Fe)	0.08	HCP	50 - 60

(2) (20)

However, in even more recent literature from 2019 and 2021, also other phase diagrams are accepted. They state that the Γ-phase is made of cubic Fe₃Zn₁₀ and that the Γ₁-phase consists of Fe₁₁Zn₄₀. (6) (21)

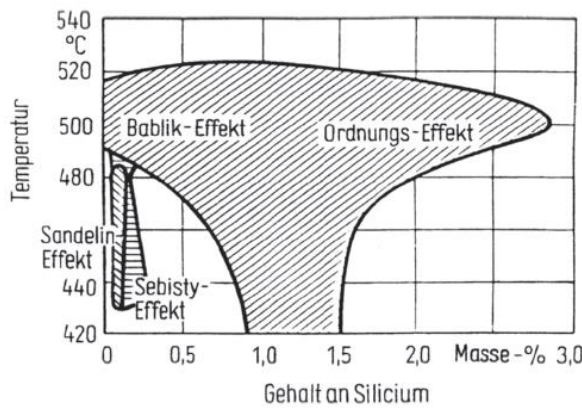


Figure 10 Influence of Si content in steel with temperature (2)

For zinc coatings in general, differences in appearance (*Figure 11* and *Figure 12*) and microstructure (*Figure 13* and *Figure 14*) are known when the steel substrate varies in Si-content. As this thesis is investigating different substrates, it is necessary to describe the effects.

The steel substrates in the Sandelin region (*Figure 10*) characteristically resemble the Si-content in a range of >0.04 wt% Si to < 0.14 wt% Si. The Sebisty – effect is proposed in a Si range from 0.12 wt% - 0.28 wt%. (2)

In the zinc-coatings a different coating growth was found at a bath temperature of $450 - 470$ °C. For adding Si to the steel substrate a linear coating growth rate is proposed in the Sandelin region (*Figure 15*), whereas in the Sebisty region a parabolic (inhibited) coating thickness growth was proposed. (2)

In the literature, for the cross section of the steel samples in the Sandelin region (*Figure 13*), the structure shows small, hardzinc crystals (ζ -phase) which are embedded in a solidified zinc melt (η -zinc). The δ -phase is hardly visibly formed. The strips vertically grown starting from the substrate show the growth direction. (2)

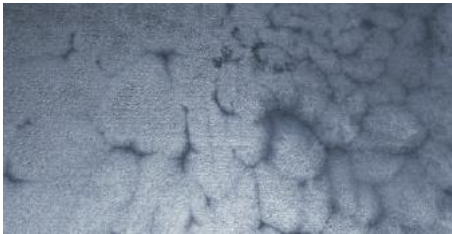


Figure 11 Visual appearance or top view of Sandelin steel zinc coated surface after surface photography (22)



Figure 12 Visual appearance or top view of Sebisty steel zinc coated surface after surface photography (22)

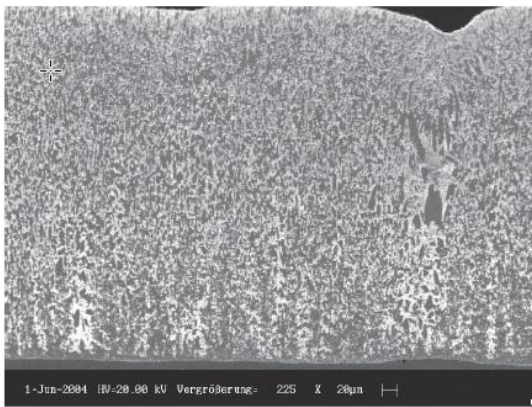


Figure 13 Cross section of zinc coated Sandelin-steel, 460°C, 10 Minutes REM (2)

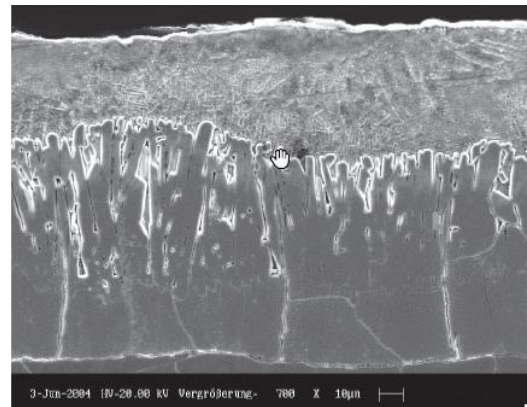


Figure 14 Cross section of zinc coating on Sebisty-steel, 460°C, 10 Minutes, REM (2)

The layer growth kinetics (*Figure 15*) of the different phases is proposed to be different when varying the dipping time. Compared to the δ -phase which is proposed to keep slow growth properties over time, the ζ -phase grows noticeably over time. (23)

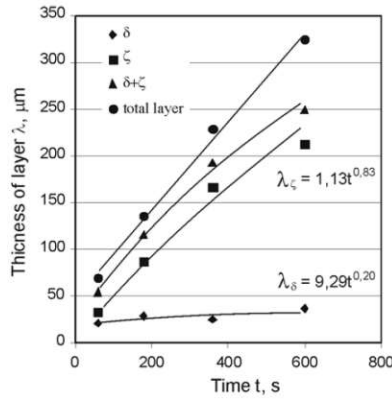


Figure 15 Growth kinetics of phases in Sandelin samples (23)

3.4.2 Properties of the Fe-Zn-Al System

The Fe/Zn and Fe/Al phase diagrams are needed to be considered regarding the double dip zinc process. With a high Al content (Fe/Al phase diagram), a very thin (15 – 20 μm) Fe-Al coating layer is formed near the substrate, which is proposed to be very stable. Furthermore, aluminium is increasing the surface tension of the zinc melt vastly. (2)

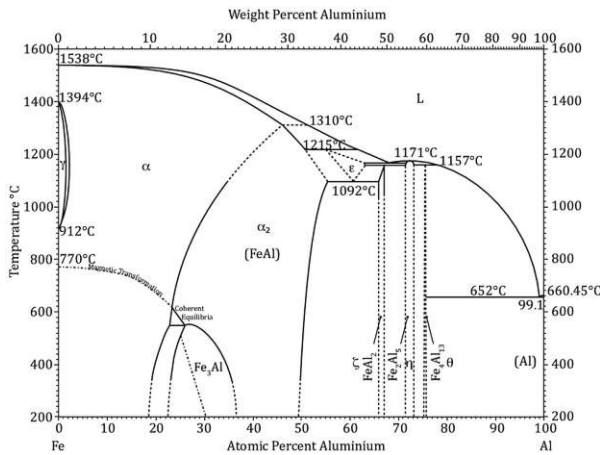


Figure 16 Phase diagram of the binary Fe/Al system (24)

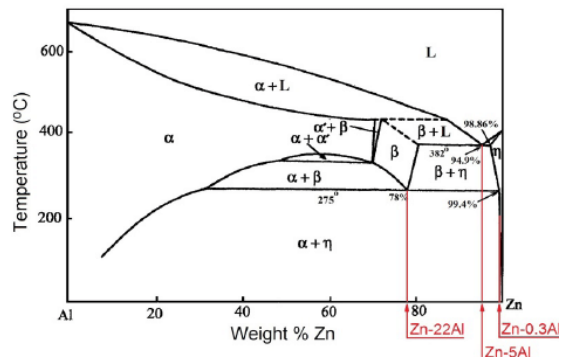


Figure 17 Phase diagram of the binary Al/Zn system (25)

The Fe/Al binary system (Figure 16) shows a Fe₂Al₅ phase called η-phase as the stable phase described above.

In the binary Al/Zn phase diagram (Figure 17) a eutectic mixture of 95 wt% Zn and 5 wt% Al is found. So, although pure Al has a melting point of 660 °C, with added zinc it forms an eutectic with a melting point of 381 °C. (26)

Double dip coatings are a young field of research, therefore not too many investigations can be found, and the influence of dipping times is not well known yet. However, Yraima Rico O. et al evaluated the mechanical properties of Zn/ZnAl double dipped coatings and provided a cross section image of a Zn/Zn-5%Al (= Galvan®) at 550 °C coated steel sheet sample. His samples showed a superficial finish which resembles continual coating quality without any roughness variations or uncoated spots. (27)

They found that the thickness of the coating increased when dipping time increased. The growth kinetics is estimated to be nonlinear after the first dip step (Zn), but after the second dip step the fast formation of the Fe-Al-Zn compounds increased the growth velocity and resulted in the large thicknesses they obtained in their experiments. The authors found a coating thickness between 450 - 650 μm after 60 - 120 s dipping time on steel plates (AISI

1020 steel, equals C22/C22E steel with of 0.1 - 0.40 wt% Si) with the dimensions of 100 mm x 38 mm x 3 mm. (27)

The zones in the microhardness tested cross section can be distinguished according to Yraima Rico O. et al (Figure 19). There are three hardness variations in the three described zones, whereas zone 1 is located closest to the steel substrate and zone 3 is the closest to the surface. Zone 1 consists mainly of the δ -phase and the pure zinc phase, significantly varying upon immersion time. Zone 2 shows the pure zinc phase appearing as a matrix, in which the δ -phase ($\text{FeZn}_{10}\text{Al}_x - \text{FeZn}_7\text{Al}_x$) and a Fe-Al-Zn micro-segregated ternary ($\text{Fe}_2\text{Al}_5\text{Zn}_x$)-phase with round morphology formed. Zone 3 consisted of the $\text{Fe}_2\text{Al}_5\text{Zn}_x$ compounds also in rounded morphology with a pure zinc phase present as well. (27)

The microhardness of zone 1 was found to be at about 254 HV, corresponding to the δ -phase ($\text{FeZn}_{10}\text{Al}_x - \text{FeZn}_7\text{Al}_x$). The pure zinc phase consists of 90HV in zone 1. The zone 2 had increased hardness values with a wide variation of 100 - 200 HV because of Fe-Al-Zn ternary layer in a hard δ -phase. Zone 3 had around 100HV, corresponding to $\text{Fe}_2\text{Al}_5\text{Zn}_x$ predicted in a pure zinc matrix, this is comparable to Galvan® coating hardness findings. This phase is also found in the ternary phase diagram (Figure 18, Figure 20). (27)

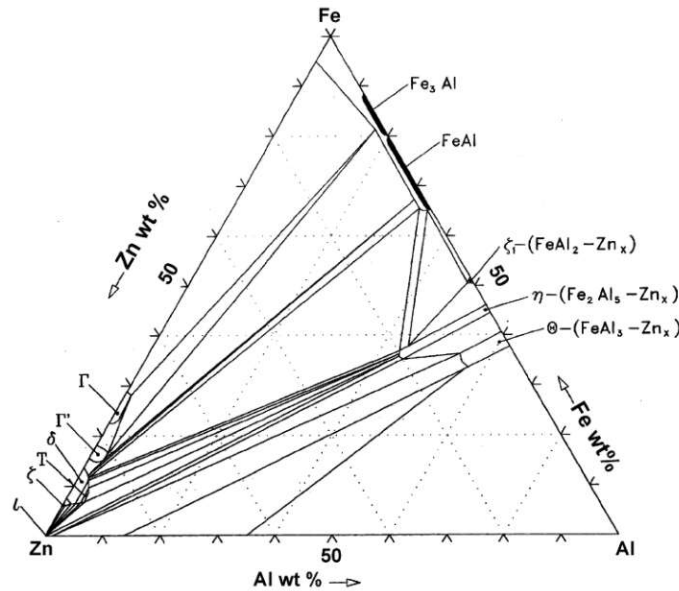


Figure 18 Ternary phase diagram Zn-Al-Fe system at 450°C (28)

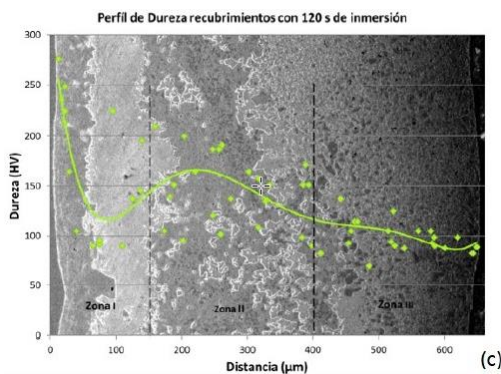


Figure 19 Microstructure of double dipped Zn/Zn-5Al sample, divided in three zones at 550°C, dipping time: 2 minutes (27)

Phase	Composition (at.%)
δ	FeZn_{10}
ζ	FeZn_{13}
Γ_1	$\text{Fe}_5\text{Zn}_{21}$
ρ	FeSi
ω	FeSi_2
θ	FeAl_3
η	Fe_2Al_5

Figure 20 Phases and compositions described from the ternary phase diagram Zn-Al-Fe (28)

4 Experimental methods

4.1 Metallography

The thin flat samples were cut with hydraulic sheet metal shears and water-cooled cutting machines ATM Brillant 250 with a 50A25 blade and an ATM Brillant 220 with a Struers 125 x 0.5 x 12.7 cm blade. For all samples the two cutting machines were used. The samples were placed in Ethanol in an ultrasonic bath for two minutes to get rid of chippings and other contamination and embedded in Opal 460 Polyfast after drying with a hairdryer.

The grinding and polishing steps were derived from the Struers suggestions and altered according to the availabilities in the lab, the steps are listed in *Table 2*. (29)

Table 2 Grinding and polishing routine

Step	Method/Machine	Time	Grit	Name	Force	Solution	Polishing agent
		min			N		
grind	Struers Labo Force 100	2	500	SiC grain size 30µm	25	water	none
clean	Rinsing	/	/	/	/	water	/
clean	Ultrasonic Bath	1	/	/	/	EtOH	/
polish	Struers Tegramin-25	3.5	9 µm	Struers MD Plan	25	Suspension blue	9 µm diamond suspension
clean	Rinsing	/	/	/	/	Water	/
clean	Ultrasonic Bath	1	/	/	/	EtOH	/
polish	Struers Tegramin-25	4.2	3 µm	Struers MD DAC	25	Suspension yellow	3 µm DP Suspension A
clean	Ultrasonic Bath	1	/	/	/	EtOH	/
polish	Struers Tegramin-25	4	1 µm	Struers MD Dur	20	Suspension yellow	1 µm DP Suspension A
clean	Ultrasonic Bath	1	/	/	/	EtOH	/

The polished samples were analysed with the light optical microscope (=LOM) and some samples of the ZN sample series were investigated in the SEM.

For the LOM pictures of the cross sections, a Leica DMRX or a Leica DM 6000 M microscope was used. The coating thickness was measured digitally, measuring the width of the cross sections of the LOM-images with the Imagic IMS software.

4.2 SEM

Before an SEM analysis was carried out, the samples were polished and inserted in a sample holder. For better connectivity a silver-strip was tapered on top of the sample connecting to the sample holder. All SEM measurements were conducted using a Zeiss Supra 40VP.

As for the microscope every measurement taken was using 15 keV, with a working distance close to 8.5 mm. The analysing detectors used were SE2 (= Secondary Electron) for surface analysis or AsB (Angle selective Backscatter). The AsB detector is utilized when in need of detecting low angle backscattered electrons. It is used in low-kV range to get a higher contrast image. For the mapping an EDX (Energy dispersive X-ray spectroscopy) was used. The suggested phases in the following chapters are theoretical proposals (= "Prop") or hypotheses according to information found in literature. The proposals are not proved in any way. (30)

4.3 Corrosion tests

The different measurement methods to acquire data regarding corrosion are explained in this section.

4.3.1 ISO 9227 Neutral Salt Spray Test

The neutral salt spray test (=NSST) is used to investigate the corrosion occurrences in an accelerated test to determine weak spots in the coatings. The test is suitable for comparative purposes.

The 5% NaCl solution is set at a pH between 6.5 - 7.2 with a 35 °C testing temperature.

The samples are placed on the grid of the chamber and are exposed to a continuous salt fog. An incline is to be established with a 15 - 25° angle. The ISO 9227 standard recommends a soft cleaning of the samples by rinsing with water and drying in air to get rid of spray solution residues. At Hilti, it is common practice to gently dry the samples with soaking up excess water using a paper tissue so white rust products stay on the samples.

For the evaluation of the results a visual inspection and photographical documentation was conducted. The test results are not representative for real life maritime applications due to the constant saline fog. (31)

4.3.2 ISO 16701 Cyclic Corrosion Test

Next to the continuous Neutral Salt Spray Test explained in 4.3.1 there is another relevant test called cyclic corrosion test (=CCT) representing real life corrosion occurrences under controlled climate conditions. The ISO 16701 test is an accelerated corrosion test to simulate atmospheric corrosion of material. The test solution contains 500 g NaCl in 20 l distilled water, with a pH of 4.2 +/- 0.1. The pH is set by adding around 50 ml of 0.025 M H₂SO₄. It is conducted in a climate chamber under monitored conditions typically for 12 weeks. The test works in continuously monitored cycles including dry phases and wet phases (*Figure 21, Figure 22*). The samples are placed with an inclined angle of 5 – 15 % without any overlaps on a single layer on the grid. At least every second week the samples were examined, and the results were documented visually via photography.

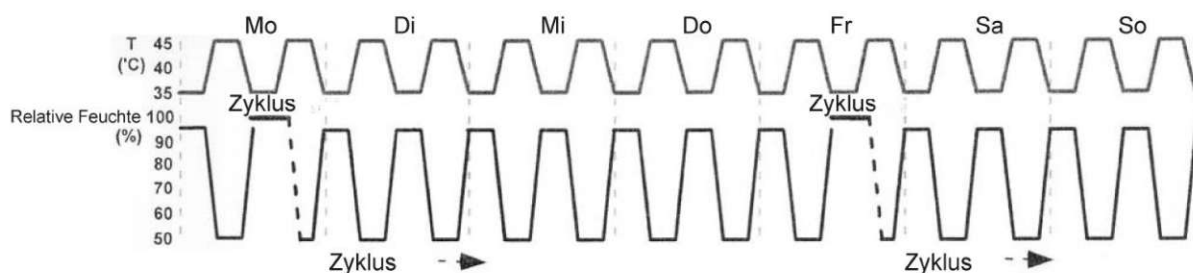


Figure 21 Full one-week cycle in CCT (32)

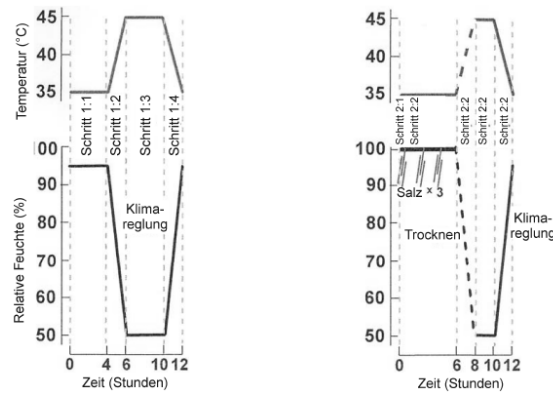


Figure 22 Spray of CCT with phase A (left) and phase B (right) (32)

The phase A (Figure 22, left cycle) is occurring multiple times a week as indicated in Figure 21. This phase of the cycle is alternating between a humidity of 50 % and a humidity of 95 % as well as altering temperatures between 35 °C and 45 °C. The changes are possible in a 2 h timeframe.

The phase B (Figure 22, right cycle) is occurring 2 times a week (marked with “Zyklus” and a humidity of 100% followed by a dashed line in Figure 21). The wet phase (humidity 100 %) of phase B has a duration of 15 minutes and sprays a 1 % NaCl solution with a pH of 4.2. It is followed by a 1 h 45 min standby period. This cycle is repeated 3 times and takes 6 h of time. After that, a dry phase completes the phase B cycle.

4.3.3 Condensation Water Test Climate DIN 50017

The condensation water test climate (=CWTC) is conducted according to DIN 50017. It is run in alternating climate cycles repeating after 24 hours in a distilled water environment. The chamber is built like indicated in Figure 23, including a thermometer, a relief valve and a floor pan where condensed water is accumulating. The samples are placed on a grid in the chamber and for the first 8 hours a constant temperature of 40 ± 3 °C and a humidity of 100 % are applied. After that, the next 16 hours the chamber is ventilated and cooled down to room temperature (18 – 28 °C). The circle repeats every 24 hours. (33)

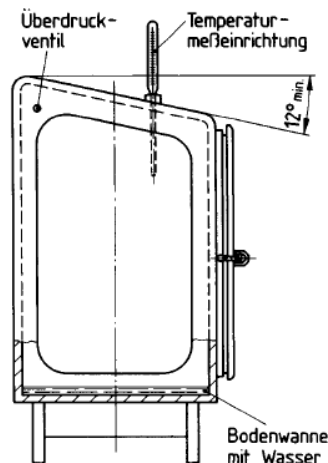


Figure 23 CWTC chamber DIN 50017 (33)

4.3.4 Electrochemical Measurements

The potentiodynamic electrochemistry measurements were conducted using a FlatCell produced by IPS. The sample is mounted to the device by being pressed against the electrolyte filled glass tank. There is a possibility to mount water or gas cooling to the glass container, but all measurements were conducted at room temperature. As electrolyte a 0.1 M NaCl solution was used. On the right side of *Figure 24*, or *Figure 25* or *Figure 26* the sample is placed, which is connected as the WE (=working electrode) to the potentiostat PGU-OEM-2A from IPS AJ/Elektroniklabor Schrems. The sample is exposed to the electrolyte with a 1.4 cm diameter circle, it is colored yellow in *Figure 26*. The CE (=counter electrode) is found on the left side of the scheme visible in *Figure 26*, made of platinum plated titanium and located inside the water tank. From the top, the reference electrode (=RE) a SE11NSK7 Ag/AgCl electrode from Xylem Analytics Sensortechnik Meinsberg (stored in a 3 M KCl solution) is mounted. The deviation of the potential of the RE to the SHE (= Standard Hydrogen Electrode) is +208 mV. (34) It is filled with a KCl electrolyte with a ceramic diaphragm. The electrode is made of glass and has a length of 155 mm and a diameter of 12/5 mm, it is suitable for applications from -5 °C to 80 °C. (35) (36)

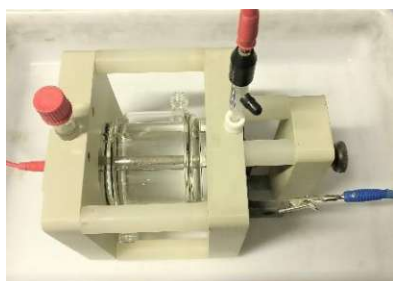


Figure 24 Overview of FlowCell buildup



Figure 25 Side view of FlowCell including flat sample

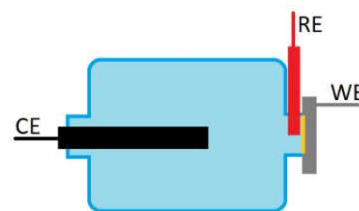


Figure 26 Explanatory image of FlowCell

The software used for documenting results was ECMWin from IPS Elektroniklabor Schrems. The programmed standard measurement used, was a OCP (open circuit potential) measurement with a duration of 2 hours first, followed by a measurement starting from a potential of -300 mV relative to the OCP to the first return point of 600 mV relative to the OCP, the second return was set to -300 mV relative to the OCP as well. For the OCP a scan rate of one measuring point per second was found to be reasonable. The polarization rate for the current density/potential curve was set to 0.2 mV/s. The polarization start was set relative to the OCP. These values were found to be suitable for zinc coating measurements in prior Hilti-projects. (36) (37)

In the end, two curves were obtained, the OCP curve shows potential over a 2 h timespan. The polarization curve shows current density over potential and is logarithmic on the current axis and shows the influence of the anodic and cathodic reaction. It is also used as a method for comparison. (36)

4.4 Sample overview

Basically, this work consists of the following work packages (WP) where various coating systems (*Table 3*) are applied on different parts or sample plates.

Table 3 Overview of work packages

Name	Description
DDZ WP1	Sample plates with different dimensions and compositions (Sandelin and low silicium) including coatings of ZN (= pure zinc bath) and DZ (technical zinc bath with usual impurities) single and double dipped (=DDZ) with various dipping times.
DDZ WP2	Hilti parts, double dipped in Zn/ZnAl
Zinc diffusion coatings	Zinc alloy diffusion and zinc nickel diffusion coatings on Hilti parts
Multilayer zinc coatings	Multilayer coatings consisting of mechanical plated coated and/or wet flake paint coatings on different Hilti samples

All parts of this work were analysed with different methods which are shown in *Table 4*.

The electrochemical measurements (= "ELCHEM") were conducted according to 4.3.4. And the Condensation Water Test Climate measurements (= "CWTC") were conducted as described under 4.3.3.

Table 4 Overview of analytic methods used for different coating technologies

	LOM CS	SEM	NSST	CCT	ELCHEM	CWTC
DDZ WP1	x	x	/	/	/	/
DDZ WP2	x	x	x	x	x	x
Zinc diffusion coatings	x	x	x	x	x	/
Multilayer zinc coatings	x	/	/	x	/	/

5 Overview of investigations

5.1 Double Dip Zinc WP1

The externally coated test plates (1500 x 1000 x 2 mm) were sorted, and photographs of all samples were documented, according to the overview provided in *Table 6*. The samples were named as seen in the overview. Single dipped (see 3.3.2) and double dipped (see 3.3.4) samples were examined. For the sample names, ZN equals a pure zinc bath and DZ means a technical zinc bath. If the ZN or DZ is followed by a time in minutes (e.g., 1m = one minute) which is given once when it is a single dip process or twice in a double dip process (e.g., 5m10m means the first dipping time was 5 minutes long followed by a 10-minute second dip). The description follows the FDS scheme (First Dip Second Dip). If there is only one time given, the samples are single dipped. In the double dipped samples, sometime the first dipping time varies, other times the second dip varies. SB stands for steel substrates in the Sandelin region, the MM samples are standard construction steel substrates. The acronym ab means the sample was quenched after Zn coating.

The steel composition of SB (=Steel in the Sandelin region) and MM samples (= Standard construction steel) of WP1 were investigated using OES (= Optical Emission Spectrometry), the results of the elements present in steel are shown in *Table 5*.

Table 5 OES analysis of steel substrate of MM and SB sample

Steel analysis	C %	Si %	Mn %	P %	S %	Cr %	Ni %
MM sample	0.025	<0.001	0.183	0.018	0.005	0.016	0.018
SB sample	0.073	0.076	1.000	0.030	0.003	0.418	0.036

Table 6 DDZ WP1 sample overview, shows dipping times in various baths, first bath with ZN or DZ and second dip ZnAl

DDZ WP1 samples		FDS	NB	FOTO	CUT	CS	LOM	SEM
Sandelin samples	ZN 1m - ZN 10m	1m	1	x	x	x	x	x
		2m	1		x	x	x	x
		5m	1		x	x	x	x
		10m	1		x	x	x	x
	DZ 1m - DZ 10m	1m	1	x	x	x	x	/
		2m	1		x	x	x	/
		5m	1		x	x	x	/
		10m	1		x	x	x	/
	ZN 1m1m – ZN 10m1m	1m1m	1	x	x	x	x	x
		2m1m	1		x	x	x	x
		5m1m	1		x	x	x	x
		10m1m	1		x	x	x	x
	DZ 1m1m - DZ 10m1m	1m1m	1	x	x	x	x	/
		2m1m	1		x	x	x	/
		5m1m	1		x	x	x	/
		10m1m	1		x	x	x	/

MM samples	ZN 5m1m - ZN 5m10m	5m1m	1	x	x	x	x	x
		5m2m	1		x	x	x	x
		5m5m	1		x	x	x	x
		5m10m	1		x	x	x	x
	DZ 5m1m - DZ 5m10m	5m1m	1	x	x	x	x	
		5m2m	1		x	x	x	
		5m5m	1		x	x	x	
		5m10m	1		x	x	x	
ZN 1m1m – ZN 10m1m	1m1m	1	x	x	x	x	x	
	2m1m	1		x	x	x	x	
	5m1m	1		x	x	x	x	
	10m1m	1		x	x	x	x	
ZN 1mab - ZN 10mab	1m ab	1	x	x	x	x		
	2m ab	1		x	x	x		
	5m ab	1		x	x	x		
	10m ab	1		x	x	x		
DZ 1m1m - DZ 10m1m	1m1m	1	x	x	x	x		
	2m1m	1		x	x	x		
	5m1m	1		x	x	x		
	10m1m	1		x	x	x		
DZ 1mab - DZ 10mab	1m ab	1	x	x	x	x		
	2m ab	1		x	x	x		
	5m ab	1		x	x	x		
	10m ab	1		x	x	x		
ZN 5m1m - ZN 5m10m	5m1m	2	x	x	x	x	x	
	5m2m	2		x	x	x	x	
	5m5m	2		x	x	x	x	
	5m10m	2		x	x	x	x	
DZ 5m1m - DZ 5m10m	5m1m	2	x	x	x	x		
	5m2m	2		x	x	x		
	5m5m	2		x	x	x		
	5m10m	2		x	x	x		
ZN 10m1m - ZN 10m10m	10m1m	2	x	x	x	x		
	10m2m	2		x	x	x		
	10m5m	2		x	x	x		
	10m10m	2		x	x	x		
DZ 10m1m - DZ 10m10m	10m1m	2	x	x	x	x		
	10m2m	2		x	x	x		
	10m5m	2		x	x	x		
	10m10m	2		x	x	x		

All samples were cut, as *Figure 27* and *Figure 28* indicate, 3 cm towards the lower edge in a 2 cm x 1 cm rectangular shape.



Figure 27 Cut location of Sandelin samples



Figure 28 Cut location of MM samples




5.2 Double Dip Zinc WP2

For this work package, the most promising coatings of WP1 were applied on actual Hilti parts.

After investigation of WP1, the likeliness for upscale ability was found to be the highest for the 5m5m samples in an industrial environment. As the dipping and removing of the bath is not possible in an instant and a dipping value of 5 minutes allows for a 4- to 6-minute dip process tolerance. The samples were inserted in a CCT and a NSST to visually inspect corrosion process and compare the results to the zinc diffusion coating and multilayer zinc samples. In addition to that, electrochemistry measurements at the starting point and after one week of water condensation test (=CWCT) were analyzed to compare them to the zinc diffusion coating sample electrochemistry results as well.

In the industrial environment the first and second dip can sometimes be weeks or even months apart. Also, previously galvanized samples from an different company can be second dipped by Hilti’s galvanizing partner. This is considered by investigation of the X-MZ samples. The “X“-terminology (Table 7) is used to describe an external coating partner. Also, in the minute terminology instead of a defined time (e.g., 5m), the term “Xm or XM” were used indicating an unknown first dip duration. The MZ stands for a special aluminum-containing coating with around 5% of Al used for the second dipping step. The other samples resemble the DZMZ coating, first dip with technical zinc and the second with the MZ (zinc-aluminum) coating.

Table 7 WP2 DDZ sample overview, on Hilti parts including three different samples, coated with the DZMZ or the X-MZ coating with various analytical methods

WP2 DDZ Samples			FOTO	CS	LOM	SEM	CCT	NSST	ELCH after CWTC
MT-C-GLP T		DZMZ 5m5m	5m5m-A	x	x	x	/	/	0w/1w
			5m5m-B	x	/	/	x	/	/
			5m5m-C	x	/	/	/	x	/
		X-MZ Xm5m	Xm5m-A	x	x	x	/	/	0w/1w
			Xm5m-B	x	/	/	x	/	/
			Xm5m-C	x	/	/	/	x	/
MT-B-02		DZMZ 5m5m	BT1	x	/	/	/	x	/
			BT2	x	/	/	/	x	/
			A	x	/	/	/	/	/
			B	x	/	/	x	/	/
			C	x	/	/	x	/	/
		DZ 5m	5m	x	/	/	x	/	/
MT-BR-40		DZMZ 5m5m	A	x	x	x	x	/	/
			B	x	x	x	x	/	/
		X-MZ Xm5m	A	x	x	x	x	/	/
			B	x	x	x	x	/	/

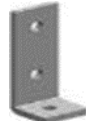


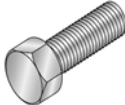

5.3 Zinc Diffusion Coatings

The diffusion coated samples (3.3.5) were actual parts of Hilti, opposed to the test plates from 5.1.

Two coating technologies have been investigated. The zinc alloy diffusion coating (ZAD) should contain slight amounts of Al and Mg, the zinc nickel diffusion coating (ZND) should contain amounts of Ni according to supplier information. More detailed information on the process was not available due to non-disclosure policy of the suppliers. *Table 8* provides an overview of the samples and the analytical investigation methods.

The number after the ZAD or ZND coating should resemble the nominal coating thickness in μm , indicated by the supplier.

Table 8 Overview Diffusion Coating samples

Product portfolio		ZAD coatings					ZND coating		
Product type and name		Picture	ZAD 60		ZAD 80	ZAD 30		ZND 60	
System Connector	MT-C-L2 OC		5x in ISO 16701		5x in ISO 16701	/		5x in ISO 16701	
System Connector	MT-C-T/1 OC		1x CS		1x CS	/		1x CS	
System Connection Mech	MT-TL M10 OC		5x in ISO 16701		/		5x in ISO 16701		5x in ISO 16701
System Connection Mech	MT-TLB OC		5x in ISO 16701	2x CS	/		5x in ISO 16701	2x CS	5x in ISO 16701 2x CS
Bracket	MT-BR-40 1000 OC		1x CS		1x CS	/		1x CS	

The preparation of the samples was conducted with the same routine as described under 4.1, except for the cutting, where no hydraulic sheet metal shears were used due to the geometry.

The system connector MT-C-L2 OC was also investigated with electrochemistry after different accelerated corrosion tests, an overview of the conducted measurements is to be seen in *Table 9*.

Table 9 Overview of ZAD and ZND coated samples after different exposure time (weeks) to accelerated corrosion tests (CCT & NSST) and the electrochemistry measurements thereafter

ZAD 60		FOTO	CUT	CS	LOM	SEM	ELCHEM
MT-C-L2 OC	CCT 0w	x	x	x	x	x	x
	CCT 7w	x	x	x	x		x
	CCT 12w	x	x	x	x		x
	NSST 12w	x	x	x	x		x
ZND 60		FOTO	CUT	CS	LOM	SEM	ELCHEM
MT-C-L2 OC	CCT 0w	x	x	x	x	x	x
	CCT 7w	x	x	x	x		x
	CCT 12w	x	x	x	x		x
	NSST 12w	x	x	x	x		x

5.4 Multilayer Coating

Furthermore, multilayer coatings, (coatings, consisting of at least two different coating layers) which are currently used for the screws of the MT-System were investigated for comparison reasons.




Three types of multilayer coatings have been investigated shown in Table 10.

Table 10 Overview of multilayer zinc coatings

	Base coating	Topcoat
MP+TC	Mechanically plated	Al/Zn flake topcoat
ZB+TC	Zinc flake basecoat	Al/Zn flake topcoat
ZAD+TC	Zn-alloy diffusion	Al/Zn flake topcoat

All the samples investigated with the proposed coatings are shown in Table 11.

Table 11 Overview Multilayer Coating samples

Product portfolio		Multilayer Coating						
Product type	Picture	MP+TC		ZB+TC		ZAD+ZT		
System Connection Mech	MT-TL M10 OC 	5x ISO 16701	1x CS	5x ISO 16701	1x CS	5x ISO 16701	1x CS	
System Connection Mech	MT-TLB OC 	5x ISO 16701		5x in ISO 16701		5x ISO 16701		
System Connection Mech	MT-TFB OC 	5x ISO 16701	1x CS	5x in ISO 16701	1x CS	5x ISO 16701	1x CS	

6 Results

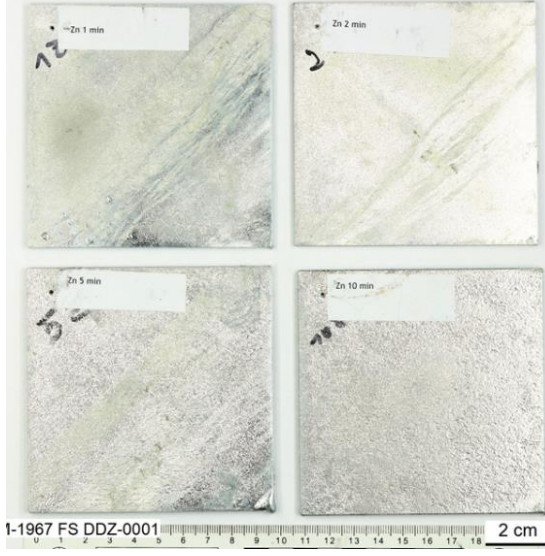
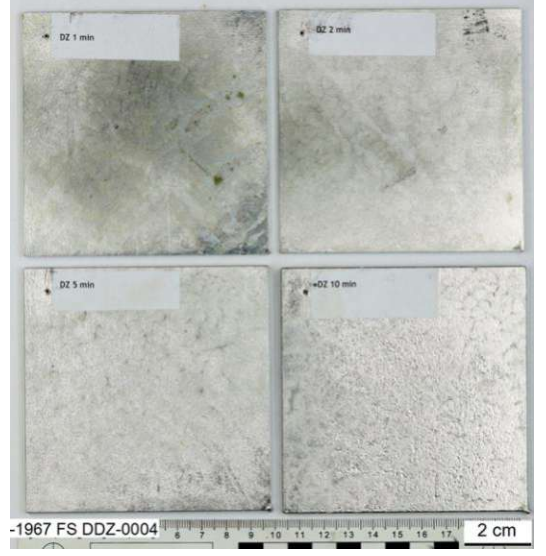
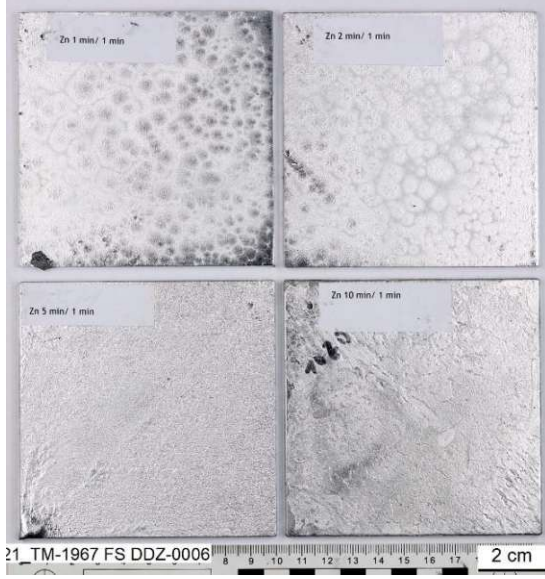
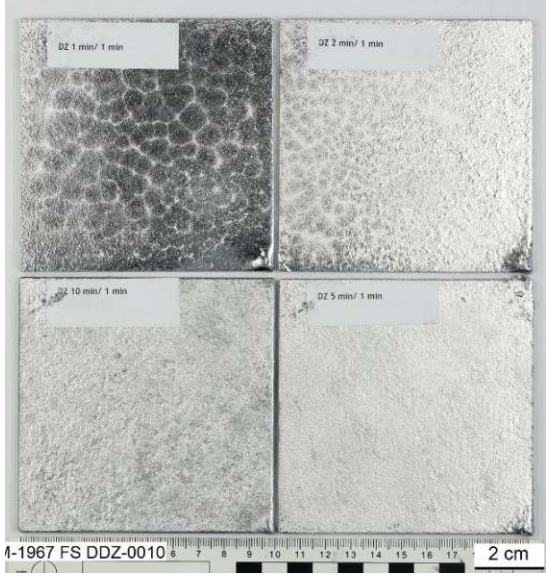
6.5 Double Dip Zinc Coatings WP1

6.5.1 Photographs of DDZ WP1

6.5.1.1 Sandelin samples

The (100 mm x 100 mm x 2 mm) Sandelin samples were galvanized by our galvanizing partner and sent to Hilti for investigation. Photographs of the received sample series and descriptions after visual inspections are shown in *Table 12*.

Table 12 Overview and descriptions of photographs of DDZ WP1 Sandelin samples

SB	ZN Sandelin samples	DZ Sandelin samples
Single dip		
	<p style="text-align: center;">1m – 10m</p> <p style="text-align: center;">Smooth surface, grey-green-blue shiny</p> <p style="text-align: center;">Visual roughness of surface increases with dipping time</p>	<p style="text-align: center;">1m – 10m</p> <p style="text-align: center;">Grey- green smooth surface,</p> <p style="text-align: center;">Visual roughness of surface increases with dipping time</p>
Double dip varying first dip, second dip 1m		
	<p style="text-align: center;">1m1m – 10m1m</p>	<p style="text-align: center;">1m1m – 10m1m</p>

Die approbierte gedruckte Originalversion dieser Diplomarbeit ist an der TU Wien Bibliothek verfügbar. The approved original version of this thesis is available in print at TU Wien Bibliothek.



	Mirror-like silvery surface, leopard-like structure visible on 1m1m and 2m1m sample and matte fine structure on others.	Mirror-like silvery surface, leopard-like structure visible on 1m1m and 2m1m sample and matte fine structure on others.
Double dip: first dip 5m, varying second dip		
	5m1m – 5m10m Silvery white shiny surface, zinc spangle flowers size increases with time	5m1m – 5m10m Silvery white shiny surface, zinc flower size increases with time

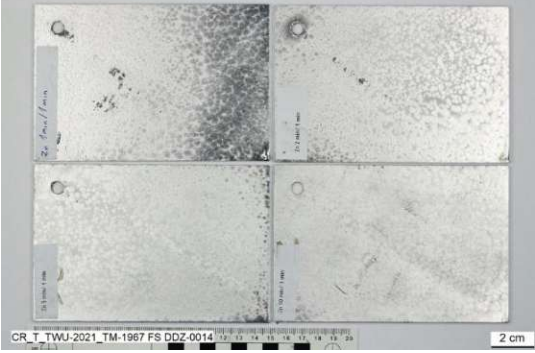
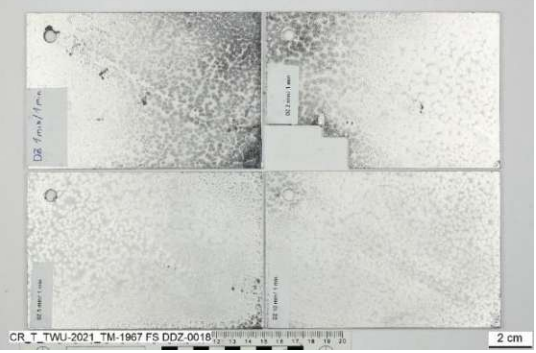
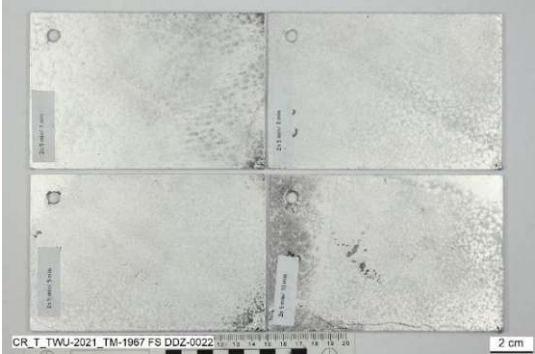
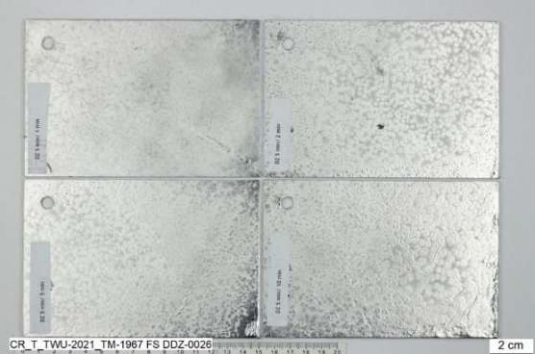
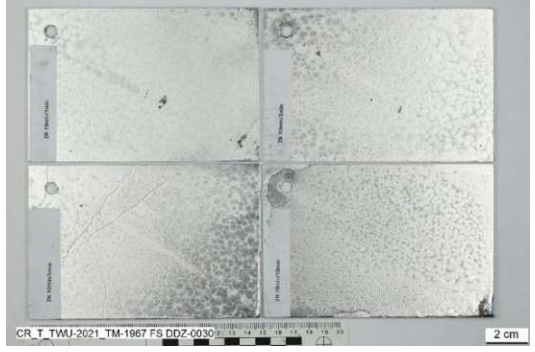
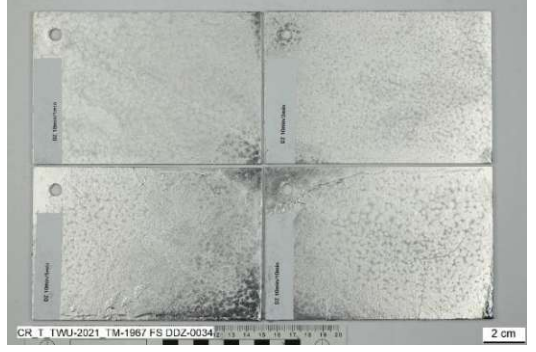
6.5.1.2 MM standard construction steel samples

The MM standard samples were also galvanized by the external galvanizing partner and sent to Hilti for investigation. Photographs of the received samples and descriptions after visual inspection are shown in Table 13.

Table 13 Overview and description of photographs of DDZ WP1 MM samples

MM	MM samples ZN	MM samples DZ
Single dip, quenched		
	1mab – 10mab Silver shiny, blue-grey matte surface	1mab – 10mab Silver shiny, green-grey matte surface

Die approbierte gedruckte Originalversion dieser Diplomarbeit ist an der TU Wien Bibliothek verfügbar
 The approved original version of this thesis is available in print at TU Wien Bibliothek.









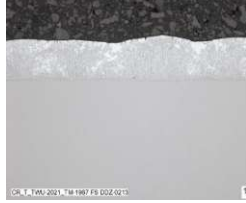

Double dip		
	<p>1m1m - 10m1m Mirror-like smooth silver coloured surface</p>	<p>1m1m - 10m1m Mirror-like smooth silver coloured surface</p>
Double dip		
	<p>5m1m - 5m10m Delamination occurs on SBZN5m10m Fine homogenous smooth silvery surface</p>	<p>5m1m - 5m10m Coating build-up on edges Fine homogenous smooth silvery surface</p>
Double dip		
	<p>10m1m- 10m10m Cracks visible on SBZN 10m5m and SBZN10m10m Fine homogenous smooth silvery surface</p>	<p>10m1m- 10m10m Delamination occurs on SBDZ10m10m. Fine homogenous smooth silvery surface</p>

6.5.2 Cross sections LOM images of DDZ WP1

6.5.2.1 Sandelin samples








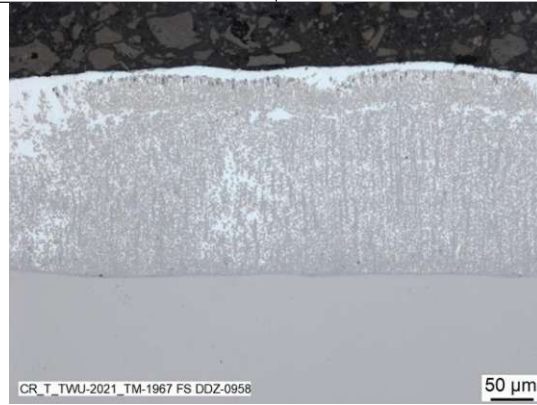
A selection of LOM obtained cross sections and description of Sandelin samples with the pure Zn coating for single dipped and Zn/ZnAl double dipped samples are shown in *Table 14*.

Table 14 WP1 DDZ CS Sandelin ZN

ZN	Sandelin samples			
Single dip				
	WP1 SBZN1m top	WP1 ZNSB2m top	WP1 SBZN5m top	WP1 SBZN10m top
				
	WP1 ZNSB2m top	WP1 SBZN10m top		
	On all single dipped samples, a gingko-leave structure of Fe-Zn phase with a Zn-rich phase on top. This is typical for HDG samples.			
Double dip: Variation in first dip				
	WP1 SBZN1m1m top	WP1 SBZN2m1m top	WP1 SBZN5m1m top	WP1 SBZN10m1m top



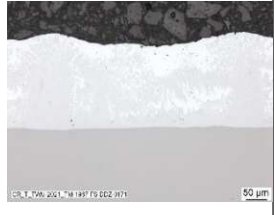

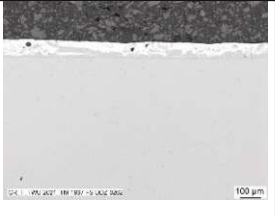
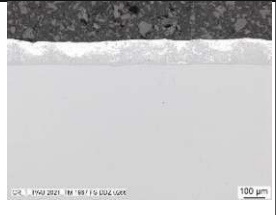
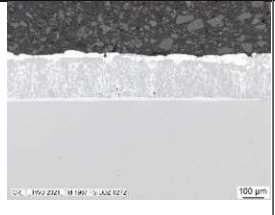
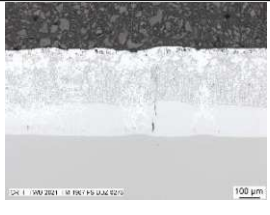




Die approbierte gedruckte Originalversion dieser Diplomarbeit ist an der TU Wien Bibliothek verfügbar. The approved original version of this thesis is available in print at TU Wien Bibliothek.



					
	WP1 SBZN2m1m top	WP1 SBZN5m1m top			
	<p>On the 1m1m and the 2m1m sample there is a Zn-rich middle coating layer and zinc rich layer visible on top.</p> <p>On the 5m1m a Fe-Zn intermetallic layer distributed towards the top is found.</p> <p>On the 10m1m sample, it appears that the second dip did not manage to be long enough to provide a homogenous coating layer.</p>				
Double dip: First dip 5m, variation in second dip					
	WP1 SBZN5m1m top	WP1 SBZN5m2m top	WP1 SBZN5m5m top	WP1 SBZN5m10m top	
					
	WP1 SBZN5m1m bot	WP1 SBZN5m10m top			
	<p>The zinc-layer on top is more dominant in short second dipped samples and appears thinner the longer the second dip time is. The Fe-Zn intermetallic phases are homogeneously distributed in a zinc matrix on SBZN5m10m.</p>				

A selection of cross sections of Sandelin samples with the DZ-Coating for single dipped and Zn/ZnAl double dipped samples is shown and described in Table 15.





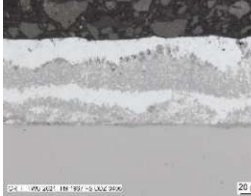

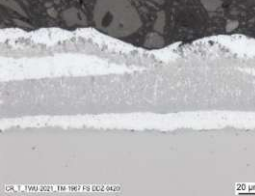





Table 15 WP1 DDZ CS Sandelin DZ

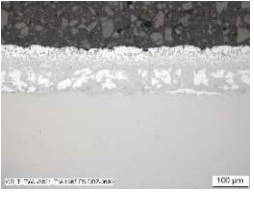



DZ	Sandelin samples			
Single dip				
	WP1 SBDZ1m top	WP1 SBDZ2m top	WP1 SBDZ5m top	WP1 SBDZ10m top
On all single dipped samples, a gingko-leave structure showing a Fe-Zn intermetallic phase shows up until top. The coating surface outline in the cross sections appear wavy.				
Double dip: Variation in first dip				
	WP1 SBDZ1m1m top	WP1 SBDZ2m1m top	WP1 SBDZ5m1m top	WP1 SBDZ10m1m top
On the 1m1m and 2m1m samples a smooth coating outline with zinc rich phase on top is seen. On the 5m1m and the 10m1m samples the intermetallic layer is distributed towards the top.				
Double dip: variation in second dip				
	WP1 SBDZ5m1m top	SBDZ5m2m top	WP1 SBDZ5m5m top	WP1 SBDZ5m10m top
An uneven coating thickness is found on the 5m1m, 5m2m and the 5m5m samples. A gingko-leave-like structure is visible all the way to the surface on 5m1m, 5m2m and 5m5m samples. The 5m10m sample shows a more even coating outline with a zinc rich layer piling up on top.				

6.5.2.2 MM samples

A selection of LOM images of the cross sections and their description of MM Samples with the Zn-coating for single dipped quenched and Zn/ZnAl double dipped samples is shown in Table 16.

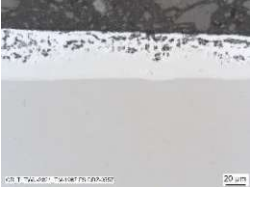



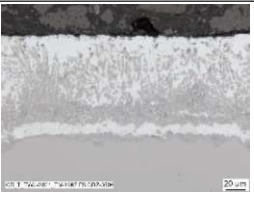

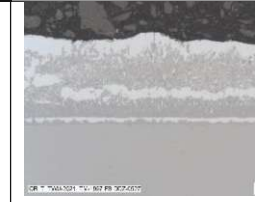
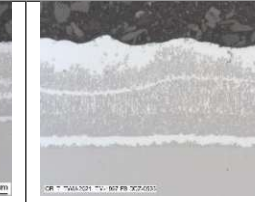
Table 16 WP1 DDZ CS MM ZN





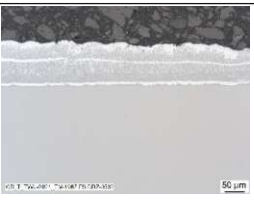


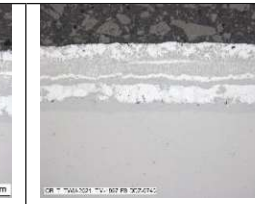
ZN	MM standard samples			
Single dip quenched				
	WP1 MMZN1m ab top	WP1 MMZN2m ab top	WP1 MMZN5m ab top	WP1 MMZN10m ab top
	An even coating thickness on all samples, including a homogeneous layer-like structure on every cross section was visible in the CS. Visible cracks on the Zn-Fe intermetallic layer next to the substrate was found on 5mab and 10mab samples.			
Double dip: variation in first dip				
	WP1 MMZN1m1m top	WP1 MMZN2m1m top	WP1 MMZN2m1m top	WP1 MMZN10m1m top
	Zinc-rich layer is found in different distances from the substrate, hints of the gingko-like structure only in the 1m1m sample. Various layer thicknesses were found, coming from a rough outline all over the coating.			
Double dip: variation in second dip				
	WP1 MMZN5m1m top	WP1 MMZN5m2m top	WP1 MMZN5m5m top	WP1 MMZN5m10m top
	Zinc rich grains are visible in 5m1m layer near the substrate. On the 5m2m, 5m5m and 5m10m many similarities are found. Near the surface a dark-grey intermetallic layer is found, on top of that a white colored zinc-rich layer is visible. Clearly defined in a horizontal line on top sits a mixed phase structure with some zinc rich grains on top.			

Double dip: variation in second dip				
	WP1 MMZN10m1m top	WP1 MMZN10m2m top	WP1 MMZN10m5m top	WP1 MMZN10m10m top
	<p>The coating thickness is found to be even over the analyzed range.</p> <p>For the 10m1m, 10m2m and 10m5m samples, the coating is showing an inhomogeneous distribution of the phases. Close to the substrate the samples show zinc rich areas surrounded by greyer coating areas.</p> <p>The 10m10m sample presents a dark-grey layer near the substrate, on top of that a white colored zinc rich layer is visible. Clearly defined in a horizontal line on top sits the mixed phase structure with some zinc rich grains on top</p>			

A selection of LOM images of the CS of MM Samples with the DZ-Coating for single dipped quenched and double dipped samples is shown in *Table 17*.

Table 17 WP1 DDZ CS MM DZ

DZ	CS of MM samples			
Single dip quenched				
	WP1 MMDZ1mab top	WP1 MMDZ2mab top	WP1 MMDZ5mab top	WP1 MMDZ10mab top
	<p>The single dipped, and quenched samples show a homogenous gingko-like intermetallic layer near the substrate. On top of that a zinc rich layer leads to a smooth surface coating. The 5m ab sample is showing a fine crack along the layer near the substrate. All samples are found to have dark spots starting from the outside and visible only in the zinc rich top layer.</p>			
Double dip: variation in first dip				
	WP1 MMDZ1m1m top	WP1 MMDZ2m1m top	WP1 MMDZ5m1m top	WP1 MMDZ10m1m top
	<p>The 1m1m sample displays a small dark-grey layer near the substrate with an overlaying zinc rich layer. On top of that, the gingko-shaped intermetallic phase is surrounded by a zinc rich layer on the outer edges.</p>			

	<p>For the 2m1m samples, the coating is showing an mixed distribution of the phases. Close to the substrate the samples show zinc rich area surrounded by greyer Fe containing areas.</p> <p>The 5m1m and 10m1m samples present a dark-grey layer near the substrate, with a white colored zinc rich layer visible on top of that first layer. Clearly defined in a horizontal line on top of the second layer sits the mixed phase structure with some white zinc rich areas on top</p>			
Double dip: variation in second dip				
	WP1 MMDZ5m1m top	WP1 MMDZ5m2m top	WP1 MMDZ5m5m top	WP1 MMDZ5m10m top
	<p>The 5m1m sample displays a mixed phase layer sprinkled randomly with zinc rich areas up to the top. The 5m2m, 5m5m and 5m10m samples are presenting a dark-grey layer near the substrate, and a white colored zinc rich layer is visible on top of that first layer. Clearly defined in a horizontal line on top of the second layer sits the mixed phase structure with some randomly distributed zinc rich areas on top</p>			
Double dip: variation in second dip				
	WP1 MMDZ10m1m top	WP1 MMDZ10m2m top	WP1 MMDZ10m5m top	WP1 MMDZ10m10m top
	<p>The 1m1m sample displays a small dark-grey layer near the surface with an overlaying very small zinc rich layer. On top of that a mixed phase structure is interrupted by a fine zinc rich layer and a zinc rich layer on the outer edge right below the surface.</p> <p>The 10m2m, 10m5m and 10m10m samples present a dark-grey layer near the substrate, and a white colored zinc rich layer is visible on top of that first layer. Clearly defined in a horizontal line on top of the second layer sits the mixed phase structure with zinc rich areas on top</p>			

6.5.3 Coating thickness measurements of DDZ WP1

The coating thickness was measured using the LOM images of the cross sections in a digital measurement using Imagic IMS software.

6.5.3.1 Sandelin samples

Bottom and top side of the samples were measured to obtain an average of both sides and diagrams to compare the coating thickness of a sample row are shown in Table 18.

Table 18 Coating thickness of SB samples, ZN and DZ coatings

	ZN	DZ
Single dip	<p>SBZN</p>	<p>SBDZ</p>
	<p>The Sandelin effect is clearly visible in the single dipped samples, where the coating thickness increases from an average of 47 μm (DZ) and 49 μm (ZN) in the 1m dip step to a average thickness of 317 μm (ZN) to 290 μm (DZ) after 10 minutes. The high standard deviation is due to a high surface roughness.</p> <p>With the Sandelin effect, the variation of the thickness also increases significantly (as shown by the higher standard deviation of the thickness measurements). This is the case for all Sandelin coated samples.</p>	
Double dip: variation in first dip	<p>SBZN 1m1m-10m1m</p>	<p>SBDZ 1m1m-10m1m</p>
	<p>The Sandelin effect is also visible in the double dipped samples with a variation in the first dip where the coating thickness increases from an average 67 μm (ZN) or 70 μm (DZ) in the 1m first dip step to a average thickness of 450 μm (ZN) to 445 μm (DZ) after a 10 minute first dip step, followed by a 1m second dip.</p>	
Double dip: variation in second dip	<p>SBZN 5m1m-5m10m</p>	<p>SBDZ 5m1m-5m10m</p>
	<p>On the double dipped samples with the fixed first dip of 5 minutes and a varying second dip step, the Sandelin effect is not visible.</p> <p>The coating thickness is between 133 μm - 216 μm for ZN samples and between 109 μm - 169 μm for DZ samples.</p>	

6.5.3.2 MM samples

For the coating thickness investigations of the MM samples, only the ZN diagrams are shown in Table 19, as the DZ results are similar.

Table 19 Coating thickness of MM samples, ZN coatings

MM	Coating Thickness Diagram	Description															
Single dip quenched	<p>MMZN 1m-10m AB</p> <table border="1"> <caption>Coating Thickness Data for MMZN 1m-10m AB</caption> <thead> <tr> <th>dipping time (min)</th> <th>Coating thickness top (µm)</th> <th>Coating thickness bot (µm)</th> </tr> </thead> <tbody> <tr> <td>1m ab</td> <td>54</td> <td>49</td> </tr> <tr> <td>2m ab</td> <td>55</td> <td>53</td> </tr> <tr> <td>5m ab</td> <td>61</td> <td>62</td> </tr> <tr> <td>10m ab</td> <td>82</td> <td>63</td> </tr> </tbody> </table>	dipping time (min)	Coating thickness top (µm)	Coating thickness bot (µm)	1m ab	54	49	2m ab	55	53	5m ab	61	62	10m ab	82	63	<p>The coating thickness lies between 49 µm – 82 µm for ZN samples and between 43 µm – 89 µm for DZ samples.</p> <p>The inhomogeneity is not very prominent, but indicated by the standard deviation also visible in the diagram. The top and bottom coating is equally thick on each sample.</p>
dipping time (min)	Coating thickness top (µm)	Coating thickness bot (µm)															
1m ab	54	49															
2m ab	55	53															
5m ab	61	62															
10m ab	82	63															
Variation in first dip, second dip: 1m	<p>MMZN 1m1m-10m1m</p> <table border="1"> <caption>Coating Thickness Data for MMZN 1m1m-10m1m</caption> <thead> <tr> <th>dipping time (min)</th> <th>Coating thickness top (µm)</th> <th>Coating thickness bot (µm)</th> </tr> </thead> <tbody> <tr> <td>1m1m</td> <td>97</td> <td>73</td> </tr> <tr> <td>2m1m</td> <td>68</td> <td>76</td> </tr> <tr> <td>5m1m</td> <td>84</td> <td>69</td> </tr> <tr> <td>10m1m</td> <td>92</td> <td>94</td> </tr> </tbody> </table>	dipping time (min)	Coating thickness top (µm)	Coating thickness bot (µm)	1m1m	97	73	2m1m	68	76	5m1m	84	69	10m1m	92	94	<p>The coating thickness lies between 68 µm – 97 µm for ZN samples and between 85 µm – 126 µm for DZ samples.</p> <p>A slight inhomogeneity is found, indicated by the standard deviation also visible in the diagram. The differences between the top side and the bottom side of the samples are not large.</p>
dipping time (min)	Coating thickness top (µm)	Coating thickness bot (µm)															
1m1m	97	73															
2m1m	68	76															
5m1m	84	69															
10m1m	92	94															
First dip: 5m, second dip varying	<p>MMZN 5m1m-5m10m</p> <table border="1"> <caption>Coating Thickness Data for MMZN 5m1m-5m10m</caption> <thead> <tr> <th>dipping time (min)</th> <th>Coating thickness top (µm)</th> <th>Coating thickness bot (µm)</th> </tr> </thead> <tbody> <tr> <td>5m1m</td> <td>115</td> <td>157</td> </tr> <tr> <td>5m2m</td> <td>102</td> <td>103</td> </tr> <tr> <td>5m5m</td> <td>128</td> <td>120</td> </tr> <tr> <td>5m10m</td> <td>135</td> <td>143</td> </tr> </tbody> </table>	dipping time (min)	Coating thickness top (µm)	Coating thickness bot (µm)	5m1m	115	157	5m2m	102	103	5m5m	128	120	5m10m	135	143	<p>The coating thickness lies between 102 µm – 157 µm for ZN samples and between 89 µm – 195 µm for DZ samples.</p> <p>There is nearly no thickness variation found. The differences between the top side and the bottom side of the samples are only found in the first sample.</p>
dipping time (min)	Coating thickness top (µm)	Coating thickness bot (µm)															
5m1m	115	157															
5m2m	102	103															
5m5m	128	120															
5m10m	135	143															
First dip: 10m, second dip varying	<p>MMZN 10m1m-10m10m</p> <table border="1"> <caption>Coating Thickness Data for MMZN 10m1m-10m10m</caption> <thead> <tr> <th>dipping time (min)</th> <th>Coating thickness top (µm)</th> <th>Coating thickness bot (µm)</th> </tr> </thead> <tbody> <tr> <td>10m1m</td> <td>132</td> <td>129</td> </tr> <tr> <td>10m2m</td> <td>147</td> <td>153</td> </tr> <tr> <td>10m5m</td> <td>150</td> <td>161</td> </tr> <tr> <td>10m10m</td> <td>201</td> <td>212</td> </tr> </tbody> </table>	dipping time (min)	Coating thickness top (µm)	Coating thickness bot (µm)	10m1m	132	129	10m2m	147	153	10m5m	150	161	10m10m	201	212	<p>The coating thickness lies between 129 µm – 212 µm for ZN samples and between 120 µm – 203 µm for DZ samples.</p> <p>There is no thickness variation found. No differences between the top side and the bottom side regarding coating thickness was found.</p>
dipping time (min)	Coating thickness top (µm)	Coating thickness bot (µm)															
10m1m	132	129															
10m2m	147	153															
10m5m	150	161															
10m10m	201	212															

6.5.4 SEM images and EDX mapping of DDZ WP1

SEM images were taken on ZN-coated samples only. Mapping (of different elements with EDX) and PID (Point identification) analysis were only carried out on specific samples, because relevant information for other samples can be concluded from the analysed samples.

6.5.4.1 Sandelin samples

Table 20 shows an overview of the SEM images of the Sandelin samples of WP1 including the mapping for Al, Fe and Zn and the PID.

Table 20 WP1 DDZ SEM Sandelin sample ZN coating

ZN	SEM Images Sandelin samples																																	
Single dip																																		
	WP1 SBZN1m top SE2	WP1 SBZN2m top SE2	WP1 SBZN5m top SE2	WP1 SBZN10m top SE2																														
Single dip mapping																																		
	WP1 SBZN1m top SE2	Zn mapping WP1 SBZN1m top SE2	Fe mapping WP1 SBZN1m top SE2	C mapping WP1 SBZN1m top SE2																														
The mapping of SBZN1m shows, that the substrate is consisting of mainly iron, the zinc layer sits on top with a small amount of iron distributed on the coating. The carbon-rich layer resembles the embedding material.																																		
Single dip PID		<table border="1"> <thead> <tr> <th></th> <th>Zn</th> <th>Fe</th> <th>Mn</th> <th>Cr</th> <th>Prop</th> </tr> </thead> <tbody> <tr> <td>No.</td> <td>Wt %</td> <td>Wt %</td> <td>Wt %</td> <td>Wt %</td> <td></td> </tr> <tr> <td>1</td> <td>94</td> <td>6</td> <td></td> <td></td> <td>ζ-phase FeZn₁₃</td> </tr> <tr> <td>2</td> <td>93</td> <td>7</td> <td></td> <td></td> <td>ζ-phase FeZn₁₃ or δ-phase</td> </tr> <tr> <td>3</td> <td></td> <td>98.5</td> <td>1</td> <td>0.5</td> <td></td> </tr> </tbody> </table>				Zn	Fe	Mn	Cr	Prop	No.	Wt %	Wt %	Wt %	Wt %		1	94	6			ζ-phase FeZn ₁₃	2	93	7			ζ-phase FeZn ₁₃ or δ-phase	3		98.5	1	0.5	
		Zn	Fe	Mn	Cr	Prop																												
No.	Wt %	Wt %	Wt %	Wt %																														
1	94	6			ζ-phase FeZn ₁₃																													
2	93	7			ζ-phase FeZn ₁₃ or δ-phase																													
3		98.5	1	0.5																														
WP1 SBZN1m top PID	WP1 SBZN1m top composition table																																	
The steel substrate is rich in iron with small amounts of 1 wt% Mn and 0.5 wt% Cr. The coating layer is Zn rich and showing a Fe content of 7 wt% near the substrate which is gradually lower towards the surface. As proposed in the theory it is mainly consisting most likely of the ζ-phase (FeZn ₁₃).																																		

Die approbierte gedruckte Originalversion dieser Diplomarbeit ist an der TU Wien Bibliothek verfügbar. The approved original version of this thesis is available in print at TU Wien Bibliothek.



Double dip: Variation in first dip, second dip: 1m																																																																			
	WP1 SBZN1m1m top AsB	WP1 SBZN2m1m top AsB	WP1 SBZN5m1m top AsB	WP1 SBZN10m1m top AsB																																																															
		Zn L series 	Al K series 	Fe K series 																																																															
	WP1 SBZN1m1m AsB	WP1 SBZN1m1m Zn Mapping	WP1 SBZN1m1m Al Mapping	WP1 SBZN1m1m Fe Mapping																																																															
		Zn L series 	Al K series 	Fe K series 																																																															
WP1 SBZN10m1m AsB	WP1 SBZN10m1m Zn Mapping	WP1 SBZN10m1m Al Mapping	WP1 SBZN10m1m Fe Mapping																																																																
	<table border="1"> <thead> <tr> <th></th> <th>Zn</th> <th>Fe</th> <th>Al</th> <th>Mn</th> <th>Cr</th> <th>Prop</th> </tr> </thead> <tbody> <tr> <td>No</td> <td>Wt %</td> <td>Wt %</td> <td>Wt %</td> <td>Wt %</td> <td>Wt %</td> <td></td> </tr> <tr> <td>1</td> <td>99</td> <td></td> <td>1</td> <td></td> <td></td> <td></td> </tr> <tr> <td>2</td> <td>80</td> <td>5</td> <td>15</td> <td></td> <td></td> <td>Fe2Al3Znx</td> </tr> <tr> <td>3</td> <td>97</td> <td>2</td> <td>1</td> <td></td> <td></td> <td>Zinc with impurities</td> </tr> <tr> <td>4</td> <td>70</td> <td>9</td> <td>21</td> <td></td> <td></td> <td>Fe2Al3Znx</td> </tr> <tr> <td>5</td> <td>54</td> <td>17</td> <td>29</td> <td></td> <td></td> <td>Fe2Al5Znx</td> </tr> <tr> <td>6</td> <td></td> <td>98.6</td> <td></td> <td>1</td> <td>0.4</td> <td></td> </tr> <tr> <td>7</td> <td>91.5</td> <td></td> <td>8.5</td> <td></td> <td></td> <td></td> </tr> </tbody> </table>					Zn	Fe	Al	Mn	Cr	Prop	No	Wt %	Wt %	Wt %	Wt %	Wt %		1	99		1				2	80	5	15			Fe2Al3Znx	3	97	2	1			Zinc with impurities	4	70	9	21			Fe2Al3Znx	5	54	17	29			Fe2Al5Znx	6		98.6		1	0.4		7	91.5		8.5			
	Zn	Fe	Al	Mn	Cr	Prop																																																													
No	Wt %	Wt %	Wt %	Wt %	Wt %																																																														
1	99		1																																																																
2	80	5	15			Fe2Al3Znx																																																													
3	97	2	1			Zinc with impurities																																																													
4	70	9	21			Fe2Al3Znx																																																													
5	54	17	29			Fe2Al5Znx																																																													
6		98.6		1	0.4																																																														
7	91.5		8.5																																																																
WP1 SBZN1m1m PID	WP1 SBZN1m1m Composition table																																																																		

		<table border="1"> <thead> <tr> <th></th> <th>Zn</th> <th>Fe</th> <th>Al</th> <th>Prop</th> </tr> <tr> <th>No.</th> <th>Wt%</th> <th>Wt%</th> <th>Wt%</th> <th></th> </tr> </thead> <tbody> <tr> <td>1</td> <td>78</td> <td>7</td> <td>15</td> <td>Fe₂Al₃Zn_x</td> </tr> <tr> <td>2</td> <td>98</td> <td>1</td> <td>1</td> <td>Pure zinc</td> </tr> <tr> <td>3</td> <td>86</td> <td>5</td> <td>9</td> <td>Fe₂Al₃Zn_x</td> </tr> <tr> <td>4</td> <td>94</td> <td>6</td> <td></td> <td>ζ-phase FeZn₁₃</td> </tr> </tbody> </table>		Zn	Fe	Al	Prop	No.	Wt%	Wt%	Wt%		1	78	7	15	Fe ₂ Al ₃ Zn _x	2	98	1	1	Pure zinc	3	86	5	9	Fe ₂ Al ₃ Zn _x	4	94	6		ζ-phase FeZn ₁₃
	Zn	Fe	Al	Prop																												
No.	Wt%	Wt%	Wt%																													
1	78	7	15	Fe ₂ Al ₃ Zn _x																												
2	98	1	1	Pure zinc																												
3	86	5	9	Fe ₂ Al ₃ Zn _x																												
4	94	6		ζ-phase FeZn ₁₃																												
	<p>WP1 SBZN10m1m PID</p>	<p>WP1 SBZN10m1m Composition table</p>																														
<p>In general, the samples 1m1m, 2m1m and 5m1m show, that Fe and Al form a ternary mixture phase consisting of 27 – 29 wt% Al, 14-17 wt% Fe and remaining zinc at the bottom close to the substrate. The layer above the dark-grey bottom coating layer is composed of 70 wt% Zn, 9 wt% Fe and 21 wt% Al. The white layer in between the bottom mixture phase and the gingko-shaped phases consists of Zn including 1-2 wt% of Fe or Al sometimes. The gingko shaped phase is consisting of 75 – 80 wt% Zn, 5 – 7 wt% Fe and 15 - 18% Al. At the top the zinc layer is present with 99 wt% zinc and 1 wt% Al.</p> <p>The 10m1m sample was too thick because of the Sandelin effect to form a uniform layer upon the second dip step. The bottom coating layer next to the steel substrate is found to be the ζ-phase (FeZn₁₃). Therefore, just a small dark-grey Fe-Al rich ternary Zn phase described above is built up on top of the undissolved first dip layer. Followed by the white layer consisting mainly of zinc. On top of that sits a grey layer with 78 wt% Zn, 7 wt% Fe and 15 wt% Al.</p>																																
<p>Double dip: First dip: 5m, variation in second dip</p>																																
	<p>WP1 SBZN5m1m top SE2</p>	<p>WP1 SBZN5m2m top SE2</p>	<p>WP1 SBZN5m5m top SE2</p>	<p>WP1 SBZN5m10m top SE2</p>																												
	<p>WP1 SBZN5m1m SE2</p>	<p>WP1 SBZN5m1m Zn Mapping</p>	<p>WP1 SBZN5m1m Al Mapping</p>	<p>WP1 SBZN5m1m Fe Mapping</p>																												

WP1 SBZN5m2m SE2	WP1 SBZN5m2m Zn Mapping	WP1 SBZN5m2m Al Mapping	WP1 SBZN5m2m Fe Mapping																																									
WP1 SBZN5m10m SE2	WP1 SBZN5m10m Zn Mapping	WP1 SBZN5m10m Al Mapping	WP1 SBZN5m10m Fe Mapping																																									
	<table border="1"> <thead> <tr> <th></th> <th>Zn</th> <th>Fe</th> <th>Al</th> <th>Prop</th> </tr> </thead> <tbody> <tr> <td>No.</td> <td>Wt %</td> <td>Wt %</td> <td>Wt %</td> <td></td> </tr> <tr> <td>1</td> <td>93</td> <td></td> <td>7</td> <td>Zn-5Al</td> </tr> <tr> <td>2</td> <td>98.8</td> <td></td> <td>1.2</td> <td>Pure zinc</td> </tr> <tr> <td>3</td> <td>93</td> <td></td> <td>7</td> <td>Zn-5Al</td> </tr> <tr> <td>4</td> <td>67 (60)</td> <td>7</td> <td>26 (33)</td> <td>Fe₂Al₅Zn_x or FeZn₁₀Al_x – FeZn₇Al_x</td> </tr> <tr> <td>5</td> <td>78</td> <td>6</td> <td>16</td> <td>Fe₂Al₃Zn_x or FeZn₁₀Al_x – FeZn₇Al_x</td> </tr> <tr> <td>6</td> <td>98.5</td> <td>0.5</td> <td>1</td> <td>Pure zic</td> </tr> </tbody> </table>					Zn	Fe	Al	Prop	No.	Wt %	Wt %	Wt %		1	93		7	Zn-5Al	2	98.8		1.2	Pure zinc	3	93		7	Zn-5Al	4	67 (60)	7	26 (33)	Fe ₂ Al ₅ Zn _x or FeZn ₁₀ Al _x – FeZn ₇ Al _x	5	78	6	16	Fe ₂ Al ₃ Zn _x or FeZn ₁₀ Al _x – FeZn ₇ Al _x	6	98.5	0.5	1	Pure zic
		Zn	Fe	Al	Prop																																							
	No.	Wt %	Wt %	Wt %																																								
	1	93		7	Zn-5Al																																							
	2	98.8		1.2	Pure zinc																																							
	3	93		7	Zn-5Al																																							
	4	67 (60)	7	26 (33)	Fe ₂ Al ₅ Zn _x or FeZn ₁₀ Al _x – FeZn ₇ Al _x																																							
5	78	6	16	Fe ₂ Al ₃ Zn _x or FeZn ₁₀ Al _x – FeZn ₇ Al _x																																								
6	98.5	0.5	1	Pure zic																																								
WP1 SBZN5m1m PID	WP1 SBZN5m1m Composition table																																											
<p>The SBZN 5m1m shows prominent zinc rich regions, surrounded by the Zn-5Al eutectic towards the surface. Below there are some ternary phases consisting of Fe₂Al₃Zn_x in just a few drops at measuring spot 4. The larger phase contains of Fe₂Al₃Zn_x towards the middle of the sample, were also some zinc rich grains are formed. On the bottom, next to the steel substrate the Fe-Al inhibition-layer is proposed.</p> <p>The phase distribution on the SBZN 5m2m sample is according to the 5m1m sample. Small differences are obtained in the layer thickness. The pure zinc layer is distributed more towards the top third in the assumed Fe₂Al₃Zn_x layer. The overall thickness of the zinc areas is smaller towards the outer surface with small Fe₂Al₅Zn_x drop-like particles, equally to the Zone 3 found in the literature.</p> <p>In the SBZN 5m5m sample the intermediate zinc rich layer is not found, it could presumably be described as a zinc matrix with a Fe₂Al₃Zn_x ternary phase formation. Between the steel substrate and the coating, a composition of 57 wt % Al, 34 wt% Fe and 9 wt % Zn was found.</p>																																												

For the SBZN 5m10m sample, the zones described in the theory are not properly distinguishable. The trends of the previous samples of the row continues as a small Al-Fe rich inhibition layer is found next to the substrate. Towards the surface there is a zinc matrix with a ternary phase obtained. The surface area is zinc rich and also shows the Zn-Al eutectic.

6.5.4.2 MM samples

Table 21 shows and overview of the MM samples of WP1 including the EDX mapping for Al, Fe and Zn and the PID.

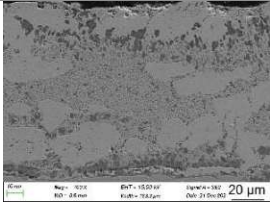
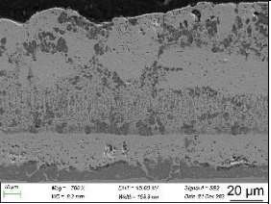
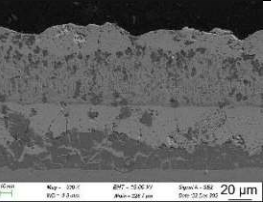
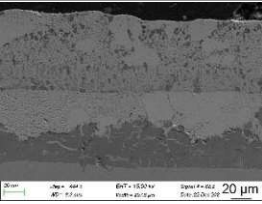
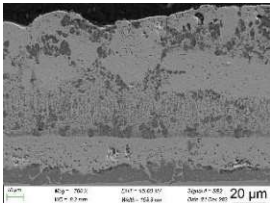
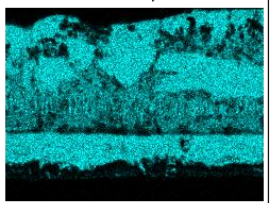
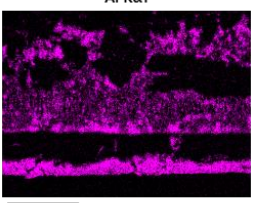
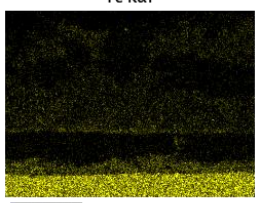
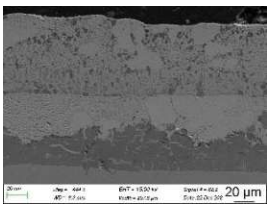
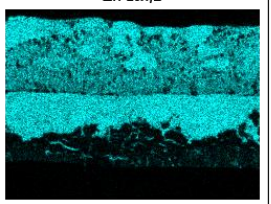
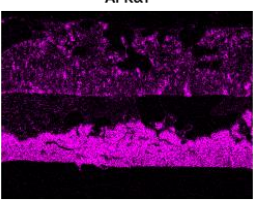
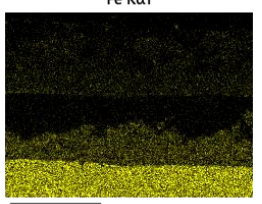
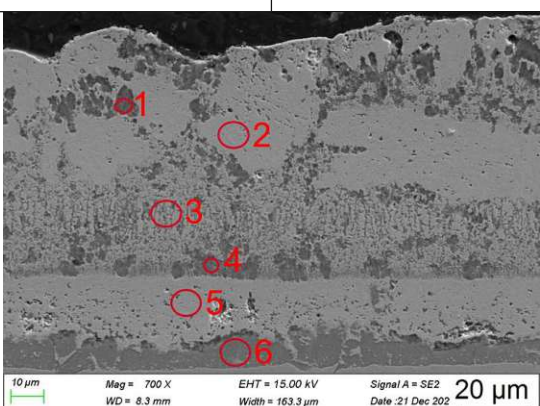
Table 21 WP1 DDZ SEM MM sample ZN coating

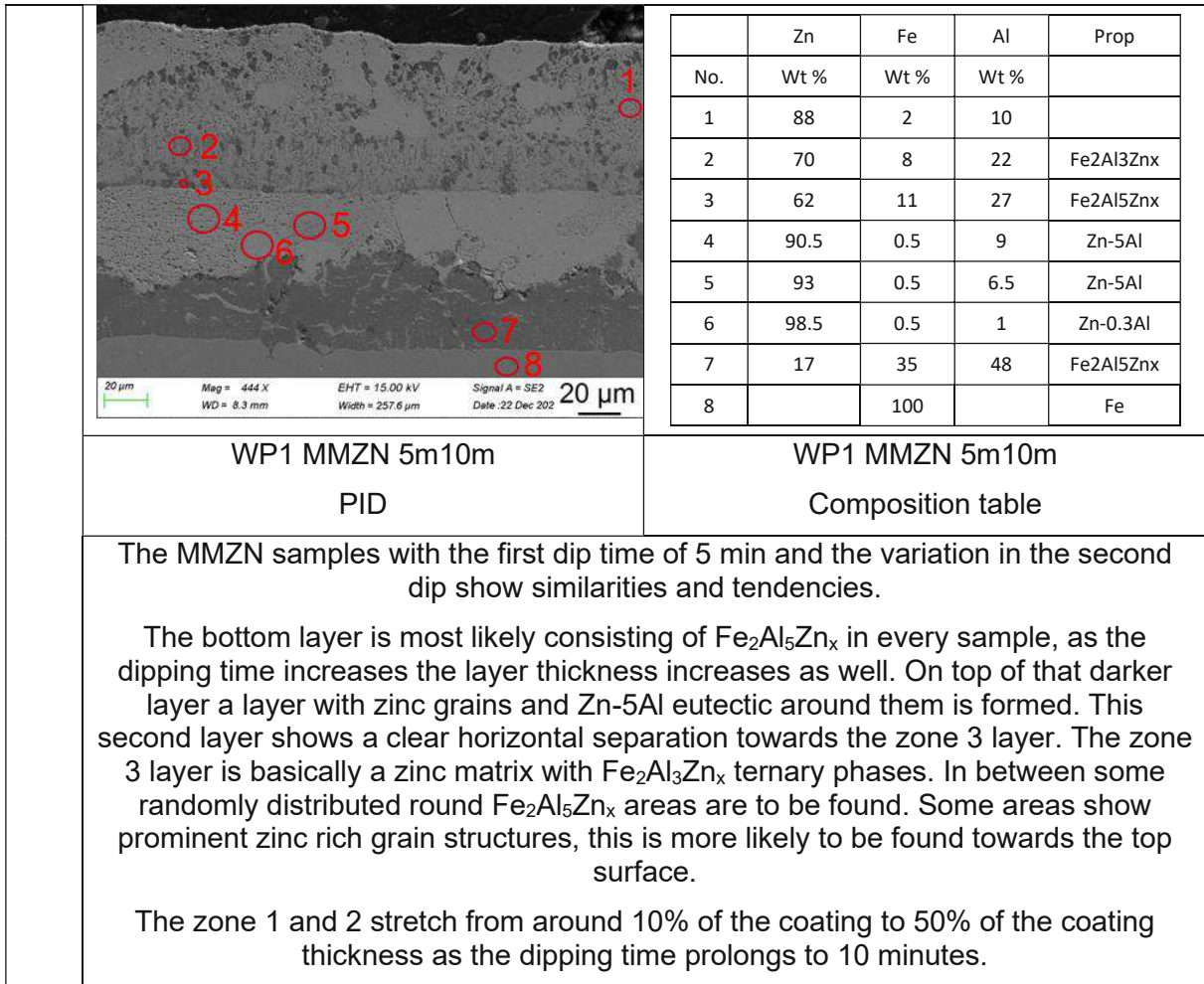
ZN	SEM Images MM samples			
Double dip: Variation in first dip time, second dip: 1m				
	WP1 MMZN1m1m top SE2	WP1 MMZN2m1m top SE2	WP1 MMZN5m1m top SE2	WP1 MMZN10m1m top SE2
	WP1 MMZN1m1m SE2	WP1 MMZN1m1m Zn Mapping	WP1 MMZN1m1m Al Mapping	WP1 MMZN1m1m Fe Mapping
WP1 MMZN2m1m SE2	WP1 MMZN2m1m Zn Mapping	WP1 MMZN2m1m Al Mapping	WP1 MMZN2m1m Fe Mapping	

Die approbierte gedruckte Originalversion dieser Diplomarbeit ist an der TU Wien Bibliothek verfügbar. The approved original version of this thesis is available in print at TU Wien Bibliothek.

<p>10 μm Mag = 700 X EHT = 15.00 kV Signal A = SE2 WD = 8.4 mm Width = 163.3 μm Date : 17 Dec 202 20 μm</p>	<table border="1"> <thead> <tr> <th></th> <th>Zn</th> <th>Fe</th> <th>Al</th> <th>Prop</th> </tr> <tr> <th>No.</th> <th>Wt %</th> <th>Wt %</th> <th>Wt %</th> <th></th> </tr> </thead> <tbody> <tr> <td>1</td> <td>99</td> <td></td> <td>1</td> <td>Zn-0.3Al</td> </tr> <tr> <td>2</td> <td>92</td> <td></td> <td>8</td> <td>Zn-5Al</td> </tr> <tr> <td>3</td> <td>72.45</td> <td>7.5</td> <td>20</td> <td>Fe₂Al₃Zn_x or FeZn₁₀Al_x – FeZn₇Al_x</td> </tr> <tr> <td>4</td> <td>94</td> <td>1</td> <td>5</td> <td>Zn-5Al</td> </tr> <tr> <td>5</td> <td>52 (38)</td> <td>14 (19)</td> <td>34 (43)</td> <td>Fe₂Al₅Zn_x or FeZn₁₀Al_x – FeZn₇Al_x</td> </tr> <tr> <td>6</td> <td>93</td> <td>1</td> <td>6</td> <td>Zn-5Al</td> </tr> <tr> <td>7</td> <td>12</td> <td>36</td> <td>52</td> <td>Fe₂Al₅Zn_x</td> </tr> </tbody> </table>		Zn	Fe	Al	Prop	No.	Wt %	Wt %	Wt %		1	99		1	Zn-0.3Al	2	92		8	Zn-5Al	3	72.45	7.5	20	Fe ₂ Al ₃ Zn _x or FeZn ₁₀ Al _x – FeZn ₇ Al _x	4	94	1	5	Zn-5Al	5	52 (38)	14 (19)	34 (43)	Fe ₂ Al ₅ Zn _x or FeZn ₁₀ Al _x – FeZn ₇ Al _x	6	93	1	6	Zn-5Al	7	12	36	52	Fe ₂ Al ₅ Zn _x
	Zn	Fe	Al	Prop																																										
No.	Wt %	Wt %	Wt %																																											
1	99		1	Zn-0.3Al																																										
2	92		8	Zn-5Al																																										
3	72.45	7.5	20	Fe ₂ Al ₃ Zn _x or FeZn ₁₀ Al _x – FeZn ₇ Al _x																																										
4	94	1	5	Zn-5Al																																										
5	52 (38)	14 (19)	34 (43)	Fe ₂ Al ₅ Zn _x or FeZn ₁₀ Al _x – FeZn ₇ Al _x																																										
6	93	1	6	Zn-5Al																																										
7	12	36	52	Fe ₂ Al ₅ Zn _x																																										
<p>WP1 MMZN1m1m PID</p>	<p>WP1 MMZN1m1m Composition table</p>																																													
<p>10 μm Mag = 800 X EHT = 15.00 kV Signal A = SE2 WD = 8.4 mm Width = 142.9 μm Date : 17 Dec 202 20 μm</p>	<table border="1"> <thead> <tr> <th></th> <th>Zn</th> <th>Fe</th> <th>Al</th> <th>Prop</th> </tr> <tr> <th>No.</th> <th>Wt %</th> <th>Wt %</th> <th>Wt %</th> <th></th> </tr> </thead> <tbody> <tr> <td>1</td> <td>18</td> <td>22</td> <td>59</td> <td>Fe₂Al₅Zn_x</td> </tr> <tr> <td>2</td> <td>93</td> <td></td> <td>7</td> <td>Zn-5Al</td> </tr> <tr> <td>3</td> <td>72</td> <td>8</td> <td>20</td> <td>Fe₂Al₃Zn_x or FeZn₁₀Al_x – FeZn₇Al_x</td> </tr> <tr> <td>4</td> <td>14</td> <td>31</td> <td>55</td> <td>Fe₂Al₅Zn_x</td> </tr> <tr> <td>5</td> <td>97</td> <td>2</td> <td>1</td> <td>Zn-0.3Al</td> </tr> <tr> <td>6</td> <td>8</td> <td>38</td> <td>54</td> <td>Fe₂Al₅Zn_x</td> </tr> </tbody> </table>		Zn	Fe	Al	Prop	No.	Wt %	Wt %	Wt %		1	18	22	59	Fe ₂ Al ₅ Zn _x	2	93		7	Zn-5Al	3	72	8	20	Fe ₂ Al ₃ Zn _x or FeZn ₁₀ Al _x – FeZn ₇ Al _x	4	14	31	55	Fe ₂ Al ₅ Zn _x	5	97	2	1	Zn-0.3Al	6	8	38	54	Fe ₂ Al ₅ Zn _x					
	Zn	Fe	Al	Prop																																										
No.	Wt %	Wt %	Wt %																																											
1	18	22	59	Fe ₂ Al ₅ Zn _x																																										
2	93		7	Zn-5Al																																										
3	72	8	20	Fe ₂ Al ₃ Zn _x or FeZn ₁₀ Al _x – FeZn ₇ Al _x																																										
4	14	31	55	Fe ₂ Al ₅ Zn _x																																										
5	97	2	1	Zn-0.3Al																																										
6	8	38	54	Fe ₂ Al ₅ Zn _x																																										
<p>WP1 MMZN5m1m PID</p>	<p>WP1 MMZN5m1m Composition table</p>																																													
<p>All four MM samples with the variation of the first dip time and a 1m second dip time, are showing a similar microstructure. Trending is the Fe-Al inhibition layer near the substrate. Thereafter a zinc rich area is obtained, on top of which either a Fe₂Al₃Zn_x layer or a FeZn₁₀Al_x – FeZn₇Al_x layer (phase δ) is found in every sample. The thickness of the Fe-Al layer is found to be not correlating to the dipping time variations.</p> <p>On the 5m1m sample, the Zn-Al eutectic areas are alternating with a zinc-rich areas and a zinc-rich matrix containing most likely Fe₂Al₃Zn_x in the middle of the coating. The area closest to the surface is shown to be rich of zinc grains surrounded by the Zn-Al eutectic.</p> <p>For the other samples in the row, most likely some Fe₂Al₅Zn_x phases with round morphology are found between the zinc-rich phases in zone 3.</p>																																														

Double dip samples: First dip 5m, variation in second dip

																																						
WP1 MMZN5m1m top SE2	WP1 MMZN5m2m top SE2	WP1 MMZN5m5m top SE2	WP1 MMZN5m10m top SE2																																			
																																						
WP1 MMZN5m2m SE2	WP1 MMZN5m2m Zn Mapping	WP1 MMZN5m2m Al Mapping	WP1 MMZN5m2m Fe Mapping																																			
																																						
WP1 MMZN5m10m SE2	WP1 MMZN5m10m Zn Mapping	WP1 MMZN5m10m Al Mapping	WP1 MMZN5m10m Fe Mapping																																			
	<table border="1"> <thead> <tr> <th>No.</th> <th>Zn Wt %</th> <th>Fe Wt %</th> <th>Al Wt %</th> <th>Prop</th> </tr> </thead> <tbody> <tr> <td>1</td> <td>23</td> <td>15</td> <td>62</td> <td>Fe2Al5Znx</td> </tr> <tr> <td>2</td> <td>99</td> <td></td> <td>1</td> <td>Zn-0.3Al</td> </tr> <tr> <td>3</td> <td>74</td> <td>7</td> <td>19</td> <td>Fe2Al3Znx</td> </tr> <tr> <td>4</td> <td>27</td> <td>17</td> <td>56</td> <td>Fe2Al5Znx</td> </tr> <tr> <td>5</td> <td>98</td> <td>1</td> <td>1</td> <td>Zn-0.3Al</td> </tr> <tr> <td>6</td> <td>23</td> <td>33</td> <td>44</td> <td>Fe2Al5Znx</td> </tr> </tbody> </table>			No.	Zn Wt %	Fe Wt %	Al Wt %	Prop	1	23	15	62	Fe2Al5Znx	2	99		1	Zn-0.3Al	3	74	7	19	Fe2Al3Znx	4	27	17	56	Fe2Al5Znx	5	98	1	1	Zn-0.3Al	6	23	33	44	Fe2Al5Znx
No.	Zn Wt %	Fe Wt %	Al Wt %	Prop																																		
1	23	15	62	Fe2Al5Znx																																		
2	99		1	Zn-0.3Al																																		
3	74	7	19	Fe2Al3Znx																																		
4	27	17	56	Fe2Al5Znx																																		
5	98	1	1	Zn-0.3Al																																		
6	23	33	44	Fe2Al5Znx																																		
WP1 MMZN5m2m PID	WP1 MMZN5m2m Composition table																																					






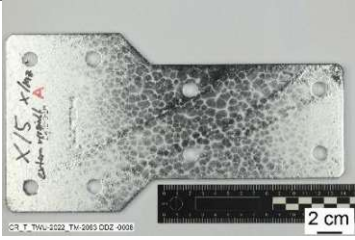
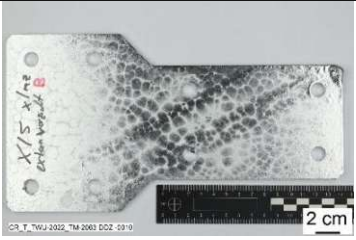


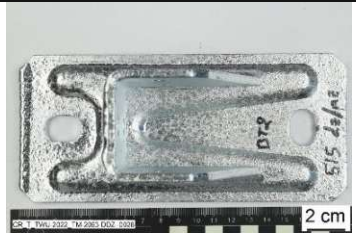



Die approbierte gedruckte Originalversion dieser Diplomarbeit ist an der TU Wien Bibliothek verfügbar
The approved original version of this thesis is available in print at TU Wien Bibliothek.



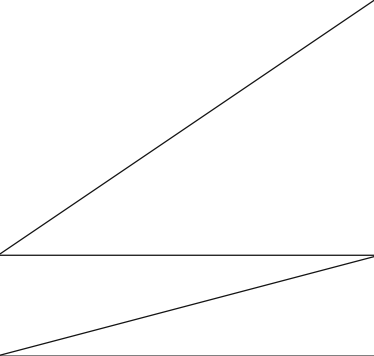
6.6 Double Dip Zinc WP2

6.6.1 Photographs of DDZ WP2

The Hilti samples were coated by the galvanizing partner and sent to Hilti for investigation. The samples were chosen in cooperation with the galvanizer based on the sample geometry. One flat sample, one welded sample and a strut channel (=chan, 2 mm thickness) with a thicker baseplate (=BP, 8 mm thickness) were investigated. Photographs and descriptions of the visual appearance of the received samples are shown in Table 22.

Table 22 Overview and descriptions of photographs of DDZ WP2 Hilti part samples

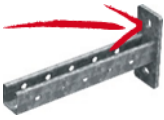
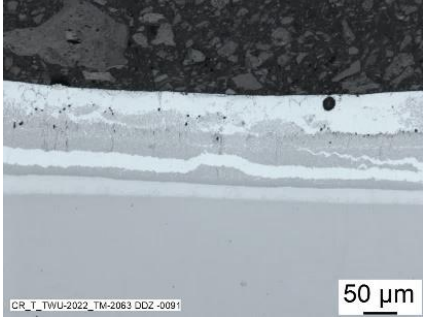
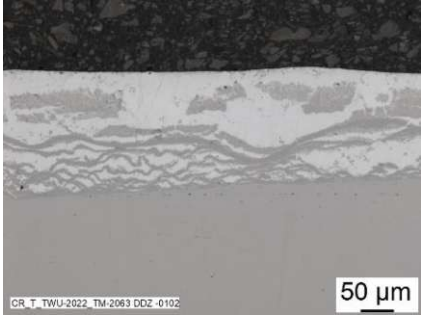

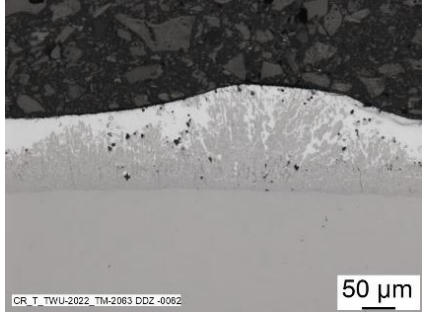
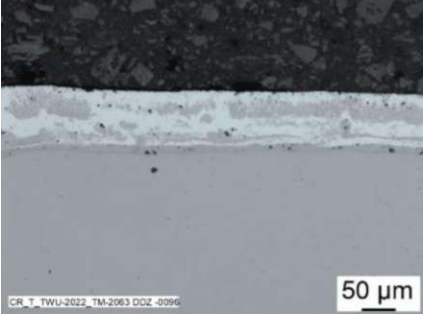
MT-C-GLP T			
	DZMZ 5m5m A	DZMZ 5m5m B	DZMZ 5m5m C
			
	X-MZ Xm5m A	X-MZ Xm5m B	X-MZ Xm5m C
	Very smooth and shiny surface finish. The externally coated samples feel smoother than the DZMZ samples. The externally coated X-MZ samples show a leopard-pattern-like visually appealing finish.		
	MT-B-02		
DZMZ 5m5m BT1		DZMZ 5m5m BT2	DZ 5m
			
DZMZ 5m5m A		DZMZ 5m5m B	DZMZ 5m5m C
The DZ 5m single dipped silver-like coating is tinted in a very light gold-tone and a needle like structure is visible.			
The samples DZMZ: BT1, BT2 A, B and C are not different from each other in terms of the coating. They show a silvery shiny finish with a slightly gritty surface feel.			



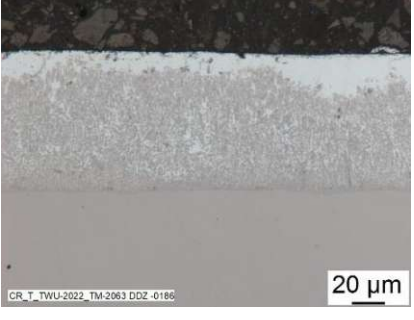

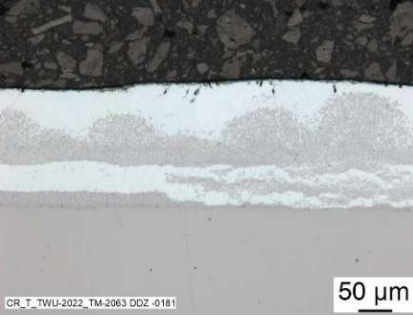
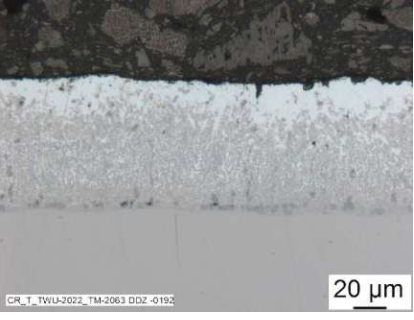
MT-BR-40-04			
	DZMZ 5m5m A is	X-MZ Xm5m A is	
	<p>The MT-BR-40-04 strut channels are of special interest, because the base plate (=BP) has a thicker substrate, than the channel itself. On the baseplate some “black” spots with insufficient coating quality were found. Overall on both samples, the coating matches the description above.</p>		

6.6.2 Cross sections LOM images of DDZ WP2

A selection of LOM obtained cross sections and a description of MT BR 40 04 samples with the DZMZ and X-MZ coating is shown in *Table 23*.

Table 23 WP2 DDZ LOM CS of DZMZ and X-MZ coated samples

	Position	DZMZ	X-MZ
MT-BR-40-04 BP	 front		
		DZMZ 5m5m A BP front	X-MZ Xm5m A BP front
	 top		
		DZMZ 5m5m A BP top	X-MZ Xm5m A BP top

MT-BR-40-04 channel	 <p>os (=outside)</p>	 <p>DZMZ 5m5m B Channel os</p>	 <p>X-MZ Xm5m B Channel os</p>
	 <p>is (= inside)</p>	 <p>DZMZ 5m5m B Channel is</p>	 <p>X-MZ Xm5m B Channel is</p>

The DZMZ 5m5m coating on the base plate of the MT-BR-40 04 sample shows various coating layers and a uniform coating thickness. There is no relation between the two different sides of the BP investigations attainable. The samples show huge differences between the top of the baseplate and the front of the baseplate.

For the X-MX Xm5m coated sample the two different spots investigated at the baseplate also show no context in their coating build up. A random build-up of the coating microstructure is possible.

For the thinner channel, the microstructure is not uniformly comprehensible on all sides investigated.

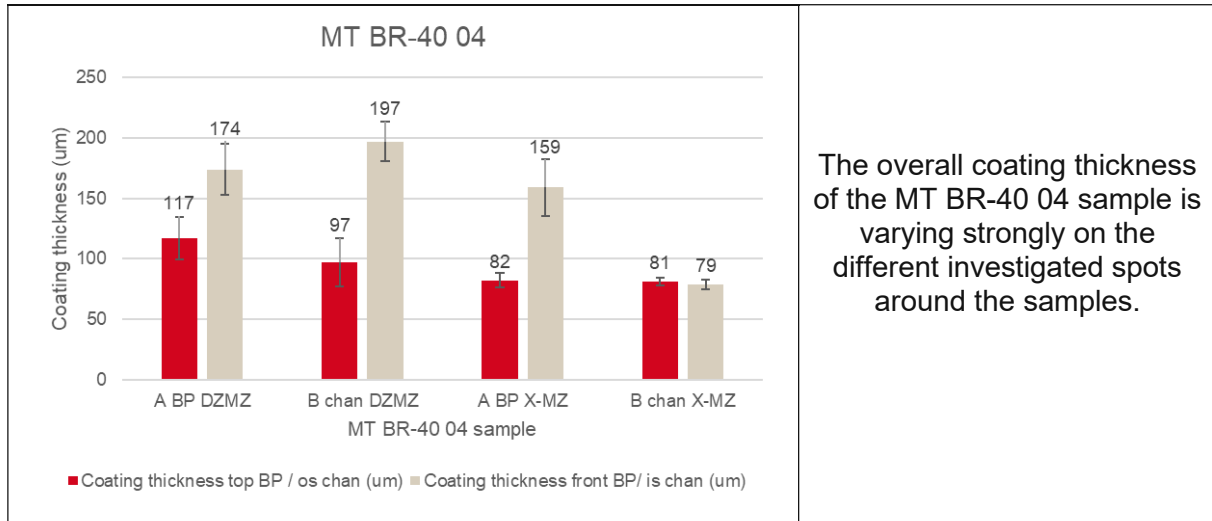
The DZMZ 5m5m coating shows small zinc-rich layers between the darker coloured mixed phases. On the outside a pile up of zinc is found.

The X-MZ coated samples are showing similarities at the outside (= os) and the inside (= is) of the channel. Next to the substrate a small darker coating layer is found, followed by a mixed phase in a zinc rich matrix. Towards the top, pure zinc is present dominantly.

6.6.3 Coating thickness measurements of DDZ WP2

The coating thickness (Table 24) was measured using the LOM images of the cross sections in a digital measurement using Imagic IMS software.

Table 24 WP2 DDZ Coating thickness of BP and chan of MT BR-40 04 coated with X-MZ and DZMZ



The DZMZ coated channel is found to have a thicker coating up to 197 µm on the inside, compared to the channel outside where it resembles at 97 µm on average. A variation of the coating thickness is found, indicated by the standard deviation. The DZMZ coated baseplate is also deviating in coating thickness and standard deviation depending on different measurement spots.

For the externally coated X-MZ samples, the baseplate shows the same deviations as the DZMZ coated sample. Only the channel of the X-MZ sample shows a comparable coating thickness of 81 µm on the outside or 79 µm on the inside with a reasonable standard deviation.

6.6.4 SEM images and EDX mapping of DDZ WP2

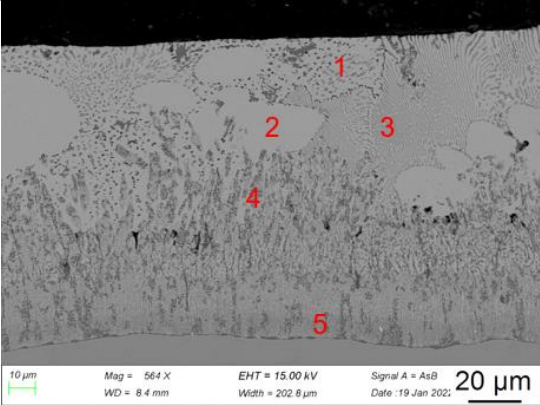
For the SEM investigation, also the DZMZ and the X-MZ coatings were analysed on the thicker baseplate and the thinner channel of the BR-40 04 Hilti part.

6.6.4.1 DZMZ coated samples

The DZMZ coated MT BR-40 04 sample was investigated on the baseplate and on the channel (Table 25).

Table 25 WP2 DDZ SEM images and EDX mapping of MT BR-40 04 with DZMZ coating on baseplate and channel

SEM images of DZMZ samples of MT BR-40 04																																																																												
MT BR-40 04 chan																																																																												
	DZMZ 5m5m B SEM os	DZMZ 5m5m B Zn mapping	DZMZ 5m5m B Al mapping	DZMZ 5m5m B Fe mapping																																																																								
		<table border="1"> <thead> <tr> <th></th> <th>Zn</th> <th>Fe</th> <th>Al</th> <th>Si</th> <th>Prop</th> </tr> <tr> <th>No.</th> <th>Wt %</th> <th>Wt %</th> <th>Wt %</th> <th>Wt %</th> <th></th> </tr> </thead> <tbody> <tr> <td>1</td> <td>99</td> <td></td> <td>0.8</td> <td></td> <td>Zn-0.3Al</td> </tr> <tr> <td>2</td> <td>92.6</td> <td></td> <td>7.4</td> <td></td> <td>Zn-5Al</td> </tr> <tr> <td>3</td> <td>79</td> <td>6</td> <td>15</td> <td></td> <td>Fe2Al3Znx</td> </tr> <tr> <td>4</td> <td>78</td> <td>6</td> <td>16</td> <td></td> <td>Fe2Al3Znx</td> </tr> <tr> <td>5</td> <td>97.6</td> <td>1.3</td> <td>1.1</td> <td></td> <td>Zn-0.3Al</td> </tr> <tr> <td>6</td> <td>68.2</td> <td>9.4</td> <td>22.2</td> <td>0.3</td> <td>Fe2Al3Znx</td> </tr> <tr> <td>7</td> <td>77</td> <td>8.8</td> <td>13.8</td> <td>0.4</td> <td>Fe2Al3Zn</td> </tr> <tr> <td>8</td> <td>18.9</td> <td>26.2</td> <td>53.7</td> <td>1.1</td> <td>Fe2Al5Znx</td> </tr> <tr> <td>9</td> <td>52.5</td> <td>15.9</td> <td>28.5</td> <td>0.6</td> <td>Fe2Al5Znx</td> </tr> <tr> <td>10</td> <td></td> <td>99.9</td> <td></td> <td></td> <td>Fe</td> </tr> </tbody> </table>					Zn	Fe	Al	Si	Prop	No.	Wt %	Wt %	Wt %	Wt %		1	99		0.8		Zn-0.3Al	2	92.6		7.4		Zn-5Al	3	79	6	15		Fe2Al3Znx	4	78	6	16		Fe2Al3Znx	5	97.6	1.3	1.1		Zn-0.3Al	6	68.2	9.4	22.2	0.3	Fe2Al3Znx	7	77	8.8	13.8	0.4	Fe2Al3Zn	8	18.9	26.2	53.7	1.1	Fe2Al5Znx	9	52.5	15.9	28.5	0.6	Fe2Al5Znx	10		99.9		
	Zn	Fe	Al	Si	Prop																																																																							
No.	Wt %	Wt %	Wt %	Wt %																																																																								
1	99		0.8		Zn-0.3Al																																																																							
2	92.6		7.4		Zn-5Al																																																																							
3	79	6	15		Fe2Al3Znx																																																																							
4	78	6	16		Fe2Al3Znx																																																																							
5	97.6	1.3	1.1		Zn-0.3Al																																																																							
6	68.2	9.4	22.2	0.3	Fe2Al3Znx																																																																							
7	77	8.8	13.8	0.4	Fe2Al3Zn																																																																							
8	18.9	26.2	53.7	1.1	Fe2Al5Znx																																																																							
9	52.5	15.9	28.5	0.6	Fe2Al5Znx																																																																							
10		99.9			Fe																																																																							
<p>For the DZMZ coated channel, near the steel substrate of the part the coating is showing darker spots, with approx. 54 wt% Al, 26 wt% Fe and 19 wt% Zn. On top of that, ternary phases rich in zinc are observed. They are consisting of 15 – 22 wt% Al, 6 – 9 wt% Fe and 77 – 80 wt% Zn. Towards the surface, the amount of zinc increases. A eutectic mixture of Zn and Al is found. Pure zinc grains are also seen.</p>																																																																												
MT BR-40 04 BP																																																																												
	DZMZ 5m5m A SEM BP	DZMZ 5m5m A Zn mapping	DZMZ 5m5m A Al mapping	DZMZ 5m5m A Fe mapping																																																																								

		Zn	Fe	Al	Si	Prop
	No.	Wt %	Wt %	Wt %	Wt %	
	1	83		17		Zn-22Al
	2	97.5	0.5	2		Zn-0.3Al
	3	85		15		Zn-22Al
	4	61	6	33		Fe2Al5Znx
5	44	15	39.2	0.8	Fe2Al5Znx or FeZn10Alx - FeZn7Alx	

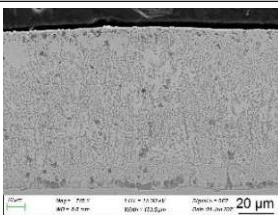
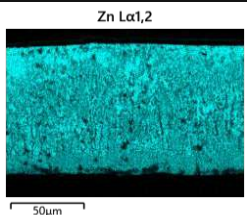
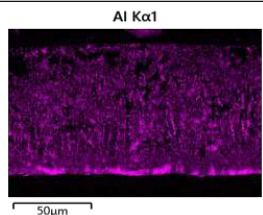
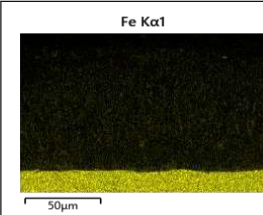
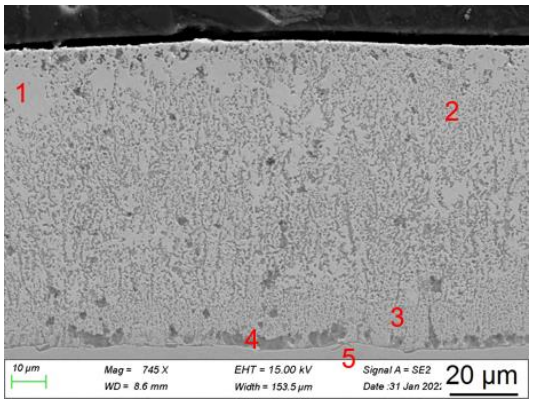
As for the 8 mm thick baseplate of the MT BR-40 04 sample, near the substrate also a high amount of aluminum (90 wt%) and iron (15 wt%) are obtained including 44 wt% Zn to form a ternary phase. For the second ternary phase, there were 33 wt% Al, 6 wt% Fe and 61 wt% Zn measured. Then a mixture of Zn and aluminum was found, consisting of 15 – 17 wt% Al and 83-85 wt% Zn.

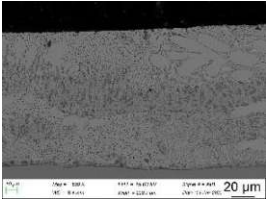
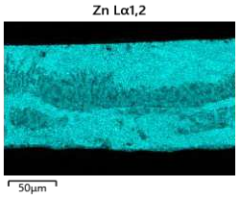
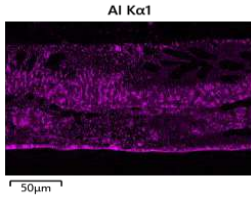
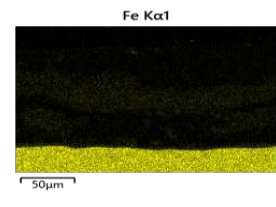
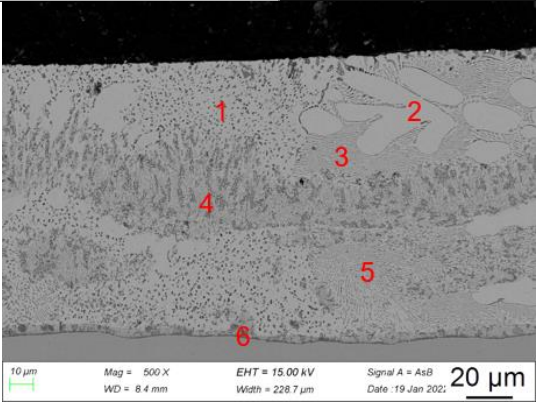
As for the tendency it follows the pattern, that the zinc amount increases towards the surface.

6.6.4.2 X-MZ coated samples

The X-MZ coated MT BR-40 04 sample was investigated on the baseplate and on the channel (Table 26).

Table 26 WP2 DDZ SEM images and EDX mapping of MT BR-40 04 with X-MZ coating on baseplate and channel

SEM images of X-MZ coated samples of MT BR-40 04							
MT BR-40 04 chan							
	X-MZ Xm5m SEM os	X-MZ Xm5m Zn mapping	X-MZ Xm5m Al mapping	X-MZ Xm5m Fe mapping			
							

<p>For the externally coated X-MZ samples, the same elements were found being present in the coating. Near the substrate a layer consisting of approximately 51 wt% Al, 29 wt% Fe and 19 wt% Zn was found. All over the cross section a ternary mixed phase was found resembling of 16 – 17 wt% Al, 6 – 9 wt% Fe and 73 – 78 wt% Zn. In between the ternary phase, pure zinc grains were found.</p>																																																				
<p>MT BR-40 04 BP</p>																																																				
	<p>X-MZ Xm5m SEM BP</p>	<p>X-MZ Xm5m Zn mapping</p>	<p>X-MZ Xm5m Al mapping</p>	<p>X-MZ Xm5m Fe mapping</p>																																																
			<table border="1"> <thead> <tr> <th></th> <th>Zn</th> <th>Fe</th> <th>Al</th> <th>Si</th> <th>Prop</th> </tr> <tr> <th>No.</th> <th>Wt %</th> <th>Wt %</th> <th>Wt %</th> <th>Wt %</th> <th></th> </tr> </thead> <tbody> <tr> <td>1</td> <td>91</td> <td></td> <td>9</td> <td></td> <td>Zn-5Al</td> </tr> <tr> <td>2</td> <td>99</td> <td></td> <td>1</td> <td></td> <td>Zn-0.3Al</td> </tr> <tr> <td>3</td> <td>93.6</td> <td>0.4</td> <td>6</td> <td></td> <td>Zn-5Al</td> </tr> <tr> <td>4</td> <td>80</td> <td>7.4</td> <td>12.3</td> <td>0.3</td> <td>Fe₂Al₃Zn_x</td> </tr> <tr> <td>5</td> <td>91</td> <td>1</td> <td>8</td> <td></td> <td>Zn-5Al</td> </tr> <tr> <td>6</td> <td>33</td> <td>16</td> <td>50</td> <td>0.9</td> <td>Fe₂Al₅Zn_x</td> </tr> </tbody> </table>				Zn	Fe	Al	Si	Prop	No.	Wt %	Wt %	Wt %	Wt %		1	91		9		Zn-5Al	2	99		1		Zn-0.3Al	3	93.6	0.4	6		Zn-5Al	4	80	7.4	12.3	0.3	Fe ₂ Al ₃ Zn _x	5	91	1	8		Zn-5Al	6	33	16	50	0.9
	Zn	Fe	Al	Si	Prop																																															
No.	Wt %	Wt %	Wt %	Wt %																																																
1	91		9		Zn-5Al																																															
2	99		1		Zn-0.3Al																																															
3	93.6	0.4	6		Zn-5Al																																															
4	80	7.4	12.3	0.3	Fe ₂ Al ₃ Zn _x																																															
5	91	1	8		Zn-5Al																																															
6	33	16	50	0.9	Fe ₂ Al ₅ Zn _x																																															
<p>On the baseplate of the X-MZ coated sample the layer closest to the substrate is coloured a little darker, indicating a ternary phase with a high content of Al (50 wt%) and Fe (16 wt%) and 33 wt% Zn. On top of that, various phases are found in a zinc rich matrix. Towards the outer coating area, the amount of zinc is found to increase, also zinc grains are visible.</p>																																																				

Die approbierte gedruckte Originalversion dieser Diplomarbeit ist an der TU Wien Bibliothek verfügbar
 The approved original version of this thesis is available in print at TU Wien Bibliothek.



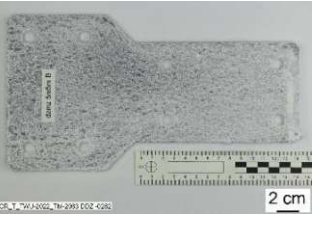

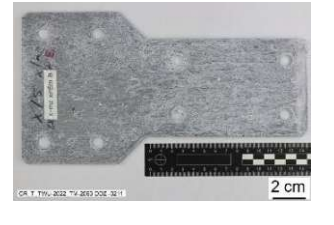
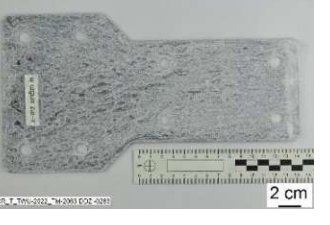
6.6.5 Accelerated corrosion: Photographs of DDZ WP2

For the accelerated corrosion test, the NSST and CCT test method were used on the samples indicated in 5.2.

6.6.5.1 WP2 DDZ CCT samples

The CCT cycle applied for the DZMZ and X-MZ coated samples shown in *Table 27* and is conducted as described under 4.3.2.

Table 27 WP2 DDZ CCT samples with X-MZ and DZMZ coating

CCT	0 weeks	2 weeks	5 weeks
DZMZ			
	DZMZ 5m5m B	DZMZ 5m5m B	DZMZ 5m5m B
X-MZ			
	X-MZ Xm5m B	X-MZ Xm5m B	X-MZ Xm5m B




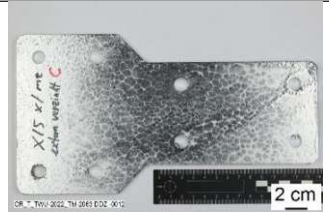


For the accelerated corrosion test the DZMZ and X-MZ samples were inserted in the CCT for a duration of 6 weeks.

After visual inspection a small white rust layer was found with an even thickness covering the entire sample. The samples were inserted in the chamber in an inclined position, where the left side was placed on a grid with a 2 cm height. The corrosion products form a wavelike pattern in the direction of the draining saltwater.

6.6.5.2 WP2 DDZ NSST samples

The NSST applied to the DZMZ and X-MZ coated samples shown in *Table 28* and is conducted as described under 4.3.1.

Table 28 WP2 DDZ NSST samples with X-MZ and DZMZ coating

NSST	0 weeks	3 weeks	6 weeks
DZMZ			
	DZMZ 5m5m C	DZMZ 5m5m C	DZMZ 5m5m C
X-MZ			
	X-MZ Xm5m C	X-MZ Xm5m C	X-MZ Xm5m C

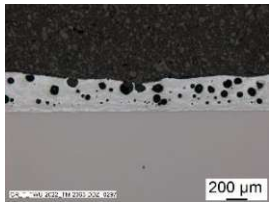
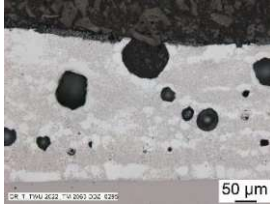
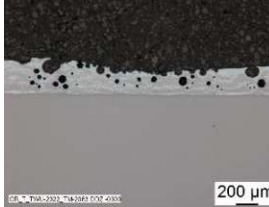
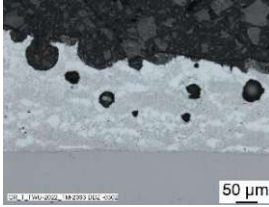

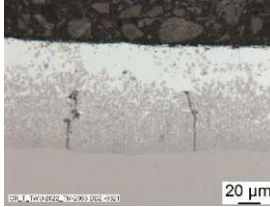
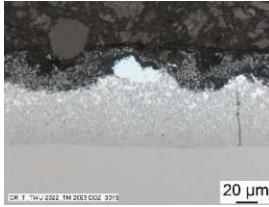

For the accelerated corrosion test the DZMZ and X-MZ samples were inserted in the neutral salt spray test for a duration of 6 weeks.

After visual inspection a voluminous white rust layer was found with a thickness of up to 5 mm at the bottom (right side of each sample photograph) but covering the entire sample. The samples were inserted in the chamber in an inclined position, where the left side was placed on a grid with a 2 cm height. The corrosion products form a wavelike pattern in the direction of the draining saltwater.

6.6.6 Accelerated corrosion: LOM of DDZ WP2

For electrochemistry tested samples, the LOM images of the cross sections of the MT-C-GLP T samples were obtained before inserting (=0w) in the CWTC and after one week (=1w) of exposure (Table 29).

Table 29 WP2 DDZ LOM images of CWTC exposed samples including electrochemistry after polarization measured spots of DZMZ and X-MZ coated samples

DZMZ				
	DZMZ 5m5m A CWTC 0w	DZMZ 5m5m A CWTC 1w	DZMZ 5m5m A ELCHEM 0w	DZMZ 5m5m A ELCHEM 1w
X-MZ				
	X-MZ Xm5m A CWTC 0w	X-MZ Xm5m A CWTC 1w	X-MZ Xm5m A ELCHEM 0w	X-MZ Xm5m A ELCHEM 1w

The specific DZMZ sample for electrochemistry is showing holes in the coating. The coating microstructure is not clearly obtainable as it is a random deposition of mixed phases in a zinc rich matrix phase. Also, the coating thickness is varying all over the sample and a lightly dark grey coloured corroded outer layer is found after visual inspection of the cross section.

The X-MZ coated samples were inserted in the CWTC and the LOM of the CS of the corroded electrochemistry measured sample spots show clear corrosion signs of the originally zinc rich outer phases of the coating, indicated by the black coloured outer coating layer of the sample. On the other hand, the investigation of the X-MZ samples on the non-electrochemistry measured areas show cracks in the layer near the substrate but other than that, they are not deviating in their appearance after 1w of CWTC.

6.6.7 Electrochemistry measurements of DDZ WP2

As WP2 was conducted after the WP1 towards the end of the thesis, the electrochemistry measurements were conducted used samples exposed to CWTC for one week.

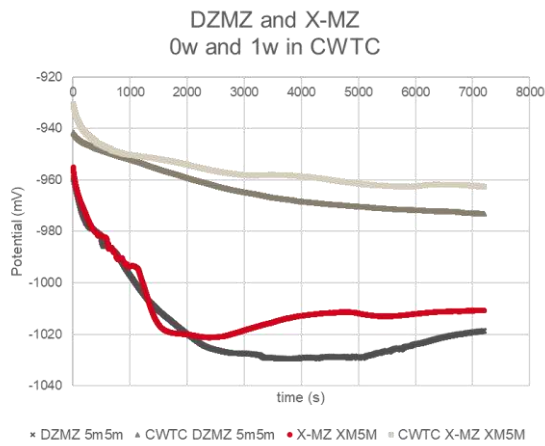


Figure 29 WP2 DZZ OCP of DZMZ and X-MZ after 0w and 1w in CWTC against Ag/AgCl (3M KCl)

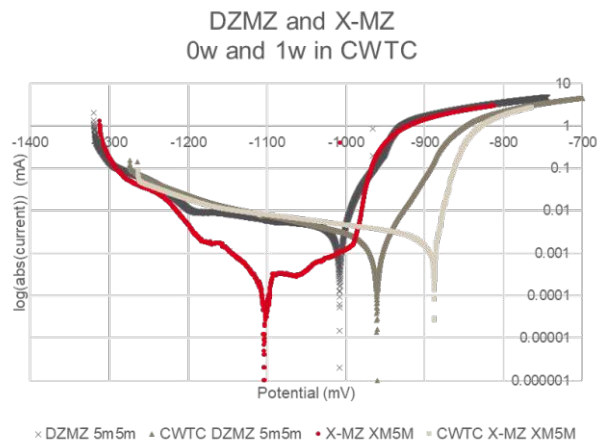


Figure 30 DZMZ and X-MZ current potential plot after 0w and 1w in CWTC against Ag/AgCl (3M KCl)

The 7 days in CWTC increased the OCP (Figure 29) in both coatings. For the DZMZ coating the starting potential was at a range of -960 mV to -1030 mV and after exposure of one week (=1w) in CWTC the OCP was increased to a range of -940 mV to -970 mV. In the individual time span the potential dropped continuously. For the X-MZ coating the starting OCP was at a range of -965 mV to -1020 mV and after exposure of 1w in CWTC the OCP was increased to a range of -930 mV to -960 mV. In the individual time span the potential dropped continuously.

For the current potential curve (Figure 30), the unexposed DZMZ and X-MX samples show a lower potential as the 1-week CWTC exposed samples.

The left branch of the polarization curve (Figure 30) indicates a cathodic reaction, like an oxide/oxygen reduction. The steady flat incline of the left branch indicates a resistance of the diffusion processes due to top layer formation. A topcoat of corrosion products can be non-conductive and lead to a flat horizontal branch. The cathodic reaction stays the same after exposure to the CWTC test on DZMZ coated samples. On the right side the anodic branch is visible, and the increased incline at the polarization curve after exposure is resembling the metal dissolution. As the increased incline of the anodic branch is the only influence after exposure, the corrosion potential is shifting to a higher potential. Which means, the corrosion potential increased when measured after exposing the samples to the corrosion test. However, the X-MZ unexposed sample curve (red) shows a passive layer formation which stays intact until to a corrosion potential of -1000 mV is reached. After that, the incline of the anodic branch is indicating that the metal is dissolving.

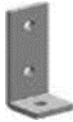











The intersection between the anodic and cathodic branch of the polarization curve indicates the corrosion current. The corrosion current stays approximately on the same level for all specimen analysed, but the red plot of the X-MZ sample, where it is not clearly measurable.









6.7 Zinc Diffusion Coatings

6.7.1 Photographs of Zinc Diffusion samples

First, the samples sent to us from special coaters from China were photographed. No information about the coating parameters were given, so it is viewed as a comparison to the DDZ. An overview of the samples is shown in *Table 30*.

Table 30 Zinc Diffusion coating sample photographs

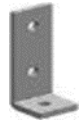
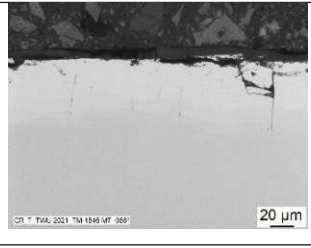
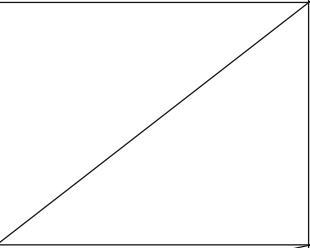

Name	Picture	ZAD	ZAD	ZND
MT-C-L2 OC				
		ZAD60	ZAD80	ZND60
		Slightly rough medium grey surface with white patches formed in strips and angles were found.	Slightly rough medium grey surface with white patches formed in strips and angles were found.	Smooth matte dark-grey surface, small bubbles found near edges. Some light grey patches were observed.
MT-C-T/1 OC				
		ZAD60	ZAD80	ZND60
		Slightly rough, medium grey surface with small white patches near edges observed	Slightly rough, medium grey surface, small white patches near edges observed	Smooth matte dark-grey surface, small bubble-shaped detachment of top coating found near edges.
MT-TL M10 OC				
		ZAD60	ZAD30	ZND60
		Fine roughness, medium grey surface, small white patches observed near edges	Matte-grey surface with small imperfections in the coating quality.	Optically flawless coating appearance.






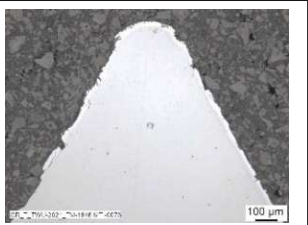
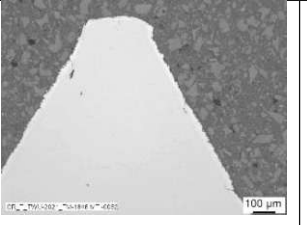
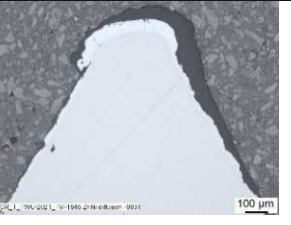

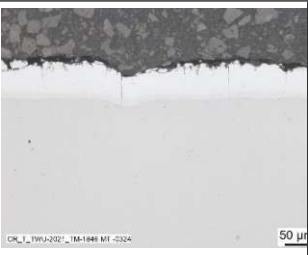
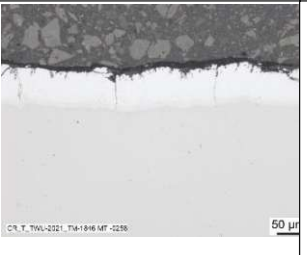
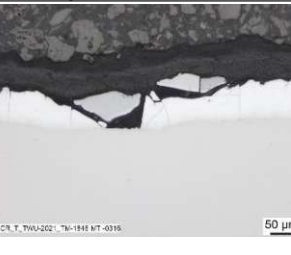
MT-TLB OC				
		ZAD60	ZAD30	ZND60
		Buildup of white appearing substance in the valleys of the thread.	Fine light-greyish sprinkles observed in thread. Head coated with fine distribution of white appearing sprinkles.	Uniform coating appearance all over thread and head.
MT-BR-40 1000 OC				
		ZAD100	ZAD120	ZND60
		Overall even coating observed, small greyish-white scratches found, suspected from handling.	Overall even coating observed, multiple fine greyish-white scratches found, suspected from handling.	Smooth matte dark-grey surface, small bubble-shaped detachment of top coating found near edges.

6.7.2 Cross sections LOM images of Zinc Diffusion coatings

A selection of cross sections of Zinc Diffusion Coatings is shown in *Table 31*.

Table 31 Zinc Diffusion Coatings CS LOM


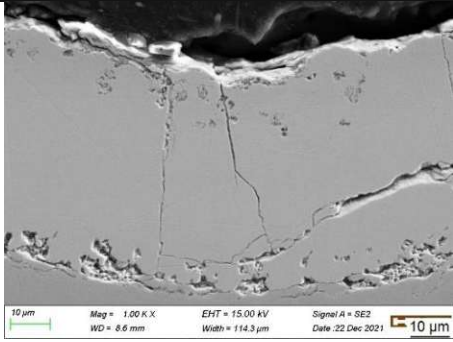
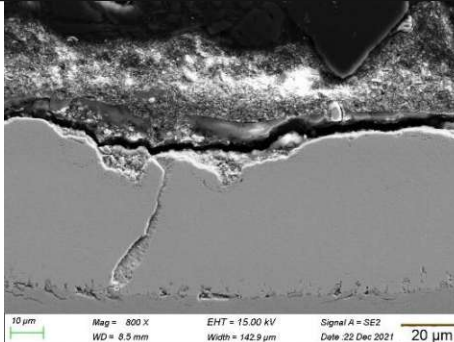
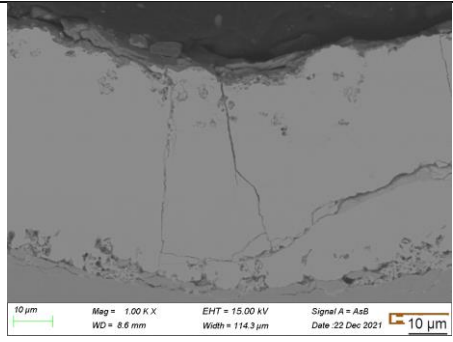
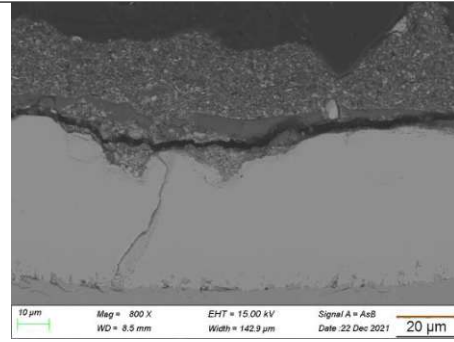
Name	Picture	ZAD	ZAD	ZND
MT-C-L2 OC				
		ZAD60 front		CCT0h_ZND front
Description		Small black layer on top, seems not to be level with the coating.		Visible black top coating layer.

<p>MT-C-T/1 OC</p> 			
<p>Description</p>	<p>ZAD 60 top</p> <p>Substrate with rough outline, coating with darker grey shade near substrate and silvery white near surface. The coating was found to be rough. Small cracks were seen prolonging towards the substrate.</p>	<p>ZAD 80 top</p> <p>Substrate is found to be uneven, coating with darker grey shade near substrate and silvery white near surface. The coating was found to be rough. Small cracks were seen prolonging towards the substrate.</p>	<p>ZND60 top</p> <p>Substrate is found to be uneven, substrate is diffusing up to the zinc rich coating layer. Small cracks were found starting from the zinc outline progressing in the direction of the substrate. Black topcoat visible.</p>
<p>MT-TLB OC</p> 			
<p>Description</p>	<p>ZAD60 thread</p> <p>Coating uneven around thread. In the valleys of the thread, a buildup of the black coating outline observed.</p>	<p>ZAD30 thread</p> <p>The diffusion coating is of equal quality on the tip and the valley of the thread.</p>	<p>ZND60 thread</p> <p>In the valleys, the coating thickness is less than on the peaks of the thread. On the peak appears to be a buildup of the zinc-rich coating. The black topcoat builds up in the valleys of the thread.</p>
<p>MT-BR-40 1000 OC</p> 			
<p>Description</p>	<p>ZAD100 is</p> <p>Even substrate layer with small grey layer on top before zinc rich coating layer. On top is a small black coating. Small cracks prolong, starting from the surface outline down to the substrate.</p>	<p>ZAD120 is</p> <p>Even substrate layer with small grey layer on top before zinc rich coating layer. On top is a small black coating. Small cracks prolong, starting from the surface outline down to the substrate.</p>	<p>ZND60 is</p> <p>Cracks and dislocations found in the metallic zinc coating, but evenly coated with black topcoat layer. No Zinc exposed to surface.</p>

6.7.3 SEM images of Zinc Diffusion Coatings

Of the MT-C-L2 OC sample CS, SEM images were obtained, to compare ZAD and ZND coatings as seen in Table 32.

Table 32 Zinc Diffusion Coatings CS SEM

Name Picture	De- tector	ZAD	ZND
MT-C- L2 OC 	SE2		
		CCT0w ZAD60 SEM top	CCT0w ZND60 SEM top
	AsB		
		CCT0w ZAD60 SEM top ASB	CCT0w ZND60 SEM top

For the ZAD coated samples close to the surface on the outline of the coating, a 90 % Zn and 10 % Fe were measured, closely matching the δ -Phase ($FeZn_{10}$) composition. Near the substrate, a composition of 80 % Zn and 20 % Fe was found matching the Fe_5Zn_{21} or Γ_1 -phase description.

For the construction steel substrate, a Mn content of 1.1 wt% was measured.

The organic coating layer of the ZND samples with the fine structure on top was measured with EDX and found to be purely organic. C and O are mainly detected in the EDX. Furthermore 17 wt% Ti, 7 wt% Ba, 3.5 wt% Ca, 2.1 wt% Pb, 1.9 wt% Zn including small quantities of other elements were found. Ti is probably added as TiO_2 filler.

For the zinc diffusion coating, a composition of 91 wt% Zn with 9 % Fe matching the δ -Phase ($FeZn_{10}$) was found near the organic layer touching the metallic coating surface. Close to the substrate, a concentration of 85 wt% Zn with 15 wt% Fe was found (Γ_1 - or Γ phase).

For the iron substrate, a construction steel, a Mn content of 1 wt% was measured.

6.7.4 Accelerated corrosion: Photographs of Zinc Diffusion Coatings












LOM images of the starting point (0w), after seven and twelve weeks in CCT and after twelve weeks in NSST are compared in *Table 33*.

The NSST samples were tested by colleagues in the Hilti China subsidiary. To have a comparison, the samples were sent to Hilti Schaan to investigate them further in terms of appearance and electrochemical properties.

Table 33 Zinc Diffusion Coatings CCT Photographs

Name	Time	ZAD	ZAD	ZND
MT-TL M10 OC	0w CCT			
		ZAD60	ZAD30	ZND60
	7w CCT			
		ZAD60	ZAD30	ZND60
	12w CCT			
		ZAD60	ZAD30	ZND60
<p>The ZAD 60 coated samples show the formation of very fine patches of white rust on the surface after 1 week in CCT. It increases over a course of 12 weeks of CCT where single thick round spots of white rust form on 1 - 3 locations of the sample surface.</p> <p>It was found that the ZAD 30 coated samples showed a fine white rust layer on the surface after 1-week CCT and red rust starting from the inner hole after 3 weeks in CCT. After 12 weeks on the surface of the sample multiple small red rust spots were obtained on the same sample.</p> <p>The ZND samples, showed a very slight hint of red rust on the hole of the inner edge after 5 weeks in CCT. The sample did not show an increase of corrosion products after visual inspection after 12 weeks in CCT.</p>				

Die approbierte gedruckte Originalversion dieser Diplomarbeit ist an der TU Wien Bibliothek verfügbar
 The approved original version of this thesis is available in print at TU Wien Bibliothek.


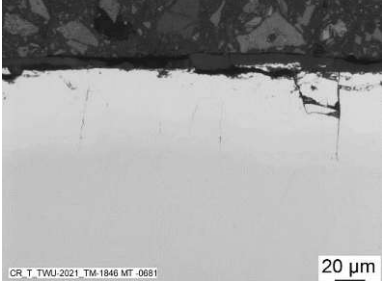

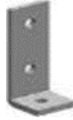
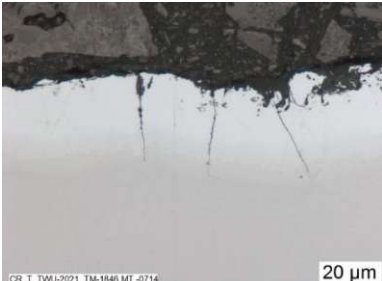




MT-C-L2 OC	0w CCT	 ZAD60	 ZAD80	 ZND60
	7w CCT	 ZAD60	 ZAD 80	 ZND60
	12w CCT	 ZAD60	 ZAD 80	 ZND60
	<p>On all MT-C-L2 OC samples no red rust was found during the 12 week CCT investigation period.</p> <p>However white rust formed on ZAD 60 after one week, at ZAD 80 after 5 weeks. The ZND 60 sample showed just one exception of a very small white rust formation after 12 weeks CCT.</p>			
	12w NSS T	 2 cm	/	 5 mm
	<p>After 12 weeks NSS T the ZAD sample showed clear red rust formations starting from single spots and are distributed aerially along the surface after time. As the samples were not placed in the same direction or rotation in the NSS T as they were in the CCT, a direct comparison is not possible.</p>			

Die approbierte gedruckte Originalversion dieser Diplomarbeit ist an der TU Wien Bibliothek verfügbar
 The approved original version of this thesis is available in print at TU Wien Bibliothek.

6.7.5 Accelerated corrosion: LOM of Zinc Diffusion Coatings

Of the obtained MT-C-L2 OC samples from 0w CCT and 12w CCT cross sections are compared in *Table 34*.

Table 34 Zinc Diffusion Coatings CCT and NSST LOM

Name	Picture	ZAD	ZND
0w CCT		 <small>CR_T_TWUJ-2021_TM-1846 MT -0681</small> 20 µm	 <small>CR_T_TWUJ-2021_TM-1846 MT -0690</small> 20 µm
		CCT0w ZAD front	CCT0w ZND front
12w CCT		 <small>CR_T_TWUJ-2021_TM-1846 MT -0714</small> 20 µm	 <small>CR_T_TWUJ-2021_TM-1846 MT -0732</small> 20 µm
		CCT12w ZAD front	CCT12w ZND front
12w NSST		 <small>CR_T_TWUJ-2021_TM-1846 MT -0793</small> 20 µm	 <small>CR_T_TWUJ-2021_TM-1846 MT -0827</small> 10 µm
		NSST12w ZAD front	NSST12w ZND front

After 12 weeks in CCT the CS of the ZAD MT-C-L2 OC sample showed corrosion signs only on the very top outer surface layer, rich in zinc. On the outer end of the coating vertical cracks, proposing pitting corrosion are found. Some dark grey spots formed as well. After 12 weeks in NSST the volume of the dark grey rusty spots increased also at the areas between the coating and the substrate. A thick red-brown outer top-layer formed as well.

The ZND coating CS of the MT-C-L2 OC sample showed minimal signs of corrosion on the outermost micrometer of the coating layer after 12 weeks in CCT. After 12 weeks in NSST more prominent corrosion products formed along the outer zinc rich phase and even between the substrate and the coating. Ocre brown spots are visible in the outer organic layer after inspection of the CS.

Die approbierte gedruckte Originalversion dieser Diplomarbeit ist an der TU Wien Bibliothek verfügbar. The approved original version of this thesis is available in print at TU Wien Bibliothek.

6.7.6 Electrochemistry of Zinc Diffusion Coatings

The open circuit potential was measured on the ZAD coated and on the ZND coated samples in different corrosion states. Every measurement series contains four samples: 0 weeks (starting point), 7 weeks and 12 weeks in CCT and 12 weeks in NSST. The measurements were carried out using the FlatCell and the ECMwin software.

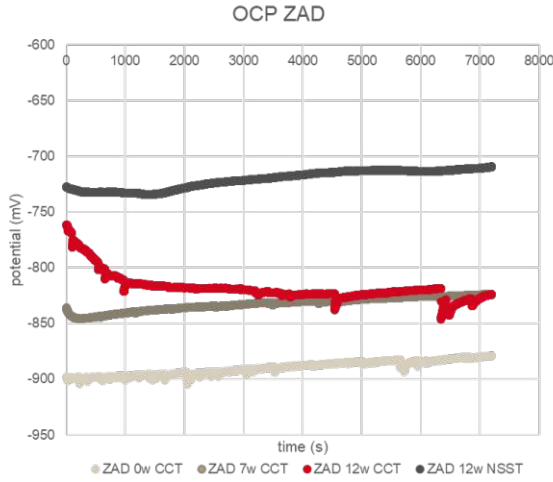


Figure 31 Electrochemistry measurement: OCP of ZAD coated zinc diffusion samples against Ag/AgCl (3M KCl) RE

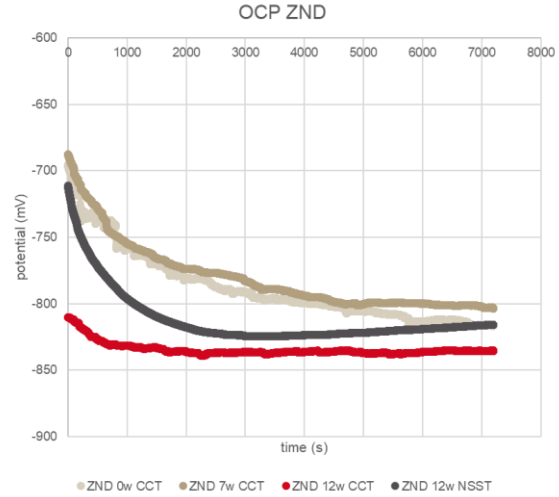


Figure 32 Electrochemistry measurement: OCP of ZND coated zinc diffusion samples against Ag/AgCl (3M KCl) RE

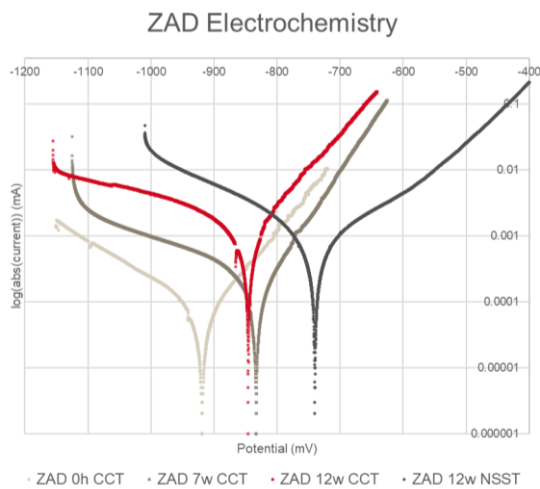


Figure 33 Electrochemistry measurement: Current-potential plot of ZAD coated zinc diffusion samples against Ag/AgCl (3M KCl) RE

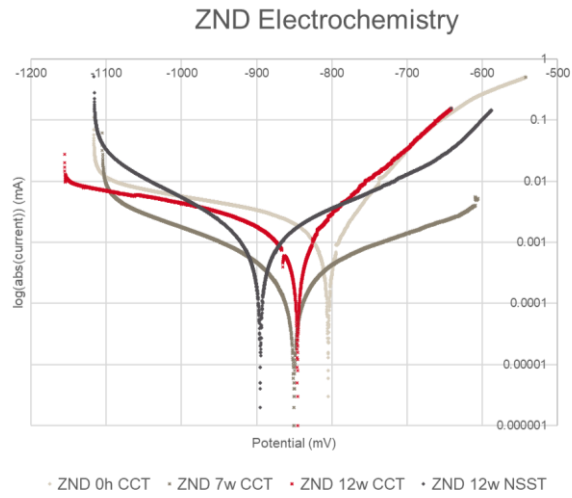


Figure 34 Electrochemistry measurement: Current-potential plot of ZND coated zinc diffusion samples against Ag/AgCl (3M KCl) RE

The OCP measurements of the different ZAD samples (Figure 31) after a measuring time of two hours is rising from -900 mV to -720 mV continuously after an increased corrosion test exposure time span of the samples.

The OCP measurements of the different ZND samples (Figure 32) after a measuring time of two hours shows lowering tendencies from -700 mV to -830 mV after an increased corrosion exposure time span of the samples. After the 12-week exposure time, the OCP is lower than after the 0 week or 7 week exposure time.

For the ZAD coating, after investigating the accelerated corrosion samples, the corrosion potentials were shifted towards a more positive direction starting from -930 mV to -740 mV (*Figure 33*). This is mainly, because the cathodic branch is clearly increasing in y-direction of the plot after the specimen were exposed to the accelerated corrosion test. As the incline of the left side of the polarization curve increases, the intersection between the anodic and cathodic branch rises as well in x- and y- direction of the plot, if every sample is compared. This explains the rise of the corrosion potential after time. Also, the corrosion current is rising with factor 10 after exposure of the specimen to the accelerated corrosion test, as more corrosion products formed over time.

For the ZND samples, the corrosion potential sank in a negative direction over a range of nearly 100 mV starting at -800 mV (*Figure 34*). If the first sample without exposure is compared to the 7 weeks and 12 weeks exposed sample, it is found, that both anodic and cathodic reactions decreased in incline. The corrosion potential sank as a result, as well as the corrosion current. After exposing the specimen to 12 weeks NSST, the cathodic branch of the polarization curve was steeper compared to all samples before. Also, the anodic branch was found to be less inclined than before exposure. This leads to an increase of the corrosion current with a further decreased corrosion potential. To sum it up, no clear tendencies are to be found in terms of the corrosion mechanism when comparing the different exposed ZND samples.













6.8 Multilayer Zinc Coating

The multilayer coating is investigated on mechanical system connection Hilti parts.

6.8.1 Photographs of Multilayer Zinc Coatings

The multilayer zinc coating samples were photographed and notes about the appearance were added to the description in *Table 35*.






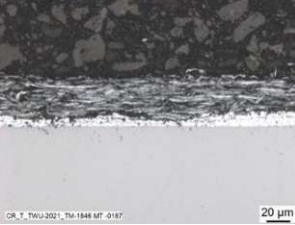


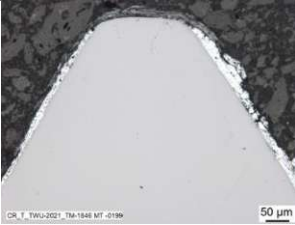
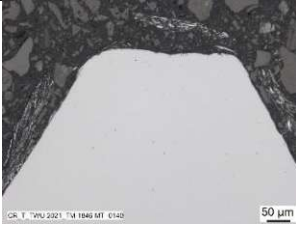
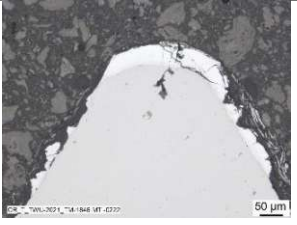
Table 35 Multilayer zinc coating photographs

Name	Picture	MP+TC	ZB+TC	ZAD +ZT
MT-TL M10 OC				
		MP+TC	ZB+TC	ZAD +ZT
Description		Grey with a slight green-yellow tint colored evenly coated samples.	Grey coating layer, shiny finish.	Silvery shiny seek coated appearance of coating.
MT-TLB OC				
		MP+TC	ZB+TC	ZAD +ZT
Description		Grey with a slight green-yellow tint colored evenly coated samples.	Grey coating layer, shiny finish, view black spots visible on edges of screwhead. Brittle coating and flakes are falling off.	View black spots on thread, even coating observed.
MT-TFB OC				
		MP+TC	ZB+TC	ZAD +ZT
Description		Gold brown silver colored, homogenous coating neither brittle nor flaky.	Grey coating layer, shiny finish, view black spots visible on edges of screwhead. Brittle coating and flakes are falling off.	Grey coating with very few black spots, very fine grains gritty finish

6.8.2 Cross sections LOM images of Multilayer Zinc Coatings

Additionally, the cross sections were investigated using the LOM. The sample images and descriptions can be found in *Table 36*.

Table 36 Multilayer Zinc Coating LOM CS

Name & Picture	MP+TC	ZB+TC	ZAD +ZT
MT-TL M10 OC 			
	MP+TC	ZB+TC	ZAD +ZT
MT-TFB OC 			
	MP+TC head	ZB+TC head	ZAD +ZT head
			
	MP+TC thread	ZB+TC thread	ZAD+ZT thread

For the MP+TC coated samples, the metallic layer right above the surface appears white and is showing spherical shaped particles in some places of the cross sections typical for mechanically plated specimen. The outer coating layer is found to be a lamellar build-up of silvery strips in a black appearing matrix (=flake coating).

On the inside of the MT- TL M10 OC sample both coating layers are thicker compared to the outside. On the MT-TFB OC there is a build-up of the white metallic layer in the valley of the thread and a build-up of the flaky top-layer on the tip of the thread.

The ZB+TC layer shows a flaky silvery layer in a black appearing matrix. The layers are distributed horizontally to the substrate. The two different coating layers cannot be distinguished visually.

In the inner corners of the MT-TL M10 OC samples a build-up of the coatings was observed. The coating is generally thinner on the outside of these samples.













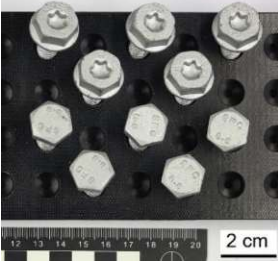
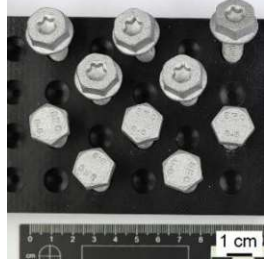
There is a build-up of the metallic layer found in the valleys of the thread of MT-TFB OC.

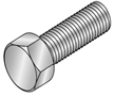

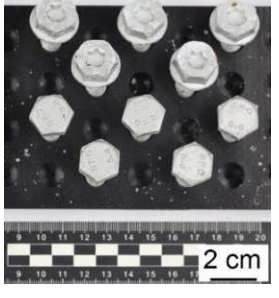
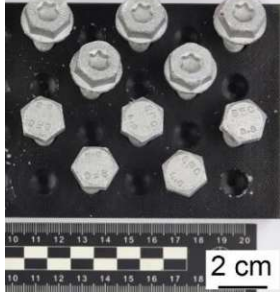



The ZAD+ZT coating is consisting of two different layers, first it appears to be a white metallic layer near the substrate and on very few spots on the sample there is also a black build-up with some silvery inlays. The metallic layer builds up on top of the thread, whereas the black layer is accumulated in the valleys. On the MT-TL M10 sample the topcoat is nearly not found on the outside of the sample.

6.8.3 Accelerated corrosion: Photographs of Multilayer Zinc Coatings

As a multilayer coating is the current standard coating for the smaller parts of the Hilti MT-System, also a variation was investigated in the accelerated corrosion CCT for 12 weeks, see Table 37.

Table 37 Multilayer Zinc Coating CCT

Name	Time	MP+TC	ZB+TC	ZAD +ZT
MT-TL M10 OC 	0w			
		MP+TC	ZB+TC	ZAD +ZT
	7w			
		MP+TC	ZB+TC	ZAD +ZT
	12w			
		MP+TC	ZB+TC	ZAD +ZT
Description		<p>Very slight hint of corrosion starting in the inner thread of MT-TL M10 after 12 weeks in CCT.</p>	<p>Corrosion starts at the edges of the hole, in the middle and thread area below the hole after 3 weeks in CCT. Some samples show little red rust on the top and bottom edge as well.</p> <p>After 12 weeks in the CCT red rust is starting to form the hole in the middle.</p>	<p>Slight occurrence of red rust on top and bottom edges after 8 weeks. Hole in the middle remains without visible corrosion phenomenon after 8 weeks in CCT.</p> <p>After 12 weeks in CCT there are red rust spots visible around the sharp edges on top and bottom and around the hole in the middle.</p>
MT-TFB OC  &	0w			
		MP+TC	ZB+TC	ZAD +ZT

<p>MT-TLB OC</p> 	7w			
		MP+TC	ZB+TC	ZAD +ZT
	12w			
		MP+TC	ZB+TC	ZAD +ZT
Description	<p>No corrosion findings after visual inspection after 12 weeks in CCT.</p>		<p>Corrosion starts at the edges of the MT-TFB OC head after 3 weeks. It starts spot-wise along the edge and after 12 weeks red rust is clearly visible over the head and on the thread of MT- TFB OC.</p> <p>For the MT-TLB samples corrosion starts after 7 weeks CCT. After 12 weeks some spots with red rust are visible on the screw head.</p>	<p>Slight occurrence of red rust on top and bottom edges after 8 weeks. After 12 weeks, a increase of the slight spots was found on MT-TFB OC samples. The MT-TLB samples show visually no corrosion phenomenon after 12 weeks CCT.</p>

7 Discussion

7.1 Double Dip Zinc WP1

7.1.1 Sandelin samples

7.1.1.1 Single Dip

The photographs of the single dipped Sandelin samples showed the typical Sandelin pattern indicated by D. Kopycinski, E. Guzik. (23). Also, the light blue shine on the outer zinc layer was found visible in the single dipped samples. (3)

The technical zinc bath (=DZ) samples showed a matte finish, this could be explained with the cooling conditions. For the cooling conditions, diffusion of iron and zinc continues after the samples are removed from the zinc bath. It is significantly slower and nearly stops at a temperature below 200 °C. If all zinc from the surface is consumed by the formation of an iron-zinc alloy the sample surface appears matte grey visually. (11)

The described linear coating growth indicated by Wolf Dieter Schulz and Marc Thiele was found as well. (2) The roughness was found to increase accordingly with the dipping time. (2) Furthermore, the high standard variations for the longer dipping times seconds this finding.

Regarding the coating thickness measurement method, it is important to mention, that the coating thickness is not representative for the whole sample. Only a small section as broad as 2 cm was cut out in the middle of the sample and the coating thickness was measured digitally on the obtained LOM images of the cross sections. The measuring distance of the three comparative measurement points on each sample side (top and bottom) were between 50 µm - 200 µm apart. This holds true for all the coating thickness measurements of the thesis.

The prominent hard zinc ζ-phase (FeZn_{13}) formed homogeneously all over the cross section of the coating embedded in a solidified zinc melt (η-zinc). (2) The coating layer is Zn rich and showing a higher Fe content near the substrate which is gradually lower towards the outer coating surface.

The surface roughness could be an effect of the thermal processing of the substrate and the high energy demand of annealing. *Figure 35* resembles the influence of annealing in a mixed structure on steel with a contaminated surface layer. This looks just like the cross sections obtained in the thesis on single dipped Sandelin samples. Very long pickling times would help to improve the surface layer of the steel, as proposed by Kuklic and Kudlacek. (11)

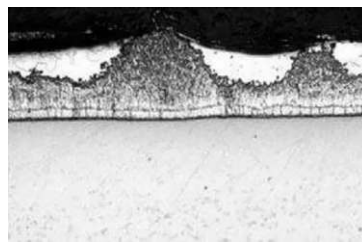


Figure 35 CS of annealing effect of zinc coated steel sample (11)

7.1.1.2 Double dip

The optical appearance is described as leopard-like in the thesis. However, this is found in literature (22) as a single dipped coating appearance. The shininess is due to Zn- and Al-rich phases towards the top, as seen in the microstructure of the samples.

The dip time was varying in the first dip as well as in the second dip step, the microstructure was as follows:

Like in theory (27) of the double dip process findings, the microstructure appeared similarly in the samples of the thesis. On most samples a thin layer consisting of the δ-phase $\text{FeZn}_{10}\text{Al}_x$ – FeZn_7Al_x has formed between substrate and coating. On top of that, in all double dipped

Sandelin samples a layer consisting of $\text{Fe}_2\text{Al}_3\text{Zn}_x$ (27), (12) in a η -zinc rich matrix was very likely found. Towards the top, just like in the literature, zinc grains are visible more often. (27), (12)

The exception holds true for the SBZN10m1m sample, where the dipping time was not long enough in the second dip bath to get a full reaction of the alloying aluminum with the steel substrate. Therefore, the bottom layer simply was the described single dip layer without the otherwise formed inhibition layer. After a clear separation of the single dipped and double dipped microstructure, a otherwise so prominent $\text{Fe}_2\text{Al}_3\text{Zn}_x$ -rich area in a zinc matrix formed in the double dipped top half.

Another issue is the variation of the second dip with a fixed 5-minute first dip. Regarding the appearance and Sandelin effect, the samples also follow the trend described for all other double dipped Sandelin samples. (22)

The inhibition layer formed prominently between substrate and coating could be the $\text{Fe}_2\text{Al}_5\text{Zn}_x$ layer, as suggested in the mappings. For these specific samples some droplets of the inhibition layer with round morphology ($\text{Fe}_2\text{Al}_5\text{Zn}_x$) were found in the EDX towards the surface of the cross section as well. While the samples show the same cross section zones as described in the literature (27), the field of study is quite new, and no approved explanations were found. Nevertheless, the theory (12) suggests the reason could be, that Al is suppressing the formation of the Zn-Fe layer. Due to a rapid formation of the FeAl_5 -rich inhibition layer, some Fe-Zn droplets form under it and perform an "outburst". This is like a mini-bomb or like a bursting bubble, forming droplets scattering towards the surface in the microstructure. This was described as ginkgo-like in this thesis after visual inspection of the CS microstructure.

Overall, an increase of the aluminium content of the second dip bath is found in the literature to lead to a more stable formation of the $\text{Fe}_2\text{Al}_5\text{Zn}_x$ inhibition layer. (12)

However, after sharing the findings with the external galvanizing partner, they indicated, due to the sheer volume of the double dip bath and the slow withdrawal of the dipped samples the one minute dipping time is not realistic for an industrial process. After scale-up a realistic immersion time would be between 3 - 7 minutes.

All in all, the Sandelin samples are not feasible to be investigated in further DDZ projects, as the process parameters in the industrial setting would lead to vastly varying coating thicknesses due to the Sandelin effect. The customer needs reliable products with clearly defined specifications and lifetime in corrosive environments.

7.1.2 MM standard construction steel samples

For all MM samples no parabolic coating thickness growth was found as it is proposed for a Sebisty steel substrate in the literature. (2)

7.1.2.1 Single Dip Zinc

The single dipped MM samples appear visually in a silvery shiny blue-grey matte surface structure equal to the pictures found in the literature. (22)

The coating thickness was found even on all samples with a lower standard deviation compared to the Sandelin samples.

For the microstructure, similarities to the low-silicon coatings are described in (2). The δ -Phase is around 25 μm thick and followed by a columnar ζ -phase with a Vickers hardness of $\text{HV} > 250$. Due to the high hardness the coating is prone to form cracks. Towards the surface the η -Phase is obtained. (2)

7.1.2.2 Double Dip Zinc

The double dipped samples are all found to have a fine, homogenous, smooth silvery surface with a mirror-like finish. Optically visual cracks or delamination occurrences are only found on 5m10m or 10m10m samples. The delamination is not progressing down to the substrate and

an overall coating is still obtained. Also, a build-up of the coating is found on the edges of the of the 5m10m dipped standard construction steel sample plates (= MM).

The microstructure on the cross sections of the double dipped MM coatings is not showing a uniform trend. Often, visible zinc-rich phases are found between ternary phases.

In the SEM and EDX analysis the series with the varying first dip and the 1m second dip as well as the series with the 5m first dip and the varying second dip time were analysed.

All four MM samples with the variation of the first dip time and a 1m second dip time, are showing a similar microstructure. Trending is the suspected $\text{Fe}_2\text{Al}_5\text{Zn}_x$ inhibition layer near the substrate (as indicated in the Sandelin samples). Thereafter a zinc rich area is obtained, on top of which either a $\text{Fe}_2\text{Al}_3\text{Zn}_x$ layer or a $\text{FeZn}_{10}\text{Al}_x - \text{FeZn}_7\text{Al}_x$ layer (phase δ) is proposed in every sample. The thickness of the $\text{Fe}_2\text{Al}_5\text{Zn}_x$ layer is found not to be correlating to the dipping time variations, increasing over time. On the 5m1m sample, the Zn-Al eutectic areas are alternating with zinc-rich grains and a zinc-rich matrix containing most likely of $\text{Fe}_2\text{Al}_3\text{Zn}_x$ in the middle of the coating. The area closest to the surface is shown to be rich of zinc grains surrounded by the Zn-Al eutectic.

For the other samples in the series, some $\text{Fe}_2\text{Al}_5\text{Zn}_x$ phases with round morphology are found between the zinc-rich phases in the outermost coating layer.

The MMZN samples with the first dip time of 5 min and the variation in the second dip also show similarities and tendencies.

The bottom layer is consisting most likely of $\text{Fe}_2\text{Al}_5\text{Zn}_x$ in every sample, as the dipping time increases, the layer thickness increases as well. On top of this darker layer, a layer with zinc grains and a Zn-Al eutectic around them, is formed. This second layer shows a clear horizontal separation towards the upper layer. The outermost layer is found to consist of a zinc matrix with a likeliness of a $\text{Fe}_2\text{Al}_3\text{Zn}_x$ ternary phases or a $\text{FeZn}_{10}\text{Al}_x - \text{FeZn}_7\text{Al}_x$ layer (phase δ) present. In between some randomly distributed round $\text{Fe}_2\text{Al}_5\text{Zn}_x$ droplets are found. The outermost areas show prominent zinc-rich grain structures, this is more likely to be found towards the top surface. The findings are similar to the literature of the Sandelin double dip sample discussion in 3.4.2.

The two bottom layers of the Fe-Al-Zn ternary layer followed by the Zn-Al eutectic stretch from around 10% of the overall coating thickness to 50% of the coating thickness as the dipping time prolongs from 1 minute to 10 minutes in the double dipped sample series.

It is likely, that proposed in the literature (12) due to the high reactivity of the FeAl_5Zn_x inhibition layer over time and by diffusion of elements, an increase of this part of the coating is formed. Whereas on top of the aluminum and iron rich layer, the surrounding liquid phase impoverishes of the more reactive elements and form a zinc-rich layer. (12)

A clear understanding of the phase formation in a thermodynamic or kinetic way is not possible, neither with the findings of the thesis, nor with the literature currently available.

Due to the above findings of 6.5, and with discussion of the galvanizing partner of Hilti, it was decided, that the most promising coating dip parameters in terms of feasibility to scale-up and corrosion protection are the 5m5m dipped plain specimen. Therefore, the Hilti-parts for 5.2 were coated with these parameters and investigated accordingly.

7.2 Double Dip Zinc WP2

The visual appearance of the double dipped DZMZ is finer than the double dipped X-MZ samples, showing a leopard like shiny smooth surface. On the MT BR-40 04 sample, different thicknesses of the base plate and the channel of the sample lead to small “black” spots.

For the cross sections obtained in the LOM there is no clear microstructure formation mechanism between the two different sides of the BP investigations attainable neither for the DZMZ coated sample, nor for the X-MZ coated sample. The microstructure is zinc-rich on the outside of both layers but shows a random distribution of the mixed phases between the substrate and the outer zinc-rich coating edge.

On both coating systems (X-MZ and DZMZ) next to the steel substrate an Al- and Fe-rich layer forms partly. Followed by ternary phases and on the outer edge by zinc-rich eutectic phases and pure zinc grains. A clear mechanism of microstructure formation cannot be found throughout the samples.

For the CCT test, both coatings performed equally and formed a thin topcoat of zinc corrosion products all over the sample after visual inspection.

The NSST showed a slightly more increased corrosion product formation on the X-MZ coated samples opposed to the DZMZ coated MT BR-40 04 samples. The thick coating layer was making cracking noises when they were removed for the photography documentation. After some time, the amorphous appearing corrosion products formed crystal-like structures. For atmospheric corrosion, the literature described the crystal formation of originally amorphous structures after a long exposure time of zinc samples in an Cl-rich environment. (38)

After the samples were exposed to the CTWC for one week, the electrochemistry measures showed, that the corrosion potential increased on all samples. The cathodic reduction branches of the specimen remained with a steady incline in all analysed specimen; a protective layer formed. The 1w CTWC exposed samples show a higher corrosion potential, as the anodic reaction is gaining more influence.

Compared to the zinc diffusion coatings, the DDZ WP2 coatings show a higher incline of the anodic branch of the current potential curve. This indicates a high reactivity in the anodic metal, thus both electrochemistry measured samples are not perfectly comparable, because of the different accelerated corrosion tests they were exposed to.

The CTWC exposed samples were also investigated regarding the cross section of the corroded samples. For the DZMZ coated sample, the cross-section microstructure shows numerous black coloured spherical appearing cavities all over the cross section even before exposure to CWTC. Thiele and Schulz (2) describe (*Figure 36*), that these are due to coating defects. They suggest that a flux containing Iron-chloride was not properly handled. It is found to be responsible for inserting humidity as of its hygroscopic properties. As due to hygroscopic properties, water is bound and the bubbles are forming in the coating, resulting in a higher coating thickness as well.

The X-MZ externally coated samples are deviating clearly on the spots exposed to the electrochemistry measurements. They form a darker corroded outer coating layer reaching about halfway through the coating. For the spots obtained in the LOM CS, not exposed to electrochemistry measurement, cracks are visible close to the substrate. It is proposed, by Thiele and Schulz (2) that the cracks are forming due to shrinkage and different thermal expansion coefficients of the steel substrate and the layer next to the substrate. The outer zinc-rich layer is cooling faster than the substrate, this induces additional stress to the sample prone to forming cracks. The cracks do not propagate to the outer surface of the coating and thus are not influencing the corrosion resistance of the outer zinc-rich layer or the cathodic protection process for the iron.

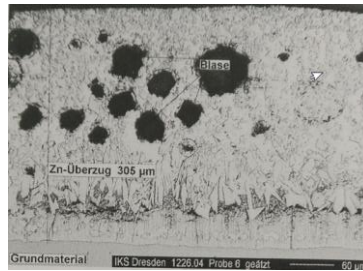


Figure 36 Bubbles forming in zinc coating due to coating mistakes (2)

7.3 Zinc Diffusion Coatings

7.3.1 ZAD Coating

After the visual inspection of the ZAD connector samples a slight roughness on a medium grey surface with small white patches near the sample edges was observed. On the screws, fine light-greyish sprinkles were found in the thread just as they were found on the head as well.

In the LOM images of the CS the substrate appeared with rough outlines resulting in a rough coating outline on some samples. The coating substrate was found to be medium-grey colored with a gradient color transitioning into the silvery white-grey colored shiny zinc diffusion coating. On the valleys of the screw thread the coating was found to be thinner than on the peaks or tips of the screw thread windings.

After the accelerated corrosion test, the ZAD MT-C-L2 OC sample showed corrosion signs only on the very top outer surface layer, rich in zinc and on the outer end of vertical coating cracks in the cross sections. After 12 weeks in NSST the volume of the dark grey rusty spots increased also at the spots between the coating and the substrate. The red rust formation after 12 weeks in NSST was also found in previous hilti projects. A thick red-brown outer top-layer formed as well.

It is found in the SEM and also in the LOM that the small black layer between specimen and embedding material, seems not to be on the same level as the zinc diffusion coating. The conclusion is, that the samples were not properly embedded and a cravis formed.

On some samples accumulated coating was found. This is mostly caused by the part geometry, as the buildup occurred mainly on threads which are especially prone to irregular coatings.

However in every sample, small cracks are found to prolong, starting from the surface outline down to the substrate. It is likely that these form due to deviating hardness and microstructure of the different phases that formed, just like described under 3.4.1.

For the microstructure the literature suggests that the darker grey layer near the α -Fe substrate is forming most likely a Γ -phase ($\text{Fe}_{11}\text{Zn}_{40}$) followed by a δ -phase (FeZn_{10}) towards the top. Typical for sherardized coatings is, that no η -zinc layer is formed towards the surface outline of the coating. (39) In some literature it is suggested that on the outer layer a very small ζ -phase (FeZn_{13}) is indicated. (6)

Due to the dominant zinc layer on top, and the higher reactivity of zinc compared to iron, an anodic oxidation reaction according to the electrochemical voltage series is assumed to happen dominantly. The main corrosion product in chloride media is simonkolleite according to literature. (6) It is likely, that Zn^{2+} ions and zinc hydroxide $\text{Zn}(\text{OH})_2$ is forming from the δ -phase. (6) (5)

While the zinc is forming the corrosion products, it is likely that the iron content in the remaining phases is increasing. The anodic dissolution is likely to slow down given the decreasing incline of the anodic branch of the polarization curve after samples were exposed to accelerated corrosion test and electrochemistry measurements were conducted. An increase of the corrosion current is found with a factor 10, as more corrosion products form over time when the samples were exposed to the accelerated corrosion test. The incline of the cathodic branch

was also suggested by literature (6). As the anodic reaction is slowing down and more cathodic reaction products occur, the cathodic reaction is suspected to be increased and this indicates an increase of the corrosion potential (E_{oc}). (6)

For the OCP potentials of the ZAD coating, after investigating the samples exposed to the accelerated corrosion test, the corrosion potentials were shifted towards a more positive direction starting from -930 mV to -740 mV against the RE.

The authors of (6) stated, a 93 wt % Zn ZAD coating was found to have a -0.75 V potential in chloride media against a Ag/AgCl (3 M KCl) electrode, which is comparable to the findings in this investigation. (6) In their paper (6), red rust on 10 μm thick ZAD coating on steel samples was found after 4 weeks in a 0.5 mol/l NaCl environment.

In this thesis no red rust formation was found after 12 weeks in CCT but also red rust was found after 12 weeks in NSST. The sample thickness in the investigated samples was at 50 – 60 μm and therefore thicker than in the comparable literature. This leads to an elongated corrosion protection of our samples compared to the literature, before red rust formation.

7.3.2 ZND Coating

Upon visual inspection a smooth matte dark-grey sample surface was found on every sample. Some showed small bubbles where the coating lifted, this was found especially near the edges of strut channels. Some light grey patches were observed on the connector.

On an overall comparison to the ZAD coated samples they were found to offer an optically flawless coating appearance with a uniform distribution all around every investigated sample.

In microstructure analyses, the typical diffusion layer was found, but surprisingly also an organic paint layer with a dark grey to black appearance was present on top of the first layer.

After investigating the ZND coated samples in the SEM, the organic layer was found to consist of carbon, oxygen, and titanium. A TiO_2 filler is predicted to be a component of the organic layer. The diffusion layer is very similar to the one of the ZAD coated samples.

Due to the organic coating found on top of the metallic-zinc diffusion layer, the cathodic reduction reaction of oxygen-rich molecules is assumed to be more dominant than the anodic (metallic) oxidation. (6) Therefore the potential after longer exposure to the accelerated corrosion test is shifting in a negative direction. After the samples were exposed to the accelerated corrosion (12 weeks in NSST) test, an incline in the cathodic branch of the polarization curve was observed. It is possible, that the organic layer is consisting of TiO_2 , which could be electrically active and therefore influencing the reaction. It is assumed, that after the samples were exposed to these harsh conditions, the organic topcoat is failing. The variation of oxygen content of the unknown organic coating is possibly leading to different availability of the electrons and therefore an unclear trend in the corrosion findings.

A differentiated view of the anodic and cathodic branch with an improved measurement set up would be helpful for the future.

7.4 Multilayer Coatings

As one of the multilayer coatings is the currently used coating for the screws in the MT-System, and the information exchange regarding the external coater is not as close as it is with the galvanizing partner for the DDZ samples, these coatings are mainly investigated to compare the findings of the new DDZ coated samples to the current standard.

For the multilayer coatings the MP+TC coating surface was coloured grey, with a light green-yellow-gold tint. The samples were evenly coated, and the coating was not brittle nor flaky.

The LOM images showed the typical spherical shapes of the particles of the mechanically plated base coating described under 3.3.6. On that zinc-rich metal coating was a topcoat containing aluminum-rich flakes in a polymer matrix, as typically used for fasteners.

The corrosion effects were evaluated visually after 12 weeks in CCT and compared to the other two multilayer coatings this one showed the best corrosion protection properties.

For the ZB+TC coating, a grey coating layer, with a shiny finish was found after visual inspection. A view black spots were also visible especially on the edges of the screw head. In general, the coating was brittle, and flakes are falling off after the slightest touch. The packaging of the samples sent to Hilti was not ideal, as there were 100 screws in a plastic bag. The coating appearance can easily be influenced by transportation and friction between the samples in the bag.

The LOM images indicate just a horizontally flaky silvery layer similar to the topcoat on the MP+TC samples. Due to the high similarity of the two layers, they cannot be distinguished in the cross section. The coating buildup was found on the inner corners of the wingnut samples. This leads to the assumption that the application was through spray or dipping in the polymer matrix rich in the metallic flakes. Maybe a spinning step was added and due to centrifugal force, a pile up in the edges formed. Otherwise, it could simply be a high surface tension forming a higher coating thickness along corners or valleys of a thread.

The results allow to conclude after three weeks in CCT pitting corrosion started to form leading to severe red rust formation around the inner holes of the connector products. Sharp edges including a small thread in the hole lead to uneven coatings and are prone for corrosion. The screw heads were showing pitting corrosion with red rust forming after 7 weeks in CCT. The corrosion protection was shown to be the worst in comparison to the other two multilayer coatings.

For the ZAD+ZT coating the optical appearance was silvery, shiny over the screws and connectors. Although on sharp edges a few black spots were found on the thread.

The LOM shows two different layers in the cross sections, first it appears to be a white metallic layer near the substrate and on very few spots on the sample there is also a black buildup with some silvery inlays. The metallic layer builds up on top of the thread, whereas the black layer is to be accumulated in the valleys of the screw samples. On the connector sample the outer layer is nearly not found on the outside of the sample.

The wingnut samples were showing red rust near the edges after eight weeks of CCT and further red rust was obtained around the inner hole with the thread after 12 weeks in CCT. One of the wingnuts started forming corrosion products on a wider surface area coating roughly 20% of the area. The screws performed better than the connector products corrosion effects were indicating small pitting corrosion around the edges of the screw and at the threads.

7.5 Comparison

The microstructure formation mechanism of the double dip zinc coatings was found to be random over various dipping times. On Sandelin and MM standard samples, an inhibition layer formation next to the substrate was found, and an increase in the zinc content towards the top of the coating was obtained. As the variation in dipping times were not investigated further in terms of corrosion protection, no conclusion on the corrosion protection benefits of a more homogeneous or layered microstructure build-up of the cross sections could be drawn.

In terms of corrosion protection of the connector parts of the MT-system after the visual inspection of the accelerated corrosion test treated samples, the best performances were found for the ZND and MP+TC coatings. The double dipped Hilti parts formed white rust easily.

After the electrochemistry test of the connector parts of the corrosion system, the slowest corrosion rate was found on the ZND coated sample. The accelerated corrosion tests all samples were exposed to were not comparable, so there is an uncertainty in the conclusion. Also, the electrochemistry test was not sufficient for measuring the screws or wingnuts covered with the standard multilayer coating, Hilti currently uses.

8 Conclusion

8.1 Single- and Double Dip Zinc coatings: plain specimen

8.1.1 Sandelin samples

- The Sandelin samples showed the typical Sandelin effect with an increased coating thickness as the dipping time increases.
- The microstructure of the single dipped Sandelin samples was found to be according to the literature.
- The double dip cross sections showed multiple phases, including a ternary Zn-Fe-Al phase in a Zn matrix and a darker grey colored inhibition layer consisting mainly of Al and Fe next to the substrate.
- No clear influencing factors or correlation between coating structure and coating process was found in the double dipped samples.

8.1.2 Standard construction steel samples

- The inhibition layer and the second layer with the Zn-Al eutectic surrounding the η -zinc layer grows from 10% of the overall coating thickness to 50% of the overall coating thickness. This happens aligned to the dipping time increase of the second dip while the first dip step remains at 5 minutes.
- The Sebigy-effect with a parabolic coating thickness growth with increasing dipping times could not be observed.

8.2 Double Dip Zinc on connectors

- The zinc rich phases increase towards the top of the coating. All ternary coatings are located toward the steel substrate. Other than that, the phase distribution is random.
- The Hilti parts are harder to be coated evenly because of their geometry and thickness. Flaws were found on the DZMZ coated Hilti parts.
- The overall visual appearance and corrosion resistance is acceptable as a thick topcoat is forming, protecting the steel substrate from corrosion.
- On Hilti parts, white rust formed fast, but no red rust was forming after 6 weeks in NSST.

8.3 Zinc Diffusion Coatings on screws and connectors

- The ZND samples, showed less corrosion signs than the ZAD samples given the investigation of screws and connector parts of the MT-System.
- After visual inspection of the 12 week accelerated corrosion samples, the ZAD coatings formed red rust indicating a more severe corrosive attack outcome as on the ZND samples, where only white rust was visible after the same time.
- The ZND samples came with an organic coating layer resulting in an unclear corrosion mechanism after electrochemistry measurements. The same measurements on the ZAD coated samples proved the findings of all corrosion tests.
- In general, the zinc diffusion coatings performed better in terms of corrosion protection than the Zn/ZnAl double dipped samples with comparable thickness.

8.4 Multilayer Zinc Coatings on screws and connectors

- The best corrosion resistance on multilayer coatings was found in the MP+TC coated samples, followed by the second best ZAD+ZT coating on screws and connectors.
- The worst performance in any of the corrosion tests of this investigation was found on ZB+TC coated screws, where red rust forms fast.

9 Outlook for the future

For the new Double Dip coating technology alloying with Mg and Al for the second dip is proposed to further increase the corrosion protection. (14)

Regarding the cost, it was estimated, that stainless-steel products, are currently 70% more expensive than Double Dip HDG products with ZnAlMg coating. Therefore, it is a logic next step to try alloying with Mg also in the second bath of the DDZ process. The investigation on Hilti parts and sample plates with varying dip times is suitable for further tests. (15)

It is expected that the corrosion protection of those DDZ ZnAlMg second dipped samples performance is even better than on Multilayer Zinc coatings or on Zinc Diffusion coatings. (37)

10 Acronyms

Acronym	Description
AsB	Angle selective Backscatter Detector
CCT	Cyclic Corrosion Test, ISO 16701
CE	Counter electrode
CS	Cross section
CWTC	Condensation water test climate, DIN 50017
DDZ	Double dip zinc
DZ	Technical zinc
EDX	Energy Dispersive X-Ray Detector
ELCHEM	Electrochemistry
EtOH	Ethanol
FDSO	First dip second dip
FOTO	Photograph
HDG	Hot dip galvanizing
LOM	Light optical microscopy
MM	Standard steel sample
No, Nb	Number
NSST	Neutral Salt Spray Test, ISO 9227
OES	Optical Emission Spectrometry
OCP	Open circuit potential
PID	Point & ID (Identification)
Prop	Proposal
RE	Reference electrode
Sandelin	Steel containing 0.04-0.14 wt.% Si
SE2	Secondary Electron Detector
SEM	Scanning electron microscope
SHE	Standard hydrogen electrode
WE	Working electrode
WP	Work package
WP1	Work package 1
WP2	Work package 2
ZN	Pure zinc

11 Table of Pictures

Figure 1 Microstructure of ZnAlMg cross section (9).....	17
Figure 2 Process schematic of continuous hot dip galvanizing (12).....	17
Figure 3 Process schematic of single dip batch hot dip galvanizing (Source: Hilti internal)..	18
Figure 4 Process schematic of double dip batch hot dip galvanizing (Source: Hilti internal) .	18
Figure 5 Microstructure example of mechanically plated sample cross section (20)	20
Figure 6 Phase diagram of Fe-Zn-system (12)	20
Figure 7 Phase diagram of Fe-Zn system (Zn-rich region) (12)	20
Figure 8 Phase diagram 2021 of Fe/Zn phase diagram including differences regarding method (21).....	21
Figure 9 Phase diagram 2021 of Fe-Zn system (Zn-rich region) differences regarding method (21).....	21
Figure 10 Influence of Si content in steel with temperature (2)	21
Figure 11 Visual appearance or top view of Sandelin steel zinc coated surface after surface photography (22).....	22
Figure 12 Visual appearance or top view of Sebisty steel zinc coated surface after surface photography (22).....	22
Figure 13 Cross section of zinc coated Sandelin-steel, 460°C, 10 Minutes REM (2)	22
Figure 14 Cross section of zinc coating on Sebisty-steel, 460°C, 10 Minutes, REM (2).....	22
Figure 15 Growth kinetics of phases in Sandelin samples (23).....	23
Figure 16 Phase diagram of the binary Fe/Al system (24)	23
Figure 17 Phase diagram of the binary Al/Zn system (25)	23
Figure 18 Ternary phase diagram Zn-Al-Fe system at 450°C (28).....	24
Figure 19 Microstructure of double dipped Zn/Zn-5Al sample, divided in three zones at 550°C, dipping time: 2 minutes (27)	24
Figure 20 Phases and compositions described from the ternary phase diagram Zn-Al-Fe (28)	24
Figure 21 Full one-week cycle in CCT (32).....	26
Figure 22 Spray of CCT with phase A (left) and phase B (right) (32)	27
Figure 23 CWTC chamber DIN 50017 (33).....	27
Figure 24 Overview of FlowCell buildup	28
Figure 25 Side view of FlowCell including flat sample	28
Figure 26 Explanatory image of FlowCell	28
Figure 27 Cut location of Sandelin samples.....	32
Figure 28 Cut location of MM samples	32
Figure 29 WP2 DZZ OCP of DZMZ and X-MZ after 0w and 1w in CWTC against Ag/AgCl (3M KCl).....	65
Figure 30 DZMZ and X-MZ current potential plot after 0w and 1w in CWTC against Ag/AgCl (3M KCl).....	65
Figure 31 Electrochemistry measurement: OCP of ZAD coated zinc diffusion samples against Ag/AgCl (3M KCl) RE	73
Figure 32 Electrochemistry measurement: OCP of ZND coated zinc diffusion samples against Ag/AgCl (3M KCl) RE	73
Figure 33 Electrochemistry measurement: Current-potential plot of ZAD coated zinc diffusion samples against Ag/AgCl (3M KCl) RE.....	73
Figure 34 Electrochemistry measurement: Current-potential plot of ZND coated zinc diffusion samples against Ag/AgCl (3M KCl) RE.....	73
Figure 35 CS of annealing effect of zinc coated steel sample (11)	79
Figure 36 Bubbles forming in zinc coating due to coating mistakes (2).....	83

12 Tables

Table 1 Phases of Fe/Zn phase diagram (2).....	21
Table 2 Grinding and polishing routine	25
Table 3 Overview of work packages	29
Table 4 Overview of analytic methods used for different coating technologies	29
Table 5 OES analysis of steel substrate of MM and SB sample	30
Table 6 DDZ WP1 sample overview, shows dipping times in various baths, first bath with ZN or DZ and second dip ZnAl	30
Table 7 WP2 DDZ sample overview, on Hilti parts including three different samples, coated with the DZMZ or the X-MZ coating with various analytical methods	33
Table 8 Overview Diffusion Coating samples	34
Table 9 Overview of ZAD and ZND coated samples after different exposure time (weeks) to accelerated corrosion tests (CCT & NSST) and the electrochemistry measurements thereafter	35
Table 10 Overview of multilayer zinc coatings	35
Table 11 Overview Multilayer Coating samples	35
Table 12 Overview and descriptions of photographs of DDZ WP1 Sandelin samples.....	36
Table 13 Overview and description of photographs of DDZ WP1 MM samples	37
Table 14 WP1 DDZ CS Sandelin ZN	39
Table 15 WP1 DDZ CS Sandelin DZ	41
Table 16 WP1 DDZ CS MM ZN	42
Table 17 WP1 DDZ CS MM DZ	43
Table 18 Coating thickness of SB samples, ZN and DZ coatings	45
Table 19 Coating thickness of MM samples, ZN coatings.....	46
Table 20 WP1 DDZ SEM Sandelin sample ZN coating.....	47
Table 21 WP1 DDZ SEM MM sample ZN coating	51
Table 22 Overview and descriptions of photographs of DDZ WP2 Hilti part samples	55
Table 23 WP2 DDZ LOM CS of DZMZ and X-MZ coated samples.....	56
Table 24 WP2 DDZ Coating thickness of BP and chan of MT BR-40 04 coated with X-MZ and DZMZ	58
Table 25 WP2 DDZ SEM images and EDX mapping of MT BR-40 04 with DZMZ coating on baseplate and channel	59
Table 26 WP2 DDZ SEM images and EDX mapping of MT BR-40 04 with X-MZ coating on baseplate and channel	60
Table 27 WP2 DDZ CCT samples with X-MZ and DZMZ coating	62
Table 28 WP2 DDZ NSST samples with X-MZ and DZMZ coating	63
Table 29 WP2 DDZ LOM images of CWTC exposed samples including electrochemistry after polarization measured spots of DZMZ and X-MZ coated samples	64
Table 30 Zinc Diffusion coating sample photographs	66
Table 31 Zinc Diffusion Coatings CS LOM	67
Table 32 Zinc Diffusion Coatings CS SEM	69
Table 33 Zinc Diffusion Coatings CCT Photographs.....	70
Table 34 Zinc Diffusion Coatings CCT and NSST LOM.....	72
Table 35 Multilayer zinc coating photographs.....	75
Table 36 Multilayer Zinc Coating LOM CS.....	76
Table 37 Multilayer Zinc Coating CCT	77

13 Equations

(FR1 1).....	14
(AR1 2).....	14
(KR1 3).....	15
(KR2 4).....	15
(KR3 5).....	15
(CR1 6).....	15
(CR2 7).....	15
(CR3 8).....	15
(CR4 9).....	15
(CR5 10).....	15
(SK1 11).....	15

Die approbierte gedruckte Originalversion dieser Diplomarbeit ist an der TU Wien Bibliothek verfügbar
The approved original version of this thesis is available in print at TU Wien Bibliothek.



14 References

1. AG, Hilti. www.hilti.com. [Online] Hilti, 2022. https://www.hilti.com/c/CLS_INSTALLATION_SYS_7134/CLS_HOTDIP_GALVANIZED_PRODUCTS_7134/CLS_MULTIDUTY_HOTDIP_GALV_PRD_7134.
2. Wolf Dieter Schulz, Marc Thiele. *Feuerverzinken von Stückgut Werkstoff-Technologien - Schichtbildung - Eigenschaften*. [ed.] Eugen G. Leuze Verlag KG. D-88348 Bad Saulgau : Leuze Verlag, 2012. Vol. 2. Auflage .
3. Wiberg, Prof. Dr Nils. *Lehrbuch der Anorganischen Chemie*. [ed.] Gerd Fischer Nils Wiberg. Berlin, München : Walter de Gruyter & Co, 2007.
4. DIN Deutsches Institut für Normung, e.V. *DIN ISO 14713-1 Zinküberzüge - Leitfäden und Empfehlungen zum Schutz von Eisen- und Stahlkonstruktionen vor Korrosion*. Berlin : Beuth Verlag GmbH Berlin, May 2010. DIN EN ISO 14713-1.
5. Graedel, Christofer Leygraf Thomas E. *Atmospheric corrosion*. USA, Sweden : Wiley Inter Science, 2000. ISBN 0471372196.
6. *The effect of the chemical composition of intermetallic phases on the corrosion of thermal diffusion zinc coatings*. A.I., Biryukov et al. 370 (2019) 166-172, Chelyabinsk, Russian Federation : Elsevier B.V., 2019, Vol. Surface & Coatings Technology.
7. *Corrosion Behaviour of a Zn/Zn-Al Double Coating in 5% NaCl solution*. Tian-yu, Weng et al. doi: 10.20964/2018.12.85, 2018, International Journal of Electrochemical Science, Vol. 13, pp. 11882-11894.
8. *Morphology and properties of hot dip Zn-Mg and Zn-Mg-Al alloy coatings on steel sheet*. Surface & Coatings Technology, Jamshedpur, India : Elsevier BV, 2010, Vol. 205. 2578-2584.
9. M. Salueiro Azevedo, C.Allely, K. Ogle, P. Volovitch. Corrosion mechanisms of Zn(Mg,Al) coated steel: 2. The effect of Mg and Al alloying on the formation and properties of corrosion products in different electrolytes. Paris, France : Elsevier Ltd. , July 2014. Corrosion Science 90 (2015) 482-490.
10. C., Yao et al. Effect of Mg content on microstructure and corrosion behavior of hot dipped Zn-Al-Mg coatings. Sichuan, China : Journal of Alloys and Compounds 670 (2016) 239-248.
11. Kuklik, Vlastimil PhD and Kudlacek, Jan PhD. *Hot-Dip Galvanizing of Steel Structures*. [ed.] Butterworth-Heinemann. Oxford UK, Cambridge USA : Elsevier Ltd., 2016.
12. Marder, A.R. *The metallurgy of zinc coated steel*. [ed.] Departement of Materials Science and Engineering Progress in Materials Science. Lehigh University Bethlehem, PA USA : E, 2000.
13. Dipl.-Ing Hans-Jörg Böttcher, Dr. Wolf-Dieter Schulz, Dipl.-Chem. Marc Thiele. *Handbuch Feuerverzinken*. [ed.] Peter Maass and Peter Peissker. Weinheim : Wiley VCH Verlag, 2008. p. 102. Vol. Third Edition.
14. Tomandl, Alexander. *B5-Report BOLT*. Schaan, FL : Hilti AG, 2016. 512510454.
15. Pol, Frederic. *Alternative Zinc Alloys TP AZA*. Schaan : Hilti AG, 2012.
16. F. Natrup, W. Graf. *Thermochemical Surface Engineering of Steels; Chapter 20: Sherardizing: corrosion protection of steels by zinc diffusion coatings*. Netherlands, Germany : Woodhead Publishing, Elsevier Ltd. , 2015. 978-0-85709-592-3.

17. Bernardo, A. Duran III. Mechanical Plating Production Process. [Online] American Galvanizers Association, 08 2010. [Cited: 02 05, 2022.] <https://galvanizeit.org/knowledgebase/article/mechanical-plating-production-process>.
18. Standardization, International Organization for. ISO 12683:2004 Mechanically deposited coatings of zinc- Specification and test methods. s.l.: International Organization for Standardization, 2004.
19. The Coatinc Company. www.coatinc.com. [Online] 2020. [Cited: 02 15, 2022.] <https://www.coatinc.com/en/processes/the-duplex-system/>.
20. *Effects of heat treatment on microstructure evolution and corrosion performance of mechanically plated zinc coatings*. PP Chung, M Esfahami, J. Wang. Surface & Coating Technology, Melbourne, Australia : Elsevier, 2019, Vol. 377. 124916.
21. *Formation and growth behavior of intermetallic compound phases in the interfacial reaction of solid Fe / liquid Zn at 450°C*. Kwangsik Han, Inho Lee, Ikuo Ohnuma, Ryosuke Kainuma. Journal of Alloys and Compounds, Tsukuba, Japan : Elsevier B.V, 2021, Vol. 88 (2021). 161562.
22. Wieggl Verwaltung GmbH & CCo KG. Einfluss der Begleitelemente im Stahl auf die Zinkschicht. [Online] 2019. [Cited: 01 17, 2022.] https://wieggl.de/fileadmin/redaktion/files-allgemein/TechnischeArbeitsblaetter/3_EinflussVerzinkungsgut/TechAB_03-1.pdf.
23. *The kinetics of zinc coating growth on hyper sandelin stells and dictile cast iron*. D. Kopycinski, E. Guzik. 4/2007 105-110, Cracow, Poland : Foundry Commission of the Polish Academy of Sciences, 2007, Vol. 7. 1897-3310.
24. Pasche, Guillaume. Interaction between liquid aluminium and solid iron Al-rich intermetallics formation. Lausanne : Ecole Polytechnique Federale de Lausanne, January 2013.
25. Muhammet Demirtas, Genecaga Purcek, Harum Yanar, Zhenjun Zhang. Effect of Chemical Composition and Grain Size of RT Superplasticity of Zn-Al alloys processed by ECAP. s.l. : Letters on Materials 5(3) , January 2015.
26. American Elements . Product Datasheet Zinc Alumium Alloy . [Online] 2022. [Cited: 02 22, 2022.] <https://www.americanelements.com/zinc-aluminum-alloy>.
27. *Evaluation of mechanical properties in of double-dip galvanized coatings on carbon steel*. Yraima Rico O., Edwain Carrasquero, Jaime Minchala. Equador : Ingenius , 2019, Vols. N.°22 (july-december) pp 80-89. <https://doi.org/10.17163/ings.n22.2019.08>.
28. *The zinc-rich corner of the 450°C isothermal section of the Zn-Al-Fe-Si quaternary system*. Shiwen Pan, Fucheng Yin, Manxiu Zhao, Ya Liu, Xuping Su. 470(2009) 600-605, Hunan, PR China : Elsevier B.V, 2008, Vol. Journal of Alloys and Compounds. doi:10.1016/j.jallcom.2008.03.032.
29. Ólafsson, Ólafur. www.struers.com. [Online] Struers GmbH Willich, Germany, 2021. [Cited: 02 09, 2022.] <https://www.struers.com/de-DE/Knowledge/Materials/Zinc-coatings#Trennen>.
30. Zeiss. microscopy@zeiss.com. [Online] 07 2020. [Cited: 02 09, 2022.] https://p.widencdn.net/od67mu/EN_aftersales-flyer_AsB-Detector_rel.2.0.
31. Deutsches Institut für Normung, e.V. Korrosionsprüfungen in künstlichen Atmosphären - Salzsprühnebelprüfungen. Berlin : Beuth Verlag GmbH Wien, 2006.
32. Deutsches Institut für Normung, e.V. Beschleunigte Korrosionsprüfungen unter zyklischer Einwirkung von Feuchte und intermittierendem Versprühen einer Salzlösung unter kontrollierten Bedingungen. *DIN EN ISO 16701*. Berlin : s.n., 2011.

33. DIN Deutsches Institut für Normung e.V. Kondenswasser Prüfklimare DIN 50017. s.l. : International Patentclassification G01 N 17/00, 1982.
34. Radiometer Analytical SAS. Titralab 870 Reference Manual D21T060. [Online] 03 08, 2021. [Cited: 03 09, 2022.] www.support.hach.com.
35. Xylem Analytics Germany, GmbH. Xylem. [Online] Sensortechnik Meinsberg, 2018. [Cited: 02 01, 2021.] <https://www.meinsberger-elektroden.de/labor/bezug.html>.
36. IPS Elektroniklabor GmbH & Co. KG. www.ips-jaissle.de. [Online] 04 2015. [Cited: 01 15, 2022.] https://ips-jaissle.de/en/corrosion_cells.html.
37. *The corrosion behavior of ZnAlMg alloys in maritime environments*. A. Tomandl, E. Labrenz. doi: 10.1002/maco.201609076, 2016, Materials and Corrosion, Wiley-Vch, Weinheim.
38. Christofer Leygraf, Thomas Graedel. *Atmospheric Corrosion*. New York, USA and Canada : Wiley - Interscience, 2000.
39. *Microstructure Characterization and Corrosion Resistance of Zinc Coating Obtained on High-Strength Grade 10.9 Bolts Using a New Thermal Diffusion Process*. Henryk Kania, Jack Sipa. 1440, Swiebodzin, Poland : MDPI, Materials Journal, 2019, Vol. 12.
40. Feldmann M, et al. *Hot dip zinc-coating of prefabricated structural steel components*. Publication Office of the European Union. Luxembourg : Joint Research Centre of the European Commission, 2010.
41. Radiometer Analytical SAS. Titralab 870 Reference Manual p.172. [Online] Hach, 03 08, 2021. [Cited: 03 08, 2022.] https://support.hach.com/app/answers/answer_view/a_id/1019350/~what-is-potential-verses-standard-hydrogen-electrode-%28she%29%3F-.
42. F., Ajersch et al. Numerical Simulation of the rate of dross formation in continuous galvanizing baths. s.l. : Iron and Steel Technology 3(8), August 2006.
43. *Electrochemical metrics for corrosion resistant alloys*. Nyby, Clara et al. 58 <https://doi.org/10.1038/s41597-021-00840-y>, 2021, nature.